

CERN-PH-EP-2012-242

Submitted to: Phys. Rev. D

Measurement of W^+W^- production in pp collisions at $\sqrt{s} = 7$ TeV with the ATLAS detector and limits on anomalous WWZ and $WW\gamma$ couplings

The ATLAS Collaboration

Abstract

This paper presents a measurement of the W^+W^- production cross section in pp collisions at $\sqrt{s} = 7$ TeV. The leptonic decay channels are analyzed using data corresponding to an integrated luminosity of 4.6 fb^{-1} collected with the ATLAS detector at the Large Hadron Collider. The W^+W^- production cross section $\sigma(pp \rightarrow W^+W^- + X)$ is measured to be 51.9 ± 2.0 (stat) ± 3.9 (syst) ± 2.0 (lumi) pb, compatible with the Standard Model prediction of $44.7^{+2.1}_{-1.9}$ pb. A measurement of the normalized fiducial cross section as a function of the leading lepton transverse momentum is also presented. The reconstructed transverse momentum distribution of the leading lepton is used to extract limits on anomalous WWZ and $WW\gamma$ couplings.

Measurement of W^+W^- production in pp collisions at $\sqrt{s} = 7$ TeV with the ATLAS detector and limits on anomalous WWZ and $WW\gamma$ couplings

The ATLAS Collaboration
(Dated: December 25, 2013)

This paper presents a measurement of the W^+W^- production cross section in pp collisions at $\sqrt{s} = 7$ TeV. The leptonic decay channels are analyzed using data corresponding to an integrated luminosity of 4.6 fb^{-1} collected with the ATLAS detector at the Large Hadron Collider. The W^+W^- production cross section $\sigma(pp \rightarrow W^+W^- + X)$ is measured to be 51.9 ± 2.0 (stat) ± 3.9 (syst) ± 2.0 (lumi) pb, compatible with the Standard Model prediction of $44.7^{+2.1}_{-1.9}$ pb. A measurement of the normalized fiducial cross section as a function of the leading lepton transverse momentum is also presented. The reconstructed transverse momentum distribution of the leading lepton is used to extract limits on anomalous WWZ and $WW\gamma$ couplings.

PACS numbers: 14.70.Fm, 12.60.Cn, 13.85.Fb, 13.38.Be

I. INTRODUCTION

Measurements of vector boson pair production at particle colliders provide important tests of the electroweak sector of the Standard Model (SM). Deviations of the production cross section or of kinematic distributions from their SM predictions could arise from anomalous triple gauge boson interactions [1] or from new particles decaying into vector bosons [2]. Vector boson pair production at the Large Hadron Collider (LHC) [3] also represents an important source of background to Higgs boson production [4] and to searches for physics beyond the SM.

This paper describes a measurement of the W^+W^- (hereafter WW) inclusive and differential production cross sections and limits on anomalous WWZ and $WW\gamma$ triple gauge couplings (TGCs) in purely leptonic decay channels $WW \rightarrow \ell\nu\ell'\nu'$ with $\ell, \ell' = e, \mu$. $WW \rightarrow \tau\nu\ell\nu$ and $WW \rightarrow \tau\nu\tau\nu$ processes with τ leptons decaying into electrons or muons with additional neutrinos are also included. Three final states are considered based on the lepton flavor, namely ee , $\mu\mu$, and $e\mu$. Leading-order (LO) Feynman diagrams for WW production at the LHC include s -channel production with either a Z boson or a virtual photon as the mediating particle or u - and t -channel quark exchange. The s - and t -channel diagrams are shown in Fig. 1. Gluon-gluon fusion processes involving box diagrams contribute about 3% to the total cross section. The SM cross section for WW production in pp collisions at $\sqrt{s} = 7$ TeV is predicted at next-to-leading order (NLO) to be $44.7^{+2.1}_{-1.9}$ pb. The calculation of the total cross section is performed using MCFM [5] with the CT10 [6] parton distribution functions (PDFs). An uncertainty of $^{+4.8\%}_{-4.2\%}$ is evaluated based on the variation of renormalization (μ_R) and factorization (μ_F) scales by a factor of two ($^{+3.6\%}_{-2.5\%}$) and CT10 PDF uncertainties derived from the eigenvector error sets as described in Ref. [7] ($^{+3.1\%}_{-3.4\%}$) added in quadrature. The contribution from SM Higgs production [4] with the Higgs boson decaying into a pair of W bosons ($H \rightarrow WW$) depends on the mass of the Higgs boson (m_H). For $m_H = 126$

GeV, the SM WW production cross section would be increased by 8%. Contributions from vector boson fusion (VBF) and double parton scattering (DPS) [8] processes are found to be less than 0.1%. The processes involving the SM Higgs boson, VBF and DPS are not included neither in the WW cross-section predictions, nor in deriving the corrected measured cross sections. Events containing two W bosons from top-quark pair production and single top-quark production are explicitly excluded from the signal definition, and are treated as background contributions.

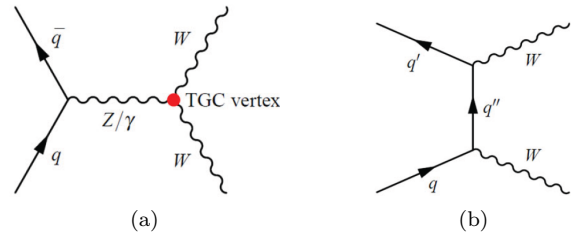


FIG. 1: SM LO Feynman diagrams for WW production through the $q\bar{q}$ initial state at the LHC for (a) the s -channel and (b) the t -channel. The s -channel diagram contains the WWZ and $WW\gamma$ TGC vertices.

The s -channel diagram contains the WWZ and $WW\gamma$ couplings. The SM predicts that these couplings are $g_{WWZ} = -e \cot \theta_W$ and $g_{WW\gamma} = -e$, where e is related to the fine-structure constant α ($= e^2/4\pi$) and θ_W is the weak mixing angle. Detailed studies of WW production allow to test the non-Abelian structure of the SM electroweak theory and probe anomalous WWZ and $WW\gamma$ TGCs, which may be sensitive to low-energy manifestations of new physics at a higher mass scale. WW production and anomalous WWZ and $WW\gamma$ TGCs have been previously studied by the LEP [9] and Tevatron [10] experiments, and were also recently studied by the LHC experiments [11–13]. The dataset used in this paper corresponds to an integrated luminosity of 4.6 fb^{-1} [14] collected with the ATLAS detector at the LHC, and the results presented supersede the previous ATLAS mea-

surements [12].

This paper is organized as follows. Section II describes the overall analysis strategy. Section III describes the ATLAS detector. Section IV summarizes the Monte Carlo (MC) simulation used for the signal and background modeling. Section V details the reconstruction of final state objects and event selection criteria. Sections VI and VII describe the WW signal and background estimation. Results are presented in Sec. VIII for inclusive and fiducial cross sections; in Sec. IX for the normalized differential fiducial cross section as a function of the transverse momentum (p_T) [15] of the lepton with higher p_T (denoted by the “leading lepton”); and in Sec. X for limits on anomalous WWZ and $WW\gamma$ TGCs. Conclusions are drawn in Sec. XI.

II. ANALYSIS STRATEGY

Candidate WW events are selected with two opposite-sign charged leptons (electrons or muons) and large missing transverse momentum (E_T^{miss}), a signature referred to “ $\ell\ell' + E_T^{\text{miss}}$ ” in this paper. The cross section is measured in a fiducial phase space and also in the total phase space. The fiducial phase space is defined in Sec. VI and is chosen to be close to the phase space defined by the offline selection criteria. The fiducial cross section σ_{WW}^{fid} for the $pp \rightarrow WW + X \rightarrow \ell\nu\ell'\nu' + X$ process is calculated according to the equation

$$\sigma_{WW}^{\text{fid}} = \frac{N_{\text{data}} - N_{\text{bkg}}}{C_{WW} \times \mathcal{L}}, \quad (1)$$

where N_{data} and N_{bkg} are the number of observed data events and estimated background events, respectively. C_{WW} is defined as the ratio of the number of events satisfying all offline selection criteria to the number of events produced in the fiducial phase space and is estimated from simulation. \mathcal{L} is the integrated luminosity of the data sample.

The total cross section σ_{WW} for the $pp \rightarrow WW + X$ process is calculated for each channel using the equation

$$\sigma_{WW} = \frac{N_{\text{data}} - N_{\text{bkg}}}{C_{WW} \times A_{WW} \times \text{BR} \times \mathcal{L}}, \quad (2)$$

where A_{WW} represents the kinematic and geometric acceptance from the total phase space to the fiducial phase space, and BR is the branching ratio for both W bosons decaying into $e\nu$ or $\mu\nu$ (including decays through τ leptons with additional neutrinos). The combined total cross section from the three channels is determined by minimizing a negative log-likelihood function as described in Sec. VIII.

To obtain the normalized differential WW cross section in the fiducial phase space ($1/\sigma_{WW}^{\text{fid}} \times d\sigma_{WW}^{\text{fid}}/dp_T$), the reconstructed leading lepton p_T distribution is corrected for detector effects after the subtraction of background contamination. The measured leading lepton p_T spectrum is also used to extract anomalous WWZ and $WW\gamma$ TGCs.

III. THE ATLAS DETECTOR

The ATLAS detector [16] is a multi-purpose particle physics detector with approximately forward-backward symmetric cylindrical geometry. The inner detector (ID) system is immersed in a 2 T axial magnetic field and provides tracking information for charged particles in the pseudorapidity range $|\eta| < 2.5$. It consists of a silicon pixel detector, a silicon microstrip detector, and a transition radiation tracker.

The calorimeter system covers the pseudorapidity range $|\eta| < 4.9$. The highly segmented electromagnetic calorimeter consists of lead absorbers with liquid-argon (LAr) as active material and covers the pseudorapidity range $|\eta| < 3.2$. In the region $|\eta| < 1.8$, a pre-sampler detector using a thin layer of LAr is used to correct for the energy lost by electrons and photons upstream of the calorimeter. The electron energy resolution is about 2–4% at $p_T = 45$ GeV. The hadronic tile calorimeter is a steel/scintillating-tile detector and is situated directly outside the envelope of the electromagnetic calorimeter. The two endcap hadronic calorimeters have LAr as the active material and copper absorbers. The calorimeter coverage is extended to $|\eta| = 4.9$ by a forward calorimeter with LAr as active material and copper and tungsten as absorber material. The jet energy resolution is about 15% at $p_T = 45$ GeV.

The muon spectrometer measures the deflection of muons in the large superconducting air-core toroid magnets. It covers the pseudorapidity range $|\eta| < 2.7$ and is instrumented with separate trigger and high-precision tracking chambers. A precision measurement of the track coordinates in the principal bending direction of the magnetic field is provided by drift tubes in the pseudorapidity range $|\eta| < 2.0$. At large pseudorapidities, cathode strip chambers with higher granularity are used in the innermost plane over $2.0 < |\eta| < 2.7$. The muon trigger system, which covers the pseudorapidity range $|\eta| < 2.4$, consists of resistive plate chambers in the barrel ($|\eta| < 1.05$) and thin gap chambers in the endcap regions ($1.05 < |\eta| < 2.4$). The muon momentum resolution is about 2–3% at $p_T = 45$ GeV.

A three-level trigger system is used to select events for offline analysis. The level-1 trigger is implemented in hardware and uses a subset of detector information to reduce the event rate to a design value of at most 75 kHz. This is followed by two software-based trigger levels, level-2 and the event filter, which together reduce the event rate to about 400 Hz which is recorded for analysis.

IV. MONTE CARLO SIMULATION

Signal WW events are modeled using MC-simulated samples, while contributions from various SM background physics processes are estimated using a combination of MC samples and control samples from data.

MC events are generated at $\sqrt{s} = 7$ TeV and processed through the full detector simulation [17] based on GEANT4 [18]. The simulation includes the modeling of additional pp interactions in the same and neighboring bunch crossings.

The simulation of the WW signal production is based on samples of $q\bar{q} \rightarrow WW$ and $gg \rightarrow WW$ events generated with MC@NLO [19] and GG2WW [20], respectively. Initial parton momenta are modeled with the CT10 PDFs. The parton showering and hadronization, and the underlying event are modeled with HERWIG [21] and JIMMY [22].

The SM background processes, which are described in Sec. VII, are simulated using ALPGEN [23] for the W +jets, Drell-Yan Z/γ^* +jets and $W\gamma$ processes, MC@NLO for the $t\bar{t}$ process, MADGRAPH [24] for the $W\gamma^*$ process, ACERMC [25] for the single top-quark process, and HERWIG for WZ and ZZ processes. The TAUOLA [26] and PHOTOS [27] programs are used to model the decay of τ leptons and QED final-state radiation of photons, respectively. The MC predictions are normalized to the data sample based on the integrated luminosity and cross sections of the physics processes. Higher-order corrections, if available, are applied. The cross section is calculated to next-to-next-to-leading-order (NNLO) accuracy for W and Z/γ^* [28], NLO plus next-to-next-to-leading-log order for $t\bar{t}$ [29], and NLO for WZ and ZZ processes [5].

To improve the agreement between data and simulation, lepton selection efficiencies are measured in both data and simulation, and correction factors are applied to the simulation to account for differences with respect to data. Furthermore, the simulation is tuned to reproduce the calorimeter energy and the muon momentum scale and resolution observed in data.

V. OBJECTS AND EVENT SELECTION

The data analyzed were selected online by a single-lepton (e or μ) trigger with a threshold on the transverse energy in the electron case and on the transverse momentum in the muon case. Different thresholds (18 GeV for muons and 20 GeV or 22 GeV for electrons) were applied for different running periods. After applying data quality requirements, the total integrated luminosity is 4.6 fb^{-1} with an uncertainty of 3.9% for all three channels ee , $\mu\mu$ and $e\mu$ [14].

Due to the presence of multiple pp collisions in a single bunch crossing, each event can have multiple vertices reconstructed. The primary vertex of the hard collision is defined as the vertex with the highest $\sum p_T^2$ of associated ID tracks. To reduce contamination due to cosmic rays, the primary vertex must have at least three associated tracks with $p_T > 0.4$ GeV.

Electrons are reconstructed from a combination of an electromagnetic cluster in the calorimeter and a track in the ID, and are required to have $p_T > 20$ GeV and

lie within the range $|\eta| < 2.47$, excluding the transition region between the barrel and endcap calorimeters ($1.37 < |\eta| < 1.52$). The electron p_T is calculated using the energy measured in the electromagnetic calorimeter and the track direction measured by the ID. Candidate electrons must satisfy the tight quality definition [30] re-optimized for 2011 data-taking conditions, which is based on the calorimeter shower shape, track quality, and track matching with the calorimeter cluster.

Muon candidates must be reconstructed in the ID and the muon spectrometer, and the combined track is required to have $p_T > 20$ GeV and $|\eta| < 2.4$. Good quality reconstruction is ensured by requiring minimum numbers of silicon microstrip and pixel hits associated with the track [31].

To ensure candidate electrons and muons originate from the primary interaction vertex, they are also required to have a longitudinal impact parameter ($|z_0|$) smaller than 1 mm and a transverse impact parameter ($|d_0|$) divided by its resolution (σ_{d_0}) smaller than ten for electrons and three for muons. These requirements reduce contamination from heavy-flavor quark decays and cosmic rays.

To suppress the contribution from hadronic jets which are misidentified as leptons, electron and muon candidates are required to be isolated in both the ID and the calorimeter. The sum of transverse energies of all clusters around the lepton but not associated with the lepton within a cone of size $\Delta R = \sqrt{(\Delta\eta)^2 + (\Delta\phi)^2} = 0.3$ is required to be less than 14% of the lepton transverse momentum. Corrections to the sum of transverse energies of all clusters around the lepton are applied to account for the energy deposition inside the isolation cone due to electron energy leakage or muon energy deposition and additional pp collisions. The sum of the p_T of all tracks with $p_T > 1$ GeV that originate from the primary vertex and are within a cone of size $\Delta R = 0.3$ around the lepton track is required to be less than 13% (15%) of the electron (muon) p_T .

Jets are reconstructed from topological clusters of energy in the calorimeter using the anti- k_t algorithm [32] with radius parameter $R = 0.4$. Topological clustering extends up to $|\eta| = 4.9$, and clusters are seeded by calorimeter cell deposits having energy exceeding 4 standard deviations of the cell noise level. Jet energies are calibrated using p_T - and η -dependent correction factors based on the simulation, and validated by collision data studies [33]. Jets are classified as originating from b -quarks by using an algorithm that combines information about the impact parameter significance of tracks in a jet which has a topology of semileptonic b - or c -hadron decays [34]. The efficiency of the b -tagging algorithm is 85% for b -jets in $t\bar{t}$ events, with an average light jet rejection factor of 10.

Since electrons are also reconstructed as jets, if a reconstructed jet and an electron satisfying the criteria mentioned above lie within $\Delta R = 0.3$ of each other, the jet is discarded. Electrons and muons are required to be sep-

arated from each other by $\Delta R > 0.1$. Since muons can radiate photons which can convert to electron-positron pairs, if a muon and an electron lie within $\Delta R = 0.1$ of each other, the electron is discarded.

The measurement of the missing transverse momentum two-dimensional vector \vec{E}_T^{miss} and its magnitude E_T^{miss} is based on the measurement of the energy collected by the electromagnetic and hadronic calorimeters, and muon tracks reconstructed by the ID and the muon spectrometer. Calorimeter cells associated with reconstructed jets with $p_T > 20$ GeV are calibrated at the hadronic energy scale, whereas calorimeter cells not associated with any object are calibrated at the electromagnetic energy scale.

Events with exactly two oppositely-charged leptons passing the lepton selection criteria above are selected. At least one of the two leptons is required to be geometrically matched to a lepton reconstructed by the trigger algorithm. In order to ensure that the lepton trigger efficiency reaches its plateau region and does not depend on the p_T of the lepton, the matching lepton is required to have $p_T > 25$ GeV. The leading lepton p_T requirement also helps to reduce the W +jets background contribution.

Events satisfying the above requirements are dominated by the contribution from the Drell-Yan process. To reject this background contribution, different requirements on the dilepton invariant mass $m_{\ell\ell'}$ and a modified missing transverse energy, $E_{T, \text{Rel}}^{\text{miss}}$, are applied to each final state. The $E_{T, \text{Rel}}^{\text{miss}}$ variable is defined as:

$$E_{T, \text{Rel}}^{\text{miss}} = \begin{cases} E_T^{\text{miss}} \times \sin(\Delta\phi) & \text{if } \Delta\phi < \pi/2 \\ E_T^{\text{miss}} & \text{if } \Delta\phi \geq \pi/2 \end{cases} \quad (3)$$

where $\Delta\phi$ is the difference in the azimuthal angle between the \vec{E}_T^{miss} and the nearest lepton or jet. The $E_{T, \text{Rel}}^{\text{miss}}$ variable is designed to reject events where the apparent E_T^{miss} arises from a mismeasurement of lepton momentum or jet energy. The selection criteria applied to $m_{\ell\ell'}$ and $E_{T, \text{Rel}}^{\text{miss}}$ are $m_{\ell\ell'} > 15, 15, 10$ GeV, $|m_{\ell\ell'} - m_Z| > 15, 15, 0$ GeV, and $E_{T, \text{Rel}}^{\text{miss}} > 45, 45, 25$ GeV for the ee , $\mu\mu$ and $e\mu$ channels, respectively. Less strict selection criteria on $m_{\ell\ell'}$ and $E_{T, \text{Rel}}^{\text{miss}}$ are employed for the $e\mu$ channel since the contribution from the Drell-Yan process is inherently smaller.

With the application of the $m_{\ell\ell'}$ and $E_{T, \text{Rel}}^{\text{miss}}$ selection criteria, the remaining background events come mainly from $t\bar{t}$ and single top-quark processes. To reject this background contribution, events are vetoed if there is at least one jet candidate with $p_T > 25$ GeV and $|\eta| < 4.5$ (this selection criterion is denoted by the term ‘‘jet veto’’ in this paper). To further reduce the Drell-Yan contribution, the transverse momentum of the dilepton system, $p_T(\ell\ell')$, is required to be greater than 30 GeV for all three channels.

Figures 2–5 show comparisons between data and simulation for the $m_{\ell\ell'}$, $E_{T, \text{Rel}}^{\text{miss}}$, jet multiplicity and $p_T(\ell\ell')$ distributions before the successive cuts are applied to the ee , $\mu\mu$ and $e\mu$ channels, respectively. The contributions

from various physics processes are estimated using MC simulation and normalized to the cross sections as described in Sect. IV. These plots indicate the discrimination power of these variables to reduce the dominant $t\bar{t}$, W +jets and Drell-Yan backgrounds and improve the signal-to-background ratio. Discrepancies between data and SM predictions based on pure MC estimates for some plots indicate the need for data-driven background estimates as are used for the WW signal extraction.

VI. WW SIGNAL ACCEPTANCE

The fractions of simulated WW signal events remaining after each step of the event selection are summarized in Table I. The fractions for direct WW decays into electrons or muons are shown separately from processes involving τ leptons ($WW \rightarrow \tau\nu\ell\nu$ and $WW \rightarrow \tau\nu\tau\nu$ processes with τ leptons decaying into electrons or muons). The acceptance for the $\mu\mu$ channel is higher than the ee channel since the identification efficiency for muons is higher than that for electrons. The acceptance for the $e\mu$ channel is the highest one due to looser selection requirements applied to $m_{\ell\ell'}$ and $E_{T, \text{Rel}}^{\text{miss}}$.

In order to minimize the theoretical uncertainty due to the extrapolation from the measured phase space to the total phase space for the cross-section measurement, a fiducial phase space is defined at the generator level by selection criteria similar to those used offline. Generator-level jets are reconstructed by running the anti- k_t algorithm with radius parameter $R = 0.4$ on all final-state particles generated with the MC@NLO and GG2WW event generators after parton showering and hadronization. The fiducial phase space is defined with the following criteria: lepton $p_T > 20$ GeV, muon pseudorapidity $|\eta| < 2.4$, electron pseudorapidity $|\eta| < 1.37$ or $1.52 < |\eta| < 2.47$, no generator-level jets with $p_T > 25$ GeV, rapidity $|y| < 4.5$ and separated from an electron by $\Delta R > 0.3$. The leading lepton p_T is required to be above 25 GeV and $p_T^{\ell\ell'} > 30$ GeV. The events are further required to have $m_{\ell\ell'} > 15, 15, 10$ GeV, $|m_{\ell\ell'} - m_Z| > 15, 15, 0$ GeV, and $p_{T, \text{Rel}}^{\nu+\bar{\nu}} > 45, 45, 25$ GeV for the ee , $\mu\mu$ and $e\mu$ channels respectively. The $p_{T, \text{Rel}}^{\nu+\bar{\nu}}$ variable is defined similarly to $E_{T, \text{Rel}}^{\text{miss}}$, where the \vec{E}_T^{miss} is replaced by the vector sum of the \vec{p}_T of the two generator-level neutrinos. To reduce the dependence on QED radiation, the electron and muon p_T include contributions from photons within $\Delta R = 0.1$ of the lepton direction.

With this definition of the fiducial phase space, the overall acceptance times efficiency can be separated into two factors A_{WW} and C_{WW} , where A_{WW} represents the extrapolation from the fiducial phase space to the total phase space, while C_{WW} represents detector effects such as lepton trigger and identification efficiencies, with a small contribution from differences in generated and measured phase spaces due to detector resolution.

Corrections to the simulation of lepton identification ef-

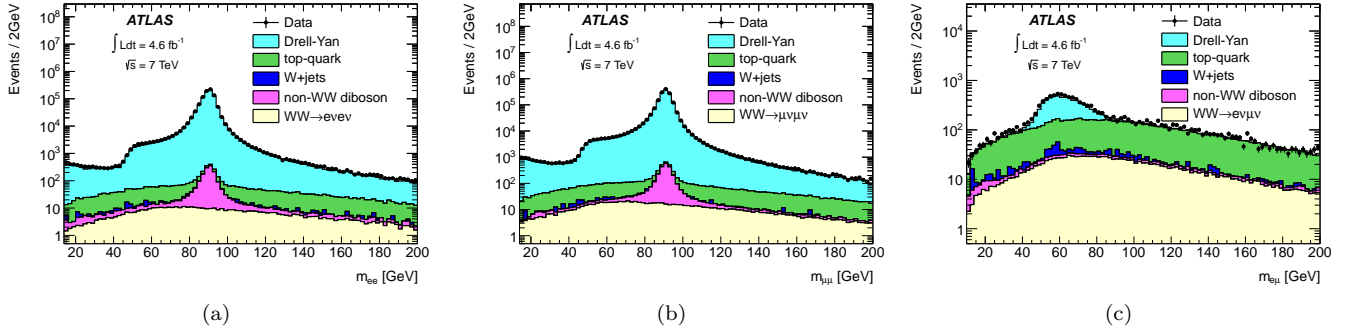


FIG. 2: Comparison between data and simulation for the dilepton invariant mass distribution before the $m_{\ell\ell'}$ cut for the (a) ee , (b) $\mu\mu$ and (c) $e\mu$ channels, respectively. The contributions from various physics processes are estimated using MC simulation and normalized to the cross sections as described in Sect. IV.

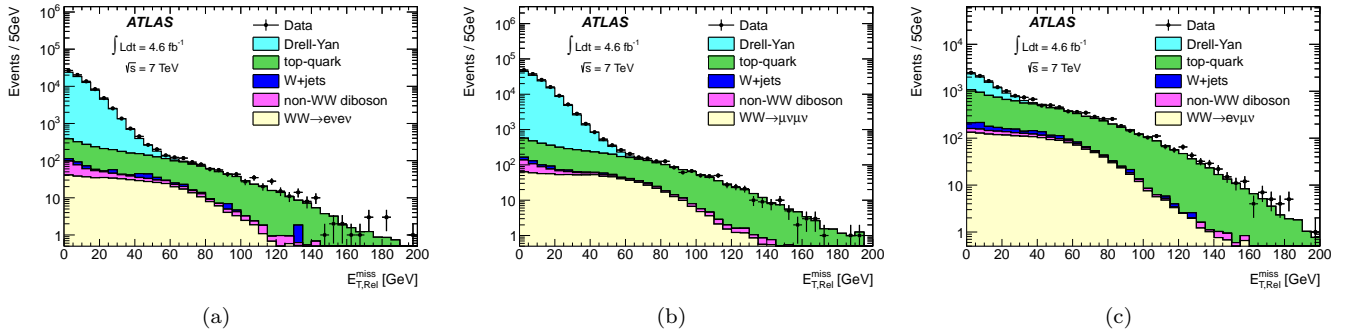


FIG. 3: Comparison between data and simulation for the $E_{T, \text{Rel}}^{\text{miss}}$ distribution before the $E_{T, \text{Rel}}^{\text{miss}}$ cut for the (a) ee , (b) $\mu\mu$ and (c) $e\mu$ channels, respectively. The contributions from various physics processes are estimated using MC simulation and normalized to the cross sections as described in Sect. IV.

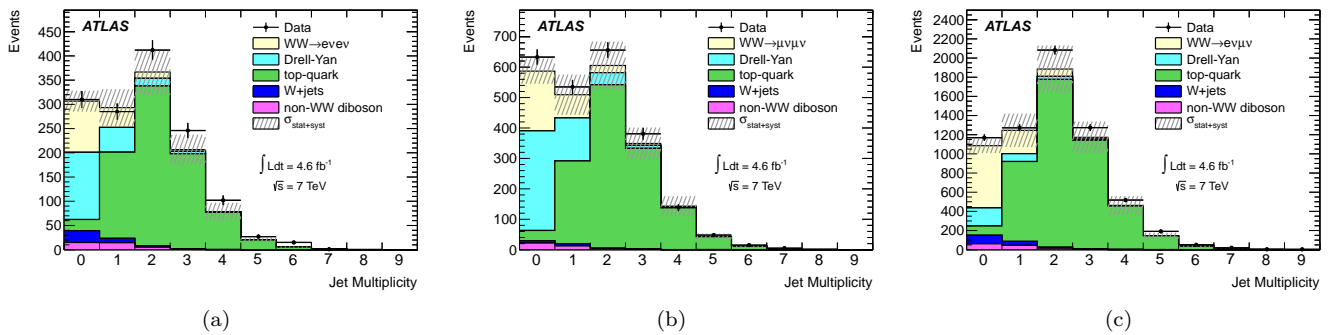


FIG. 4: Comparison between data and simulation for the jet multiplicity distribution of jets with $p_T > 25$ GeV before jet veto requirement for the (a) ee , (b) $\mu\mu$ and (c) $e\mu$ channels, respectively. The contributions from various physics processes are estimated using MC simulation and normalized to the cross sections as described in Sect. IV. The error band on each plot includes both statistical and systematic uncertainties on the signal and background estimations. Systematic uncertainties on the signal estimation are described in Sect. VI. Systematic uncertainties on background estimations include uncertainties on lepton, jet and E_T^{miss} reconstruction and identification, as well as uncertainties on theoretical production cross sections for these processes.

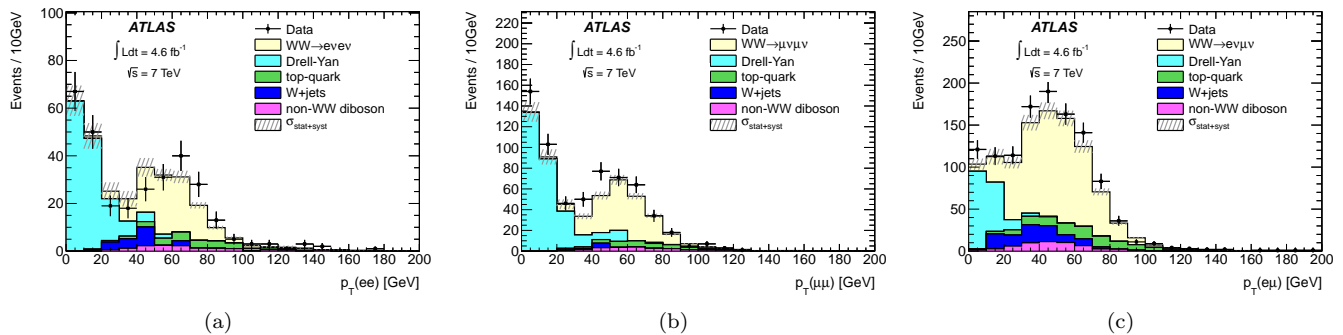


FIG. 5: Comparison between data and simulation for the dilepton p_T distribution before the $p_T(\ell\ell')$ cut for the (a) ee , (b) $\mu\mu$ and (c) $e\mu$ channels, respectively. The contributions from various physics processes are estimated using MC simulation and normalized to the cross sections as described in Sect. IV. The error band on each plot includes both statistical and systematic uncertainties on the signal and background estimations. Systematic uncertainties on the signal estimation are described in Sect. VI. Systematic uncertainties on background estimations include uncertainties on lepton, jet and E_T^{miss} reconstruction and identification, as well as uncertainties on theoretical production cross sections for these processes.

iciencies and resolutions are discussed in Sec. IV. A correction to the modelling of the jet veto efficiency (the fraction of events with zero reconstructed jets) is determined as the ratio of data to MC jet veto efficiencies for the $Z/\gamma^* \rightarrow \ell\ell$ process. This ratio is applied to WW MC [35] as

$$P_{\text{pred}}^{WW} = \frac{P_{Z/\gamma^*}^{\text{data}}}{P_{Z/\gamma^*}^{\text{MC}}} \times P_{WW}^{\text{MC}}, \quad (4)$$

where P_{pred}^{WW} is the corrected jet veto efficiency for $pp \rightarrow WW$, P_{WW}^{MC} is the MC estimate of this efficiency, and $P_{Z/\gamma^*}^{\text{data}}$ ($P_{Z/\gamma^*}^{\text{MC}}$) is the efficiency determined using $Z/\gamma^* \rightarrow \ell\ell$ events selected with two leptons satisfying the lepton selection criteria and $|m_{\ell\ell} - m_Z| < 15$ GeV in data (MC). By applying this correction, experimental uncertainties associated with the jet veto efficiency are significantly reduced, in particular, the uncertainty on the jet energy scale. The dominant uncertainty is due to the theoretical prediction of the differences in jet energy spectra between the WW and Z/γ^* processes, which are both modelled with MC@NLO + HERWIG for this correction.

For the factor C_{WW} (A_{WW}), the dominant uncertainty is the theoretical uncertainty on $P_{Z/\gamma^*}^{\text{MC}}$ (P_{WW}^{MC}). The theoretical uncertainty from missing higher-order corrections is evaluated by varying renormalization and factorization scales up and down by a factor of 2 for both the inclusive (≥ 0) and exclusive (≥ 1) jet cross sections and adding these two uncertainties in quadrature [36]. Uncertainties associated with the parton shower and hadronization models are evaluated by comparing the PYTHIA and HERWIG models, interfaced to the MC generating the process of interest. Uncertainties due to PDFs are computed using the CT10 error eigenvectors, and using the difference between the central CT10 and MSTW2008NLO [38] PDF sets. Including uncertainties from the jet energy scale (JES) and jet energy resolution (JER), P_{pred}^{WW} is es-

timated to be 0.624 ± 0.023 , 0.625 ± 0.023 and 0.633 ± 0.023 for the ee , $\mu\mu$ and $e\mu$ channels, respectively.

Additional theoretical uncertainties on A_{WW} are evaluated using the same procedures as for the jet veto efficiency. Additional uncertainties on C_{WW} are calculated using uncertainties on the lepton trigger, reconstruction and isolation efficiencies, as well as energy scale and resolution uncertainties on the reconstruction of lepton, jet, soft clustered energy in the calorimeter, and energy deposits from additional pp collisions. The uncertainty on the single-lepton trigger efficiency is less than 0.5% [39]. Electron and muon reconstruction and identification efficiency uncertainties are less than 2.0% and 0.4%, respectively [40]. The lepton isolation efficiency is determined with an uncertainty of 0.3% and 0.2% for electrons and muons, respectively. The simulation is corrected for the differences with respect to the data in lepton energy scale and resolution. The uncertainty is less than 1.0% and 0.1% on the energy scale and less than 0.6% and 5.0% on the resolution, for electrons and muons, respectively [30]. Uncertainties on the JES range from 2.5% to 8%, varying with jet p_T and η [41]. Uncertainties on the JER range from 9–17% for jet $p_T \simeq 30$ GeV to about 5–9% for jets with $p_T > 180$ GeV depending on jet η [41]. The uncertainties on the lepton energy scale and resolution, JES and JER are propagated to the E_T^{miss} , which also receives contributions from energy deposits due to additional pp collisions in the same or close by bunch crossings, and from energy deposits not associated with any reconstructed object [42].

All systematic uncertainties described above are propagated to the calculations of A_{WW} , C_{WW} and $A_{WW} \times C_{WW}$. The overall systematic uncertainty on A_{WW} is 5.7% for all three channels. The contributions from all systematic sources for A_{WW} are listed in Table II. The overall systematic uncertainty on C_{WW} is 4.2%, 3.1% and 3.2% for the ee , $\mu\mu$ and $e\mu$ channels, respectively.

The contributions from all systematic sources for C_{WW} are listed in Table III.

The product of $A_{WW} \times C_{WW}$ is defined as the ratio of events satisfying all offline selection criteria to the number of events produced in the total phase space. The systematic uncertainty on $A_{WW} \times C_{WW}$ is 4.9%, 4.0% and 4.1% for the ee , $\mu\mu$ and $e\mu$ channels. Owing to the presence of correlations between A and C , these uncertainties are smaller than those obtained by adding in quadrature the uncertainties from the PDFs, μ_F , μ_R , and parton shower model. As a result, the uncertainty on $A_{WW} \times C_{WW}$ is used for the calculation of the total cross-section uncertainty in each individual channel. Table IV summarizes the central value and also the statistical and systematic uncertainties on A_{WW} , C_{WW} and $A_{WW} \times C_{WW}$ for all three channels.

VII. BACKGROUND ESTIMATION

SM processes producing the $\ell\ell' + E_T^{\text{miss}}$ signature with no reconstructed jets in the final state are top-quark production, when additional jets in the final state are not reconstructed or identified (denoted by “top-quark background”); W production in association with jets (denoted by “ W +jets background”) when one jet is reconstructed as a lepton; Z/γ^* production in association with jets (denoted by “Drell-Yan background”) when apparent E_T^{miss} is generated from the mismeasurement of the p_T of the two leptons from Z/γ^* boson decay; WZ and ZZ processes when only two leptons are reconstructed in the final state; and the $W\gamma$ process when the photon converts into electrons. The contribution from QCD multi-jet production when two jets are reconstructed as leptons is found to be negligible.

A. Background contribution from SM non- WW diboson production processes

The expected background contributions from SM non- WW diboson processes (WZ , ZZ and $W\gamma$) are estimated using simulation. The total number of selected non- WW diboson background events corresponding to 4.6 fb^{-1} is estimated to be 13 ± 1 (stat) ± 2 (syst), 21 ± 1 (stat) ± 2 (syst), and 44 ± 2 (stat) ± 6 (syst) for the ee , $\mu\mu$ and $e\mu$ channels, respectively. The systematic uncertainties arise mainly from theoretical uncertainties on the non- WW diboson production cross sections and uncertainties on the lepton, jet and E_T^{miss} modeling in the simulation.

B. Background contribution from SM top-quark production processes

Background contributions from top-quark production processes are suppressed by the jet veto requirement. However, top-quark events containing no reconstructed

jets with $p_T > 25 \text{ GeV}$ and $|\eta| < 4.5$ could still mimic the signature of WW candidates. The top-quark background contribution is estimated using a data-driven method.

An extended signal region (ESR) is defined after the $E_{T, \text{Rel}}^{\text{miss}}$ cut but before applying the jet veto and $p_T(\ell\ell')$ criteria. In addition, a control region (CR) is defined as a subset of the ESR, which contains events having at least one b -tagged jet with $p_T > 20 \text{ GeV}$. The jet multiplicity distribution for top-quark events in the ESR, $T_{\text{data}}^{\text{ESR}}$, is estimated from the jet multiplicity distribution in the CR, $T_{\text{data}}^{\text{CR}}$. In a first step, the non-top-quark background distribution $T_{\text{MC,nt}}^{\text{CR}}$ in the CR is estimated with simulation, scaled by a normalization factor f'_n and then subtracted from the measured $T_{\text{data}}^{\text{CR}}$ distribution. Subsequently, the resulting distribution is extrapolated bin-by-bin from the CR to the ESR via the MC prediction of the ratio $T_{\text{MC},i}^{\text{ESR}}/T_{\text{MC},i}^{\text{CR}}$ for each jet multiplicity bin i . The method can be summarized by the following equation for each jet multiplicity bin:

$$T_{\text{data}}^{\text{ESR}} = \frac{T_{\text{MC}}^{\text{ESR}}}{T_{\text{MC}}^{\text{CR}}} (T_{\text{data}}^{\text{CR}} - f'_n \times T_{\text{MC,nt}}^{\text{CR}}), \quad (5)$$

where each symbol T represents a full jet multiplicity distribution. The normalization scale factor f'_n for the non-top-quark background contributions in the CR is determined from events in the ESR by fitting the jet multiplicity distribution observed in data with the templates constructed from the data in the CR for top-quark contributions and from simulation for non-top-quark contributions. The value of f'_n is found to be 1.07 ± 0.03 . In a final step, the number of top-quark background events in the signal region is estimated using the number of top-quark events in the ESR observed in data scaled by the ratio of top-quark events in the signal region to the number in the ESR in the MC simulation for the zero-jet bin.

The number of top-quark background events in the signal region is estimated to be 22 ± 12 (stat) ± 3 (syst), 32 ± 14 (stat) ± 5 (syst), and 87 ± 23 (stat) ± 13 (syst) for the ee , $\mu\mu$ and $e\mu$ channels, respectively. The statistical uncertainty is mainly due to the limited number of data events observed in the CR. The systematic uncertainties are dominated by the b -tagging uncertainty.

An alternative data-driven method is used to cross-check the top-quark background estimation. To reduce the associated uncertainties on the jet veto probability, a data-based correction is derived from a top-quark dominated sample based on the WW selection but with the requirement of at least one b -jet with $p_T > 25 \text{ GeV}$ [12]. In this sample, the ratio P_1 of events with one jet to the total number of events is sensitive to the modeling of the jet energy spectrum in top-quark events. A multiplicative correction based on the ratio $P_1^{\text{data}}/P_1^{\text{MC}}$ is applied to reduce the uncertainties resulting from the jet veto requirement. The results from the two data-driven methods are found to be consistent with each other within their uncertainties.

Selection criteria	ee		$\mu\mu$		$e\mu$	
	$e\nu e\nu$	$\tau\nu l\nu$	$\mu\nu\mu\nu$	$\tau\nu l\nu$	$e\nu\mu\nu$	$\tau\nu l\nu$
Exactly two opposite-sign leptons	22.8%	7.3%	39.0%	11.4%	30.2%	9.1%
$m_{\ell\ell'} > 15, 15, 10$ GeV	22.7%	7.3%	38.8%	11.4%	30.2%	9.1%
$ m_{\ell\ell'} - m_Z > 15, 15, 0$ GeV	17.6%	5.4%	29.9%	8.5%	30.2%	9.1%
$E_{T, \text{Rel}}^{\text{miss}} > 45, 45, 25$ GeV	6.4%	1.4%	11.9%	2.6%	19.0%	5.1%
Jet veto	4.0%	0.8%	7.4%	1.6%	12.1%	3.1%
$p_T(\ell\ell') > 30$ GeV	3.9%	0.7%	7.1%	1.5%	10.1%	2.6%

TABLE I: The product of acceptance times efficiency for the WW simulated sample at each event selection step. The $\tau\nu l\nu$ sample for the ee channel includes both $WW \rightarrow \tau\nu e\nu$ and $WW \rightarrow \tau\nu\tau\nu$ processes that result in two electrons in the final state; and accordingly for the $\tau\nu l\nu$ samples for the $\mu\mu$ and $e\mu$ channels.

Source of uncertainty	Relative uncertainty		
	ee	$\mu\mu$	$e\mu$
PDFs	0.9%	0.9%	0.9%
μ_R and μ_F scales	0.5%	0.5%	0.6%
Jet veto	5.6%	5.6%	5.6%
Total	5.7%	5.7%	5.7%

TABLE II: Relative uncertainties on the estimate of A_{WW} for the ee , $\mu\mu$ and $e\mu$ channels.

Source of uncertainty	Relative uncertainty		
	ee	$\mu\mu$	$e\mu$
Trigger efficiency	0.1%	0.6%	0.3%
Lepton efficiency	2.9%	0.7%	1.4%
Lepton p_T scale and resolution	0.9%	0.8%	0.6%
Jet energy scale and resolution	0.6%	0.5%	0.5%
E_T^{miss} modeling	0.5%	0.2%	0.4%
Jet veto scale factor	2.8%	2.8%	2.7%
PDFs, μ_R and μ_F scales	0.7%	0.7%	0.3%
Total	4.2%	3.1%	3.2%

TABLE III: Relative uncertainties on the estimate of C_{WW} for the ee , $\mu\mu$ and $e\mu$ channels.

	ee	$\mu\mu$	$e\mu$
A_{WW}	$(7.5 \pm 0.1 \pm 0.4)\%$	$(8.1 \pm 0.1 \pm 0.5)\%$	$(15.9 \pm 0.1 \pm 0.9)\%$
C_{WW}	$(40.3 \pm 0.5 \pm 1.7)\%$	$(68.7 \pm 0.5 \pm 2.1)\%$	$(50.5 \pm 0.2 \pm 1.6)\%$
$A_{WW} \times C_{WW}$	$(3.0 \pm 0.1 \pm 0.1)\%$	$(5.6 \pm 0.1 \pm 0.2)\%$	$(8.0 \pm 0.1 \pm 0.3)\%$

TABLE IV: Acceptances A_{WW} , C_{WW} and $A_{WW} \times C_{WW}$ for the ee , $\mu\mu$ and $e\mu$ channels. The first and second uncertainties represent the statistical and systematic uncertainties.

C. Background contribution from W +jets production process

The W +jets process can produce the $\ell\ell' + E_T^{\text{miss}}$ signature when one jet is reconstructed as a charged lepton. Since the probability for a jet to be identified as a lepton may not be accurately modeled in the MC simulation, a data-driven method is employed to estimate this contribution. A leptonlike jet is defined as a jet that passes all lepton selection criteria but fails the lepton isolation requirement in the muon case, and fails at least one of the isolation or tight quality requirements in the electron case. The ratio f_ℓ is then calculated as the ratio of jets satisfying the full lepton identification criteria

to the number of leptonlike jets. A jet-enriched data sample is selected containing one lepton that passes all lepton selection criteria and a leptonlike jet. The number of events in this sample is then scaled by the ratio f_ℓ to obtain the expected number of W +jets events in the signal region. The ratio f_ℓ is measured as a function of the jet p_T and η from a jet-enriched sample for electrons and muons separately. The number of W +jets background events in the signal regions is estimated to be 21 ± 1 (stat) ± 11 (syst), 7 ± 1 (stat) ± 3 (syst), and 70 ± 2 (stat) ± 31 (syst) for the ee , $\mu\mu$ and $e\mu$ channels, respectively. The dominant source of systematic uncertainties stems from the f_ℓ measurement. The same method is applied to a W +jets-enriched sample selected

with the requirement of two same-sign leptons to validate the W +jets estimation method. Consistent results are obtained for the number of observed and predicted events in this control region.

An alternative method is used to check the W +jets estimation in the signal region. This method defines leptons with two different sets of quality criteria, one with the standard lepton selection criteria (called tight lepton here) and the other one with less restrictive lepton identification criteria (called loose lepton here). For loose muons, the isolation requirement is dropped. For loose electrons, the medium electron identification criteria as defined in Ref. [30] are used and the isolation requirement is also dropped. Events with two loose leptons are assigned to one of four categories depending on whether both leptons, only the leading lepton, only the trailing lepton or neither of the two leptons, satisfy the tight lepton identification criteria. The corresponding numbers of events are denoted by N_{TT} , N_{TL} , N_{LT} and N_{LL} . The sample composition can be solved from a linear system of equations:

$$(N_{TT}, N_{TL}, N_{LT}, N_{LL})^T = \mathcal{E} (N_{\ell\ell'}, N_{\ell j}, N_{j\ell'}, N_{jj})^T \quad (6)$$

where $N_{\ell\ell'}$ is the number of events with two prompt leptons, $N_{\ell j}$ ($N_{j\ell'}$) is the number of events where only the leading (trailing) lepton is a prompt lepton, N_{jj} is the number of events where neither of the two leptons are prompt leptons. The 4×4 matrix \mathcal{E} contains the probabilities for a loose quality lepton to pass the tight quality selection for both prompt leptons and jets. These probabilities are estimated by applying the loose and tight selections to $Z/\gamma^* \rightarrow \ell\ell'$ events and to a sample of dijet events, respectively. To take into account the lepton p_T dependence of these two probabilities, the matrix equation is inverted for each event, giving four weights, corresponding to these four combinations. These weights are then summed over all events in the signal region with loose lepton requirements to yield the estimated total number of background events from W +jets and dijet processes. The results from the two data-driven methods are found to be consistent with each other within their uncertainties.

D. Background contribution from Drell-Yan production process

The Drell-Yan background is one of the dominant background contributions in the ee and $\mu\mu$ channels. Its contribution is suppressed by the requirements on $m_{\ell\ell'}$, $E_{T, \text{Rel}}^{\text{miss}}$ and $p_T(\ell\ell')$. A control region dominated by the Drell-Yan process is defined by applying the same set of selection cuts as used for the signal region and reversing the $p_T(\ell\ell')$ cut. The Drell-Yan background in the signal region is estimated from the number of events observed in this control region, after subtracting other background contributions using MC expectations, scaled by the ratio

of the number of MC Z +jets events in the signal region to the number in the control region. The number of Drell-Yan background events in the signal region is estimated to be 12 ± 3 (stat) ± 3 (syst), 34 ± 6 (stat) ± 10 (syst) and 5 ± 2 (stat) ± 1 (syst) events in the ee , $\mu\mu$ and $e\mu$ channels, respectively. As a cross-check, the results obtained above are compared to the predictions from simulation. Good agreement between the two estimates is found.

VIII. INCLUSIVE AND FIDUCIAL CROSS-SECTION RESULTS

Table V shows the number of events selected in data and the estimated background contributions with statistical and systematic uncertainties for the three individual channels and the combined channel. The expected numbers of WW signal events for the individual and the combined channels are also shown. In total $1325 \ell\ell' + E_T^{\text{miss}}$ candidates are observed in data with 824 ± 4 (stat) ± 69 (syst) signal events expected from the WW process and 369 ± 31 (stat) ± 53 (syst) background events expected from non- WW processes. The WW processes mediated by a SM Higgs boson with a mass of 126 GeV would contribute an additional 3, 7 and 17 events in the ee , $\mu\mu$ and $e\mu$ channels, respectively. Figure 6 shows the comparison between data and predictions for the leading lepton p_T , azimuthal angle difference between the two leptons, p_T and the transverse mass m_T of the $\ell\ell' + E_T^{\text{miss}}$ system, where m_T is calculated as $\sqrt{(E_T^\ell + E_T^{\ell'} + E_T^{\text{miss}})^2 - (\vec{p}_T^\ell + \vec{p}_T^{\ell'} + \vec{E}_T^{\text{miss}})^2}$ with \vec{p}_T^ℓ and $\vec{p}_T^{\ell'}$ being the transverse momentum vectors of the two leptons. The shapes of the Drell-Yan and top-quark distributions are taken from simulation and are scaled according to the data-driven estimates of the respective background. The W +jets background contribution is based on the data-driven method as described in Sec. VII C, and the non- WW diboson background contributions are estimated using simulation.

The fiducial and total cross sections for the WW process for the three individual decay channels are calculated using Eqs. (1) and (2), respectively. The results are shown in Table VI together with the SM predictions. Reasonable agreement is found between the measured cross sections and the theoretical predictions. For the total cross-section measurement, the relative statistical uncertainty is 12%, 8% and 5% for the ee , $\mu\mu$ and $e\mu$ channels, respectively, and the overall relative systematic uncertainty is 18%, 10% and 8%, respectively.

The combined total cross section from the three decay channels is determined by minimizing the negative log-likelihood function:

$$L = -\ln \prod_{i=1}^3 \frac{e^{-(\mu_s^i + \mu_b^i)} \times (\mu_s^i + \mu_b^i)^{N_{\text{obs}}^i}}{N_{\text{obs}}^i!} \quad (7)$$

where $i = 1, 2, 3$ runs over the three channels, μ_s^i and μ_b^i represent the expected WW signal and estimated back-

ground for the i -th channel, and N_{obs}^i represents the number of observed data events. The expected WW signal is computed as $\mu_s^i = \sigma_{WW} \times \text{BR} \times \mathcal{L} \times A_{WW}^i \times C_{WW}^i$, where A_{WW}^i and C_{WW}^i are the corresponding A_{WW} and C_{WW} in the i -th channel.

The combined total cross section is $\sigma_{WW} = 51.9 \pm 2.0$ (stat) ± 3.9 (syst) ± 2.0 (lumi) pb and is also shown in Table VI. The statistical uncertainty is estimated by taking the difference between the cross section at the minimum of the negative log-likelihood function and the cross section where the negative log-likelihood is 0.5 units above the minimum. Systematic uncertainties include all sources except luminosity and are taken into account by convolving the Poisson probability distributions for signal and background with the corresponding Gaussian distributions. Correlations between the signal and background uncertainties due to common sources of systematic uncertainties are taken into account in the definition of the likelihood.

IX. NORMALIZED DIFFERENTIAL FIDUCIAL CROSS SECTION

The measured leading lepton p_T distribution is unfolded to remove all experimental effects due to detector acceptance, resolution and lepton reconstruction efficiencies. The unfolded distribution provides a differential cross-section measurement in the fiducial phase space and allows a comparison with different theoretical models. A Bayesian unfolding technique [43] with three iterative steps is used in this analysis.

In unfolding of binned data, effects of the experimental acceptance and resolution are expressed in a response matrix, whose elements are the probability of an event in the i th bin at the generator level being reconstructed in the j th measured bin. The lepton p_T bins are chosen to be wider than the detector resolution to minimize migration effects and to maintain a sufficient number of events in each bin. The bin purity is found to be above 80%, implying small bin-to-bin migration effects.

The measured leading lepton p_T distribution in data is then corrected using a regularized inversion of the response matrix. Finally, the distribution is corrected for efficiency and acceptance calculated from simulation.

Figure 7 shows the normalized fiducial cross sections ($1/\sigma_{WW}^{\text{fid}} \times d\sigma_{WW}^{\text{fid}}/dp_T$) extracted in bins of the leading lepton p_T together with the SM predictions. The combined fiducial cross section σ_{WW}^{fid} is defined as the sum of the fiducial cross sections in each decay channel. The corresponding numerical values and the correlation matrix are shown in Table VII. The overall uncertainty is about 5% for leading lepton $p_T < 80$ GeV and increases to 40% for leading lepton $p_T > 140$ GeV. The dominant source of uncertainty on the normalized differential cross section is statistical and is determined from MC ensembles. Two thousand pseudoexperimental spectra are generated by fluctuating the content of each bin accord-

ing to a Poisson distribution with a mean that is equal to the bin content. The unfolding procedure is applied to each pseudoexperiment, and the root mean square of the results is taken as the statistical uncertainty.

Systematic uncertainties on the normalized differential cross section mainly arise from uncertainties which directly impact the shape of the leading lepton p_T spectrum, i.e. the lepton energy scale and resolution, identification and isolation efficiencies, jet and E_T^{miss} modeling, and background estimations. The systematic uncertainties are evaluated by varying the response matrix for each uncertainty, and combining the resulting changes in the unfolded spectrum. Uncertainties on the expected background shapes and contributions are treated in a similar way. The performance of the unfolding procedure was verified by comparing the true and unfolded spectrum generated using pseudo-experiments. The unfolded results are stable with different numbers of iterations used and different input distributions.

X. ANOMALOUS WWZ AND $WW\gamma$ COUPLINGS

The reconstructed leading lepton p_T distribution is used to set limits on anomalous WWZ and $WW\gamma$ TGCs. The Lorentz invariant Lagrangian describing the WWZ and $WW\gamma$ interactions [44] has 14 independent coupling parameters. Assuming electromagnetic gauge invariance and C and P conservations, the number of independent parameters reduces to five: g_1^Z , κ_Z , κ_γ , λ_Z and λ_γ . In the SM, the coupling parameters have the following values: $g_1^Z = \kappa_Z = \kappa_\gamma = 1$ and $\lambda_Z = \lambda_\gamma = 0$. Deviations of these coupling parameters from their SM values $\Delta g_1^Z (\equiv g_1^Z - 1)$, $\Delta \kappa_Z (\equiv \kappa_Z - 1)$, $\Delta \kappa_\gamma (\equiv \kappa_\gamma - 1)$, λ_Z and λ_γ , all equal to zero in the SM, would result in an increase of the production cross section and alter kinematic distributions, especially for large values of the leading lepton p_T . Since unitarity restricts the WWZ and $WW\gamma$ couplings to their SM values at asymptotically high energies, each of the couplings is usually modified by $\alpha(\hat{s}) = \alpha_0/(1 + \hat{s}/\Lambda^2)^2$, where α corresponds to one of the five couplings, α_0 is the value of the anomalous coupling at low energy, \hat{s} is the square of the invariant mass of the WW system, and Λ is the mass scale at which new physics affecting anomalous couplings would be introduced.

Limits on these couplings can be obtained under the assumption that the WWZ and $WW\gamma$ couplings are equal (denoted by the ‘‘equal couplings scenario’’) ($\Delta \kappa_Z = \Delta \kappa_\gamma$, $\lambda_Z = \lambda_\gamma$, and $g_1^Z = 1$). Two other different sets of parameters are also considered. One, motivated by $SU(2) \times U(1)$ gauge invariance, was used by the LEP collaborations (denoted by the ‘‘LEP scenario’’) [45] and assumes $\Delta \kappa_\gamma = (\cos^2 \theta_W / \sin^2 \theta_W)(\Delta g_1^Z - \Delta \kappa_Z)$, and $\lambda_Z = \lambda_\gamma$. The other one (denoted by the ‘‘HISZ scenario’’) [46] assumes $\Delta g_1^Z = \Delta \kappa_Z / (\cos^2 \theta_W - \sin^2 \theta_W)$, $\Delta \kappa_\gamma = 2\Delta \kappa_Z \cos^2 \theta_W / (\cos^2 \theta_W - \sin^2 \theta_W)$, and $\lambda_Z = \lambda_\gamma$. Due to the constraints mentioned above, the number of

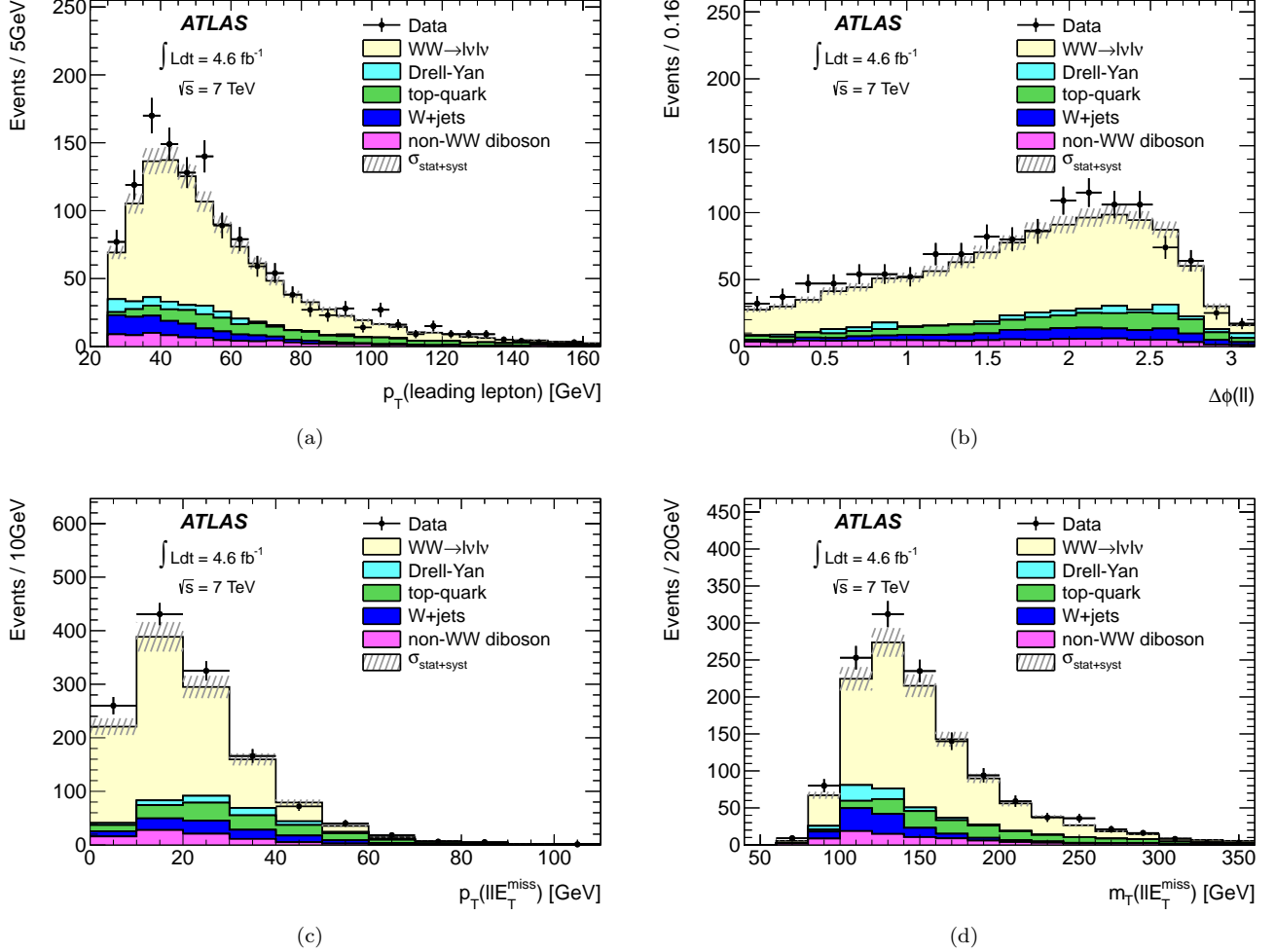


FIG. 6: Distributions for WW candidates with all selection criteria applied and combining ee , $\mu\mu$ and $e\mu$ channels: (a) leading lepton p_T (b) opening angle between the two leptons ($\Delta\phi(\ell\ell')$), (c) p_T and (d) m_T of the $\ell\ell' + E_T^{\text{miss}}$ system. The points represent data. The statistical and systematic uncertainties are shown as grey bands. The stacked histograms are from MC predictions except the background contributions from the Drell-Yan, top-quark and W +jets processes, which are obtained from data-driven methods. The prediction of the SM WW contribution is normalized to the inclusive theoretical cross section of 44.7 pb.

	ee	$\mu\mu$	$e\mu$	Combined
Data	174	330	821	1325
WW	$100 \pm 2 \pm 9$	$186 \pm 2 \pm 15$	$538 \pm 3 \pm 45$	$824 \pm 4 \pm 69$
Top	$22 \pm 12 \pm 3$	$32 \pm 14 \pm 5$	$87 \pm 23 \pm 13$	$141 \pm 30 \pm 22$
W +jets	$21 \pm 1 \pm 11$	$7 \pm 1 \pm 3$	$70 \pm 2 \pm 31$	$98 \pm 2 \pm 43$
Drell-Yan	$12 \pm 3 \pm 3$	$34 \pm 6 \pm 10$	$5 \pm 2 \pm 1$	$51 \pm 7 \pm 12$
Other dibosons	$13 \pm 1 \pm 2$	$21 \pm 1 \pm 2$	$44 \pm 2 \pm 6$	$78 \pm 2 \pm 10$
Total background	$68 \pm 12 \pm 13$	$94 \pm 15 \pm 13$	$206 \pm 24 \pm 35$	$369 \pm 31 \pm 53$
Total expected	$169 \pm 12 \pm 16$	$280 \pm 16 \pm 20$	$744 \pm 24 \pm 57$	$1192 \pm 31 \pm 87$

TABLE V: Summary of observed and expected numbers of signal and background events in three individual channels and their combination (contributions from SM Higgs, VBF and DPS processes are not included). The prediction of the SM WW contribution is normalized to the inclusive theoretical cross section of 44.7 pb. The first and second uncertainties represent the statistical and systematic uncertainties, respectively.

	Measured σ_{WW}^{fid} (fb)	Predicted σ_{WW}^{fid} (fb)	Measured σ_{WW} (pb)	Predicted σ_{WW} (pb)
ee	$56.4 \pm 6.8 \pm 9.8 \pm 2.2$	54.6 ± 3.7	$46.9 \pm 5.7 \pm 8.2 \pm 1.8$	$44.7^{+2.1}_{-1.9}$
$\mu\mu$	$73.9 \pm 5.9 \pm 6.9 \pm 2.9$	58.9 ± 4.0	$56.7 \pm 4.5 \pm 5.5 \pm 2.2$	$44.7^{+2.1}_{-1.9}$
$e\mu$	$262.3 \pm 12.3 \pm 20.7 \pm 10.2$	231.4 ± 15.7	$51.1 \pm 2.4 \pm 4.2 \pm 2.0$	$44.7^{+2.1}_{-1.9}$
Combined	$51.9 \pm 2.0 \pm 3.9 \pm 2.0$	$44.7^{+2.1}_{-1.9}$

TABLE VI: The measured fiducial and total cross sections for the three channels separately and also the total cross section for the combined channels, compared with theoretical predictions. The fiducial cross sections include the branching ratio for both W bosons decaying into $e\nu$ or $\mu\nu$ (including decays through τ leptons with additional neutrinos). For the measured cross sections, the first uncertainty is statistical, the second is systematic without luminosity uncertainty and the third is the luminosity uncertainty.

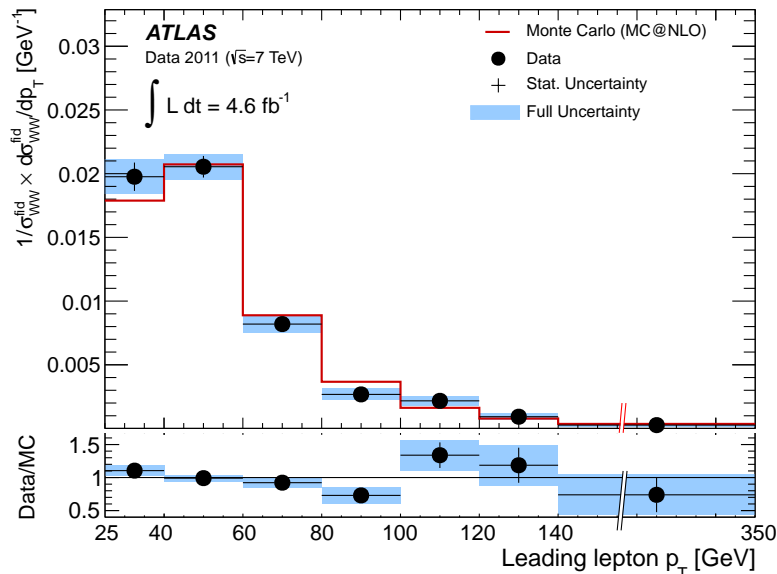


FIG. 7: The normalized differential WW fiducial cross section as a function of the leading lepton p_T compared to the SM prediction.

independent parameters is only two for the Equal Couplings scenario and the HISZ scenario, and three for the LEP scenario. Limits are also set assuming no relationships among these five parameters.

A reweighting method is applied to SM WW events generated with MC@NLO and processed through the full detector simulation to obtain the leading lepton p_T distribution with anomalous couplings. The reweighting method uses an event weight to predict the rate with which a given event would be generated if anomalous couplings were present. The event weight is the ratio of the squared matrix elements with and without anomalous couplings i.e., $|\mathcal{M}|^2/|\mathcal{M}|_{\text{SM}}^2$, where $|\mathcal{M}|^2$ is the matrix element squared in the presence of anomalous couplings and $|\mathcal{M}|_{\text{SM}}^2$ is the matrix element squared in the SM. The event generator BHO [47] is used for the calculation of the two matrix elements. Generator-level comparisons of WW production between MC@NLO and BHO with all anomalous couplings set to zero are performed and consistent results are obtained. Samples with different sets of anomalous couplings are generated and the ratio of

the leading lepton p_T distribution to the SM prediction is parameterized as a function of the input anomalous coupling parameters. This function is then used to interpolate the leading lepton p_T distribution for any given anomalous couplings. To verify the reweighting method, the event weights for a given set of anomalous couplings are calculated and applied to events generated with BHO assuming no anomalous couplings. The reweighted distributions are compared to those predicted by the BHO generator, and good agreement is observed for the inclusive cross section and for the kinematic distributions as shown in Fig. 8(a).

Figure 8(b) compares the reconstructed leading lepton p_T spectrum in data with that from the sum of expected signal and background contributions. The predicted leading lepton p_T distributions for three different anomalous TGC values are also shown. Events at high values of the leading lepton p_T distribution are sensitive to anomalous TGCs. Limits on anomalous TGCs are obtained by forming a likelihood test incorporating the observed number of candidate events, the expected signal as

Leading lepton p_T [GeV]	[25,40]	[40,60]	[60,80]	[80,100]	[100,120]	[120,140]	[140, 350]
Weighted bin center [GeV]	33.6	50.2	70.2	89.1	107.1	127.5	180.4
$1/\sigma_{WW}^{\text{fid}} \times d\sigma_{WW}^{\text{fid}}/dp_T$ [GeV $^{-1}$]	2.0×10^{-2}	2.1×10^{-2}	8.2×10^{-3}	2.7×10^{-3}	2.2×10^{-3}	9.5×10^{-4}	6.2×10^{-5}
Relative uncertainty	6.7%	4.8%	8.2%	17.0%	17.1%	25.5%	41.0%
Correlation	1	-0.43	-0.33	-0.27	-0.27	-0.13	-0.29
		1	-0.29	-0.29	-0.23	-0.30	-0.15
			1	-0.01	-0.04	0.02	0.03
				1	0.21	0.11	0.14
					1	0.23	0.11
						1	0.27
							1

TABLE VII: Normalized fiducial cross section together with the overall uncertainty in bins of the leading lepton p_T . The weighted bin center is calculated as the cross-section-weighted average of the leading lepton p_T in each bin derived from MC@NLO and **gg2WW**. The correlation coefficients between different leading lepton p_T bins are also shown. Only half of the symmetric correlation matrix is presented.

a function of anomalous TGCs and the estimated number of background events in each p_T bin. The systematic uncertainties are included in the likelihood function as nuisance parameters with correlations taken into account. The 95% confidence level (C.L.) intervals on anomalous TGC parameters include all values of anomalous TGC parameters for which the negative log-likelihood functions increase by no more than 1.92 (2.99) units above the minimum for the one (two)-dimensional case.

Table VIII shows expected and observed 95% C.L. limits on anomalous WWZ and $WW\gamma$ couplings for three scenarios (LEP, HISZ and equal couplings) with two scales, $\Lambda = 6$ TeV and $\Lambda = \infty$. The $\Lambda = 6$ TeV scale is chosen as it is the rounded largest value which still preserves unitarity for all extracted anomalous TGC limits of this analysis. Table IX shows the results assuming no relationships between the five couplings. Figure 9 shows the two-dimensional 95% C.L. contour limits of $\Delta\kappa_Z$ vs. λ_Z , $\Delta\kappa_Z$ vs. Δg_1^Z , $\Delta\kappa_\gamma$ vs. Δg_1^Z and λ_Z vs. Δg_1^Z for the LEP scenario. Except for the anomalous coupling parameter(s) under study, all other parameters are set to their SM values.

Limits in the LEP scenario are compared with limits obtained from the CMS [13], CDF [10], DØ [10] and LEP [9] experiments in Fig. 10. Due to higher energy and higher WW production cross section at the LHC, the limits obtained in this paper are better than the Tevatron results and approach the precision of the combined limits from the LEP experiments.

XI. CONCLUSION

The WW production cross section in pp collisions at $\sqrt{s} = 7$ TeV is measured using 4.6 fb^{-1} of data collected with the ATLAS detector at the LHC. The measurement is conducted using the $WW \rightarrow \ell\nu\ell'\nu'$ ($\ell, \ell' = e, \mu$) channels including decays through τ leptons with additional neutrinos. In total 1325 candidates are selected with an estimated background of 369 ± 61 events for the three decay channels into ee , $\mu\mu$ and $e\mu$ final states. The

combined production cross section $\sigma(pp \rightarrow WW + X)$ is 51.9 ± 2.0 (stat) ± 3.9 (syst) ± 2.0 (lumi) pb, compatible with the SM NLO prediction of $44.7^{+2.1}_{-1.9}$ pb. The overall statistical and systematic uncertainty is 9% and an improvement of 30% has been achieved compared with the previous ATLAS measurement [12]. The results presented supersede the previous results obtained with 1 fb^{-1} of data. Cross sections are also measured in a fiducial phase space.

The leading lepton p_T distribution is unfolded to obtain the normalized differential fiducial cross section in the chosen fiducial phase space. Reasonable agreement is observed between the measured distribution and theoretical predictions using MC@NLO.

Anomalous WWZ and $WW\gamma$ couplings are probed using the reconstructed leading lepton p_T distribution of the selected WW events. With the assumption that WWZ and $WW\gamma$ couplings are equal, 95% C.L. limits are set on $\Delta\kappa_Z$ and λ_Z in the intervals $[-0.061, 0.093]$ and $[-0.062, 0.065]$ respectively for a scale of $\Lambda = 6$ TeV. Limits on these anomalous couplings are also reported for three other scenarios and two scales $\Lambda = 6$ TeV and $\Lambda = \infty$. The limits on anomalous TGCs obtained approach the precision of the combined limits from the four LEP experiments.

XII. ACKNOWLEDGMENTS

We thank CERN for the very successful operation of the LHC, as well as the support staff from our institutions without whom ATLAS could not be operated efficiently.

We acknowledge the support of ANPCyT, Argentina; YerPhI, Armenia; ARC, Australia; BMWF and FWF, Austria; ANAS, Azerbaijan; SSTC, Belarus; CNPq and FAPESP, Brazil; NSERC, NRC and CFI, Canada; CERN; CONICYT, Chile; CAS, MOST and NSFC, China; COLCIENCIAS, Colombia; MSMT CR, MPO CR and VSC CR, Czech Republic; DNRF, DNSRC and Lundbeck Foundation, Denmark; EPLANET and ERC, European Union; IN2P3-CNRS,

Scenario	Parameter	Expected	Observed	Expected	Observed
		($\Lambda = 6$ TeV)	($\Lambda = 6$ TeV)	($\Lambda = \infty$)	($\Lambda = \infty$)
LEP	$\Delta\kappa_Z$	[-0.043, 0.040]	[-0.045, 0.044]	[-0.039, 0.039]	[-0.043, 0.043]
	$\lambda_Z = \lambda_\gamma$	[-0.060, 0.062]	[-0.062, 0.065]	[-0.060, 0.056]	[-0.062, 0.059]
	Δg_1^Z	[-0.034, 0.062]	[-0.036, 0.066]	[-0.038, 0.047]	[-0.039, 0.052]
HISZ	$\Delta\kappa_Z$	[-0.040, 0.054]	[-0.039, 0.057]	[-0.037, 0.054]	[-0.036, 0.057]
	$\lambda_Z = \lambda_\gamma$	[-0.064, 0.062]	[-0.066, 0.065]	[-0.061, 0.060]	[-0.063, 0.063]
Equal Couplings	$\Delta\kappa_Z$	[-0.058, 0.089]	[-0.061, 0.093]	[-0.057, 0.080]	[-0.061, 0.083]
	$\lambda_Z = \lambda_\gamma$	[-0.060, 0.062]	[-0.062, 0.065]	[-0.060, 0.056]	[-0.062, 0.059]

TABLE VIII: The 95% C.L. expected and observed limits on anomalous TGCs in the LEP, HISZ and Equal Couplings scenarios. Except for the coupling under study, all other anomalous couplings are set to zero. The results are shown for two scales $\Lambda = 6$ TeV and $\Lambda = \infty$.

Parameter	Expected	Observed
	($\Lambda = \infty$)	($\Lambda = \infty$)
$\Delta\kappa_Z$	[-0.077, 0.086]	[-0.078, 0.092]
λ_Z	[-0.071, 0.069]	[-0.074, 0.073]
λ_γ	[-0.144, 0.135]	[-0.152, 0.146]
Δg_1^Z	[-0.449, 0.546]	[-0.373, 0.562]
$\Delta\kappa_\gamma$	[-0.128, 0.176]	[-0.135, 0.190]

TABLE IX: The 95% C.L. expected and observed limits on anomalous TGCs assuming no relationships between these five coupling parameters for $\Lambda = \infty$. Except for the coupling under study, all other anomalous couplings are set to zero.

CEA-DSM/IRFU, France; GNSF, Georgia; BMBF, DFG, HGF, MPG and AvH Foundation, Germany; GSRT, Greece; ISF, MINERVA, GIF, DIP and Benozziyo Center, Israel; INFN, Italy; MEXT and JSPS, Japan; CNRST, Morocco; FOM and NWO, Netherlands; BRF and RCN, Norway; MNiSW, Poland; GRICES and FCT, Portugal; MERYM (MECTS), Romania; MES of Russia and ROSATOM, Russian Federation; JINR; MSTD, Serbia; MSSR, Slovakia; ARRS and MVZT, Slovenia; DST/NRF, South Africa; MICINN, Spain; SRC and Wallenberg Foundation, Sweden; SER, SNSF and Cantons of Bern and Geneva, Switzerland; NSC, Taiwan;

TAEK, Turkey; STFC, the Royal Society and Leverhulme Trust, United Kingdom; DOE and NSF, United States of America.

The crucial computing support from all WLCG partners is acknowledged gratefully, in particular from CERN and the ATLAS Tier-1 facilities at TRIUMF (Canada), NDGF (Denmark, Norway, Sweden), CC-IN2P3 (France), KIT/GridKA (Germany), INFN-CNAF (Italy), NL-T1 (Netherlands), PIC (Spain), ASGC (Taiwan), RAL (UK) and BNL (USA) and in the Tier-2 facilities worldwide.

-
- [1] K. Hagiwara, S. Ishihara, R. Szalapski, and D. Zeppenfeld, *Phys. Rev. D* **48**, 2182 (1993).
- [2] J. C. Pati and A. Salam, *Phys. Rev. D* **10**, 275 (1974); **11** 703(E) (1975); G. Altarelli, B. Mele, and M. Ruiz-Altaba, *Z. Phys. C* **45**, 109 (1989); **47**, 676(E) (1990); H. Davoudiasl, J. L. Hewett, and T. G. Rizzo, *Phys. Rev. D* **63**, 075004 (2001); H. He *et al.*, *Phys. Rev. D* **78**, 031701 (2008).
- [3] L. Evans and P. Bryant (eds) *JINST* **3**, S08001 (2008).
- [4] ATLAS Collaboration, *Phys. Lett. B* **716**, 1 (2012); CMS Collaboration, *Phys. Lett. B* **716**, 30 (2012).
- [5] J. M. Campbell, R. K. Ellis, and D. J. Rainwater, *Phys. Rev. D* **68**, 094021 (2003). Version 6.2 is used.
- [6] P. M. Nadolsky *et al.*, *Phys. Rev. D* **78**, 013004 (2008).
- [7] J. M. Campbell, J. W. Huston and W. J. Stirling, *Rept. Prog. Phys.* **70**, 89 (2007).
- [8] A. Del Fabro and D. Treleani, *Phys. Rev. D* **63**, 057901 (2001).
- [9] S. Schael *et al.* (ALEPH Collaboration), *Phys. Lett. B* **614**, 7 (2005); J. Abdallah *et al.* (DELPHI Collaboration), *Eur. Phys. J. C* **54**, 345 (2008); P. Achard *et al.* (L3 Collaboration), *Phys. Lett. B* **586**, 151 (2004); G. Abbiendi *et al.* (OPAL Collaboration), *Eur. Phys. J. C* **33**, 463 (2004).
- [10] T. Aaltonen *et al.* (CDF Collaboration), *Phys. Rev. Lett.* **104**, 201801 (2010); V. Abazov *et al.* (D0 Collaboration), *Phys. Rev. Lett.* **103**, 191801 (2009); *ibid.*, *Phys. Rev. D* **80**, 053012 (2009).
- [11] ATLAS Collaboration, *Phys. Rev. Lett.* **107**, 041802 (2011).
- [12] ATLAS Collaboration, *Phys. Lett. B* **712**, 289 (2012).
- [13] CMS Collaboration, *Phys. Lett. B* **699**, 25 (2011).
- [14] ATLAS Collaboration, *Eur. Phys. J. C* **71**, 1630 (2011).
- [15] The ATLAS reference system is a Cartesian right-handed coordinate system with its origin at the nominal interaction point (IP) in the center of the detector and the z -axis

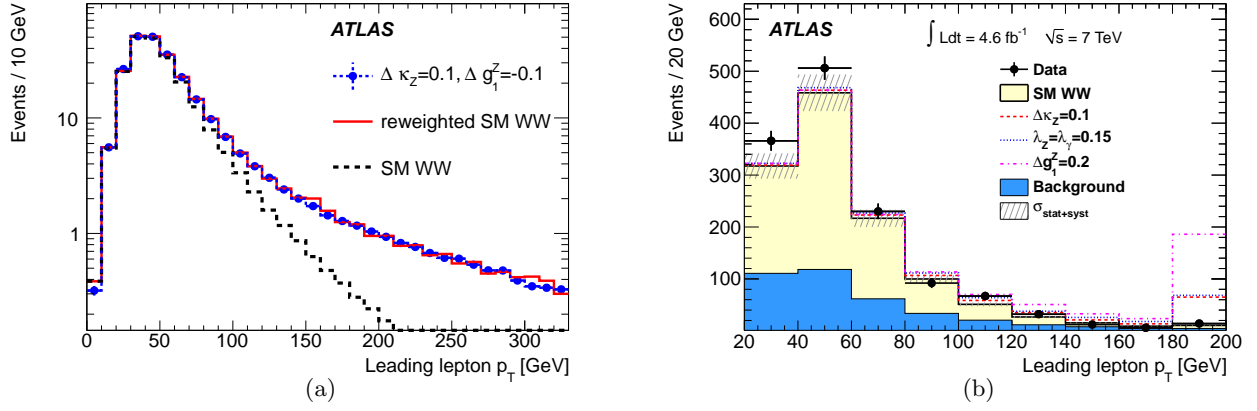


FIG. 8: (a) The leading lepton p_T spectrum from the SM prediction, compared with a prediction using BHO and by reweighting the SM prediction assuming the LEP scenario with $\Delta\kappa_z = 0.1$, $\lambda_z = 0$, $\Delta g_1^Z = -0.1$ and $\Lambda = \infty$; (b) The reconstructed leading lepton p_T spectrum in data and sum of MC signal and background for the SM prediction and for three different anomalous TGC predictions. The shaded band corresponds to the total statistical and systematic uncertainties. The rightmost bin shows the sum of all events with leading lepton p_T above 180 GeV.

along the beam direction. The x -axis points from the IP to the center of the LHC ring, and the y -axis points upward. Cylindrical coordinates (r, ϕ) are used in the transverse plane, ϕ being the azimuthal angle around the beam direction. The pseudorapidity is defined in terms of the polar angle θ as $\eta = -\ln \tan(\theta/2)$. Transverse momentum (p_T) is defined relative to the beam axis.

- [16] ATLAS Collaboration, JINST **3**, S08003 (2008).
 [17] ATLAS Collaboration, Eur. Phys. J. C **70**, 823 (2010).
 [18] S. Agostinelli *et al.*, Nucl. Instr. Meth. A **506**, 250 (2003).
 [19] S. Frixione and B. R. Webber, JHEP **0206** (2002) 029.
 [20] T. Binoth, M. Ciccolini, N. Kauer, and M. Krämer, JHEP **0612** (2006) 046.
 [21] G. Corcella *et al.*, JHEP **0101** (2001) 010.
 [22] J.M. Butterworth, J.R. Forshaw, and M.H. Seymour, Z. Phys. C **72**, 637 (1996).
 [23] M.L. Mangano, F. Piccinini, A.D. Polosa, M. Moretti, and R. Pittau, JHEP **07** (2003) 001.
 [24] T. Stelzer and W. F. Long, Comput. Phys. Commun. **81**, 357 (1994); J. Alwall, M. Herquet, F. Maltoni, O. Mattelaer, T. Stelzer, JHEP **6** (2011) 128.
 [25] B.P. Kersevan and E. Richter-Was, arXiv:hep-ph/0405247.
 [26] S. Jadach, Z. Was, R. Decker, and J.H. Kuhn, Comput. Phys. Commun. **76**, 361 (1993).
 [27] P. Golonka and Z. Was, Eur. Phys. J. C **45**, 97 (2006).
 [28] R. Gavin, Y. Li, F. Petriello, and S. Quackenbush, Comput. Phys. Commun. **182**, 2388 (2011).
 [29] S. Moch and P. Uwer, Phys. Rev. D **78**, 034003 (2008).
 [30] ATLAS Collaboration, Eur. Phys. J. C **72**, 1909 (2012).
 [31] ATLAS Collaboration, Phys. Lett. B **707**, 438 (2012).
 [32] M. Cacciari, G. P. Salam, and G. Soyez, JHEP **0804** (2008) 063.
 [33] ATLAS Collaboration, ATLAS-CONF-2011-032, available at <http://cdsweb.cern.ch/record/1337782>.
 [34] ATLAS Collaboration, ATLAS-CONF-2011-102, available at <http://cdsweb.cern.ch/record/1369219>.
 [35] J.M. Campbell, E. Castaneda-Miranda, Y. Fang, N. Kauer, B. Mellado, S. L. Wu, Phys. Rev. D **80**, 054023 (2009).
 [36] I.W. Stewart and F.J. Tackmann, Phys. Rev. D **85**, 034011 (2012).
 [37] T. Sjöstrand, S. Mrenna, and P. Skands, JHEP **0605** (2006) 026.
 [38] A. D. Martin, W. J. Stirling, R. S. Thorne, and G. Watt, Eur. Phys. J. C **63**, 189 (2009).
 [39] ATLAS Collaboration, Eur. Phys. J. C **72**, 1849 (2012); ATLAS Collaboration, ATLAS-CONF-2012-099, available at <https://cdsweb.cern.ch/record/1462601>.
 [40] ATLAS Collaboration, JHEP **12** (2010), 060.
 [41] ATLAS Collaboration, Eur. Phys. J. C **73**, 2304 (2013).
 [42] ATLAS Collaboration, Eur. Phys. J. C **72**, 1844 (2012).
 [43] G. D'Agostini, Nucl. Instr. Meth. A **362**, 487 (1995).
 [44] K. Hagiwara, R. D. Peccei, D. Zeppenfeld, and K. Hikasa, Nucl. Phys. B **282**, 253 (1987).
 [45] G. Gounaris *et al.*, arXiv:hep-ph/9601233.
 [46] K. Hagiwara, S. Ishihara, R. Szalapski, and D. Zeppenfeld, Phys. Lett. B **283**, 353 (1992); *ibid.*, Phys. Rev. D **48**, 2182 (1993).
 [47] U. Baur, T. Han, and J. Ohnemus, Phys. Rev. D **53**, 1098 (1996).

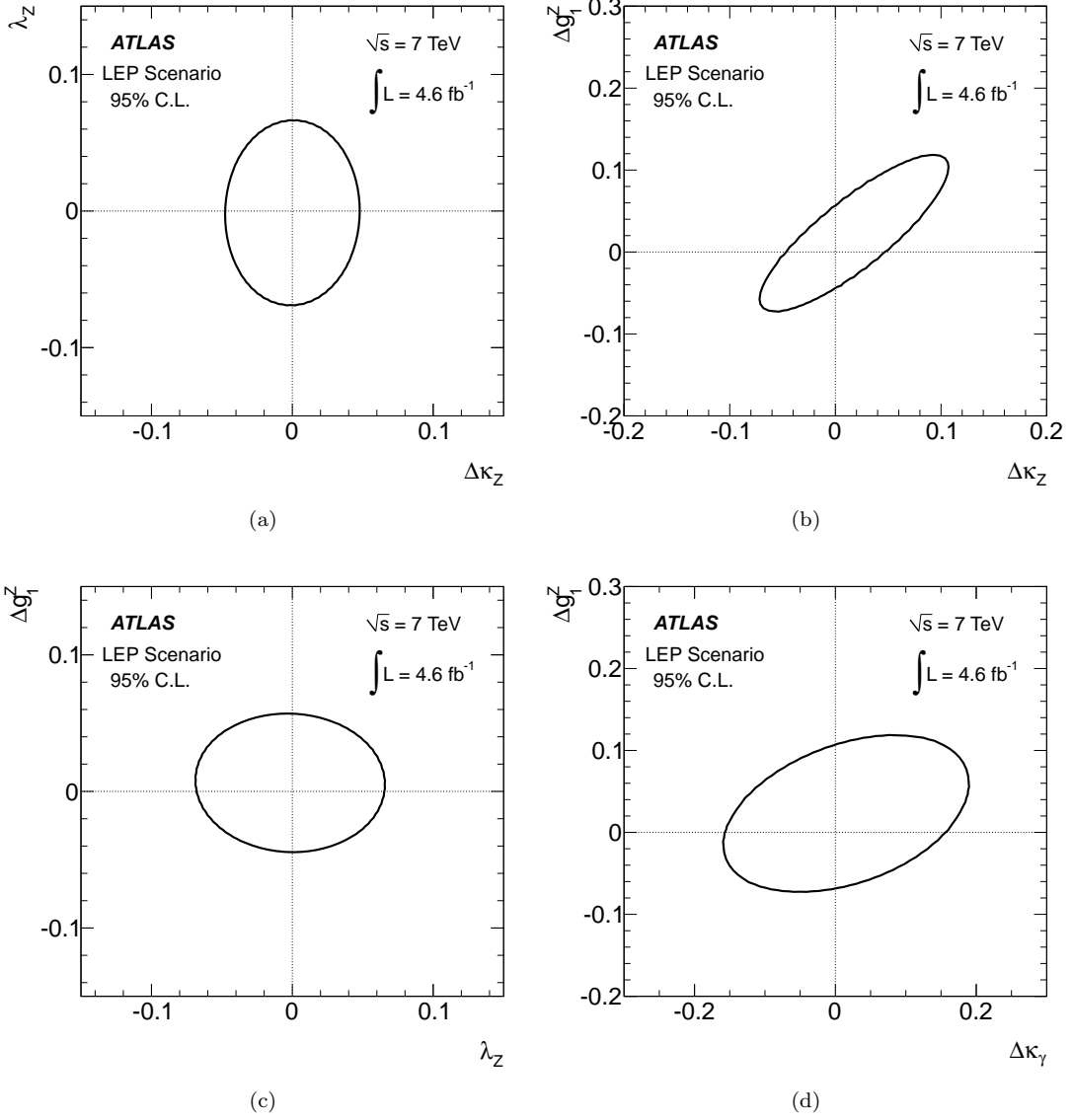


FIG. 9: Two-dimensional 95% C.L. contour limits on (a) λ_Z vs $\Delta\kappa_Z$, (b) Δg_1^Z vs $\Delta\kappa_Z$, (c) Δg_1^Z vs λ_Z and (d) Δg_1^Z vs $\Delta\kappa_\gamma$ for the LEP scenario for $\Lambda = \infty$. Except for the two parameters under study, all other anomalous couplings are set to zero.

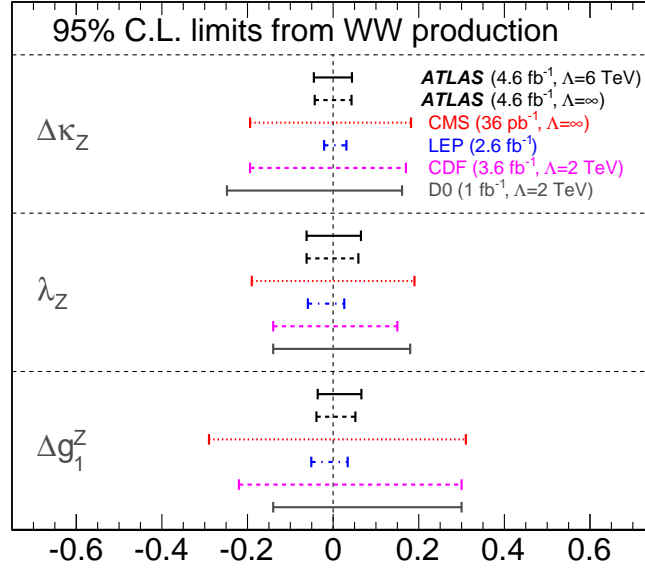


FIG. 10: Comparison of anomalous TGC limits from ATLAS, CMS, CDF, DØ and LEP experiments for the LEP scenario. The $\Delta\kappa_Z$ result in the LEP scenario from CMS was obtained using the $\Delta\kappa_\gamma$ limit in the HISZ scenario [13] and inserting it in the LEP scenario assuming $\Delta g_1^Z = 0$.

The ATLAS Collaboration

G. Aad⁴⁸, T. Abajyan²¹, B. Abbott¹¹¹, J. Abdallah¹², S. Abdel Khalek¹¹⁵, A.A. Abdelalim⁴⁹, O. Abdinov¹¹,
 R. Aben¹⁰⁵, B. Abi¹¹², M. Abolins⁸⁸, O.S. AbouZeid¹⁵⁸, H. Abramowicz¹⁵³, H. Abreu¹³⁶, B.S. Acharya^{164a,164b},
 L. Adamczyk³⁸, D.L. Adams²⁵, T.N. Addy⁵⁶, J. Adelman¹⁷⁶, S. Adomeit⁹⁸, P. Adragna⁷⁵, T. Adye¹²⁹, S. Aefsky²³,
 J.A. Aguilar-Saavedra^{124b,a}, M. Agustoni¹⁷, M. Aharrouche⁸¹, S.P. Ahlen²², F. Ahles⁴⁸, A. Ahmad¹⁴⁸, M. Ahsan⁴¹,
 G. Aielli^{133a,133b}, T. Akdogan^{19a}, T.P.A. Åkesson⁷⁹, G. Akimoto¹⁵⁵, A.V. Akimov⁹⁴, M.S. Alam², M.A. Alam⁷⁶,
 J. Albert¹⁶⁹, S. Albrand⁵⁵, M. Aleksa³⁰, I.N. Aleksandrov⁶⁴, F. Alessandria^{89a}, C. Alexa^{26a}, G. Alexander¹⁵³,
 G. Alexandre⁴⁹, T. Alexopoulos¹⁰, M. Alhroob^{164a,164c}, M. Aliev¹⁶, G. Alimonti^{89a}, J. Alison¹²⁰,
 B.M.M. Allbrooke¹⁸, P.P. Allport⁷³, S.E. Allwood-Spiers⁵³, J. Almond⁸², A. Aloisio^{102a,102b}, R. Alon¹⁷²,
 A. Alonso⁷⁹, F. Alonso⁷⁰, A. Altheimer³⁵, B. Alvarez Gonzalez⁸⁸, M.G. Alviggi^{102a,102b}, K. Amako⁶⁵, C. Amelung²³,
 V.V. Ammosov^{128,*}, S.P. Amor Dos Santos^{124a}, A. Amorim^{124a,b}, N. Amram¹⁵³, C. Anastopoulos³⁰, L.S. Ancu¹⁷,
 N. Andari¹¹⁵, T. Andeen³⁵, C.F. Anders^{58b}, G. Anders^{58a}, K.J. Anderson³¹, A. Andreazza^{89a,89b}, V. Andrei^{58a},
 M-L. Andrieux⁵⁵, X.S. Anduaga⁷⁰, S. Angelidakis⁹, P. Anger⁴⁴, A. Angerami³⁵, F. Anghinolfi³⁰, A. Anisenkov¹⁰⁷,
 N. Anjos^{124a}, A. Annovi⁴⁷, A. Antonaki⁹, M. Antonelli⁴⁷, A. Antonov⁹⁶, J. Antos^{144b}, F. Anulli^{132a}, M. Aoki¹⁰¹,
 S. Aoun⁸³, L. Aperio Bella⁵, R. Apolle^{118,c}, G. Arabidze⁸⁸, I. Aracena¹⁴³, Y. Arai⁶⁵, A.T.H. Arce⁴⁵, S. Arfaoui¹⁴⁸,
 J-F. Arguin⁹³, E. Arik^{19a,*}, M. Arik^{19a}, A.J. Armbruster⁸⁷, O. Arnaez⁸¹, V. Arnal⁸⁰, C. Arnault¹¹⁵,
 A. Artamonov⁹⁵, G. Artoni^{132a,132b}, D. Arutinov²¹, S. Asai¹⁵⁵, S. Ask²⁸, B. Åsman^{146a,146b}, L. Asquith⁶,
 K. Assamagan²⁵, A. Astbury¹⁶⁹, M. Atkinson¹⁶⁵, B. Aubert⁵, E. Auge¹¹⁵, K. Augsten¹²⁷, M. Aourousseau^{145a},
 G. Avolio³⁰, R. Avramidou¹⁰, D. Axen¹⁶⁸, G. Azuelos^{93,d}, Y. Azuma¹⁵⁵, M.A. Baak³⁰, G. Baccaglioni^{89a},
 C. Bacci^{134a,134b}, A.M. Bach¹⁵, H. Bachacou¹³⁶, K. Bachas³⁰, M. Backes⁴⁹, M. Backhaus²¹, J. Backus Mayes¹⁴³,
 E. Badescu^{26a}, P. Bagnaia^{132a,132b}, S. Bahinipati³, Y. Bai^{33a}, D.C. Bailey¹⁵⁸, T. Bain¹⁵⁸, J.T. Baines¹²⁹,
 O.K. Baker¹⁷⁶, M.D. Baker²⁵, S. Baker⁷⁷, P. Balek¹²⁶, E. Banas³⁹, P. Banerjee⁹³, Sw. Banerjee¹⁷³, D. Banfi³⁰,
 A. Bangert¹⁵⁰, V. Bansal¹⁶⁹, H.S. Bansil¹⁸, L. Barak¹⁷², S.P. Baranov⁹⁴, A. Barbaro Galtieri¹⁵, T. Barber⁴⁸,
 E.L. Barberio⁸⁶, D. Barberis^{50a,50b}, M. Barbero²¹, D.Y. Bardin⁶⁴, T. Barillari⁹⁹, M. Barisonzi¹⁷⁵, T. Barklow¹⁴³,
 N. Barlow²⁸, B.M. Barnett¹²⁹, R.M. Barnett¹⁵, A. Baroncelli^{134a}, G. Barone⁴⁹, A.J. Barr¹¹⁸, F. Barreiro⁸⁰,
 J. Barreiro Guimarães da Costa⁵⁷, P. Barrillon¹¹⁵, R. Bartoldus¹⁴³, A.E. Barton⁷¹, V. Bartsch¹⁴⁹, A. Basye¹⁶⁵,
 R.L. Bates⁵³, L. Batkova^{144a}, J.R. Batley²⁸, A. Battaglia¹⁷, M. Battistin³⁰, F. Bauer¹³⁶, H.S. Bawa^{143,e}, S. Beale⁹⁸,
 T. Beau⁷⁸, P.H. Beauchemin¹⁶¹, R. Beccherle^{50a}, P. Bechtel²¹, H.P. Beck¹⁷, A.K. Becker¹⁷⁵, S. Becker⁹⁸,
 M. Beckingham¹³⁸, K.H. Becks¹⁷⁵, A.J. Beddall^{19c}, A. Beddall^{19c}, S. Bedikian¹⁷⁶, V.A. Bednyakov⁶⁴, C.P. Bee⁸³,
 L.J. Beamster¹⁰⁵, M. Begel²⁵, S. Behar Harpaz¹⁵², P.K. Behera⁶², M. Beimforde⁹⁹, C. Belanger-Champagne⁸⁵,
 P.J. Bell⁴⁹, W.H. Bell⁴⁹, G. Bella¹⁵³, L. Bellagamba^{20a}, M. Bellomo³⁰, A. Belloni⁵⁷, O. Beloborodova^{107,f},
 K. Belotskiy⁹⁶, O. Beltramello³⁰, O. Benary¹⁵³, D. Bencheikroun^{135a}, K. Bendtz^{146a,146b}, N. Benekos¹⁶⁵,
 Y. Benhammou¹⁵³, E. Benhar Noccioli⁴⁹, J.A. Benitez Garcia^{159b}, D.P. Benjamin⁴⁵, M. Benoit¹¹⁵, J.R. Bensinger²³,
 K. Benslama¹³⁰, S. Bentvelsen¹⁰⁵, D. Berge³⁰, E. Bergeas Kuutmann⁴², N. Berger⁵, F. Berghaus¹⁶⁹,
 E. Berglund¹⁰⁵, J. Beringer¹⁵, P. Bernat⁷⁷, R. Bernhard⁴⁸, C. Bernius²⁵, T. Berry⁷⁶, C. Bertella⁸³, A. Bertin^{20a,20b},
 F. Bertolucci^{122a,122b}, M.I. Besana^{89a,89b}, G.J. Besjes¹⁰⁴, N. Besson¹³⁶, S. Bethke⁹⁹, W. Bhimji⁴⁶, R.M. Bianchi³⁰,
 L. Bianchini²³, M. Bianco^{72a,72b}, O. Biebel⁹⁸, S.P. Bieniek⁷⁷, K. Bierwagen⁵⁴, J. Biesiada¹⁵, M. Biglietti^{134a},
 H. Bilokon⁴⁷, M. Bindi^{20a,20b}, S. Binet¹¹⁵, A. Bingul^{19c}, C. Bini^{132a,132b}, C. Biscarat¹⁷⁸, B. Bittner⁹⁹, K.M. Black²²,
 R.E. Blair⁶, J.-B. Blanchard¹³⁶, G. Blanchot³⁰, T. Blazek^{144a}, I. Bloch⁴², C. Blocker²³, J. Blocki³⁹, A. Blondel⁴⁹,
 W. Blum⁸¹, U. Blumenschein⁵⁴, G.J. Bobbink¹⁰⁵, V.B. Bobrovnikov¹⁰⁷, S.S. Bocchetta⁷⁹, A. Bocchi⁴⁵,
 C.R. Boddy¹¹⁸, M. Boehler⁴⁸, J. Boek¹⁷⁵, N. Boelaert³⁶, J.A. Bogaerts³⁰, A. Bogdanchikov¹⁰⁷, A. Bogouch^{90,*},
 C. Bohm^{146a}, J. Bohm¹²⁵, V. Boisvert⁷⁶, T. Bold³⁸, V. Boldea^{26a}, N.M. Bolnet¹³⁶, M. Bomben⁷⁸, M. Bona⁷⁵,
 M. Boonekamp¹³⁶, S. Bordon⁷⁸, C. Borer¹⁷, A. Borisov¹²⁸, G. Borissov⁷¹, I. Borjanovic^{13a}, M. Borri⁸², S. Borroni⁸⁷,
 J. Bortfeldt⁹⁸, V. Bortolotto^{134a,134b}, K. Bos¹⁰⁵, D. Boscherini^{20a}, M. Bosman¹², H. Boterenbrood¹⁰⁵,
 J. Bouchami⁹³, J. Boudreau¹²³, E.V. Bouhova-Thacker⁷¹, D. Boumediene³⁴, C. Bourdarios¹¹⁵, N. Bousson⁸³,
 A. Boveia³¹, J. Boyd³⁰, I.R. Boyko⁶⁴, I. Bozovic-Jelisavcic^{13b}, J. Bracinik¹⁸, P. Branchini^{134a}, A. Brandt⁸,
 G. Brandt¹¹⁸, O. Brandt⁵⁴, U. Bratzler¹⁵⁶, B. Brau⁸⁴, J.E. Brau¹¹⁴, H.M. Braun^{175,*}, S.F. Brazzale^{164a,164c},
 B. Brelier¹⁵⁸, J. Bremer³⁰, K. Brendlinger¹²⁰, R. Brenner¹⁶⁶, S. Bressler¹⁷², D. Britton⁵³, F.M. Brochu²⁸, I. Brock²¹,
 R. Brock⁸⁸, F. Broggi^{89a}, C. Bromberg⁸⁸, J. Bronner⁹⁹, G. Brooijmans³⁵, T. Brooks⁷⁶, W.K. Brooks^{32b}, G. Brown⁸²,
 H. Brown⁸, P.A. Bruckman de Renstrom³⁹, D. Bruncko^{144b}, R. Bruneliere⁴⁸, S. Brunet⁶⁰, A. Bruni^{20a}, G. Bruni^{20a},
 M. Bruschi^{20a}, T. Buanes¹⁴, Q. Buat⁵⁵, F. Bucci⁴⁹, J. Buchanan¹¹⁸, P. Buchholz¹⁴¹, R.M. Buckingham¹¹⁸,
 A.G. Buckley⁴⁶, S.I. Buda^{26a}, I.A. Budagov⁶⁴, B. Budick¹⁰⁸, V. Büscher⁸¹, L. Bugge¹¹⁷, O. Bulekov⁹⁶,
 A.C. Bundock⁷³, M. Bunse⁴³, T. Buran¹¹⁷, H. Burckhart³⁰, S. Burdin⁷³, T. Burgess¹⁴, S. Burke¹²⁹, E. Busato³⁴,
 P. Bussey⁵³, C.P. Buszello¹⁶⁶, B. Butler¹⁴³, J.M. Butler²², C.M. Buttar⁵³, J.M. Butterworth⁷⁷, W. Buttinger²⁸,
 M. Byszewski³⁰, S. Cabrera Urbán¹⁶⁷, D. Caforio^{20a,20b}, O. Cakir^{4a}, P. Calafiura¹⁵, G. Calderini⁷⁸, P. Calfayan⁹⁸,
 R. Calkins¹⁰⁶, L.P. Caloba^{24a}, R. Caloi^{132a,132b}, D. Calvet³⁴, S. Calvet³⁴, R. Camacho Toro³⁴, P. Camarri^{133a,133b},
 D. Cameron¹¹⁷, L.M. Caminada¹⁵, R. Caminal Armadans¹², S. Campana³⁰, M. Campanelli⁷⁷, V. Canale^{102a,102b},

F. Canelli^{31,g}, A. Canepa^{159a}, J. Cantero⁸⁰, R. Cantrill⁷⁶, L. Capasso^{102a,102b}, M.D.M. Capeans Garrido³⁰, I. Caprini^{26a}, M. Caprini^{26a}, D. Capriotti⁹⁹, M. Capua^{37a,37b}, R. Caputo⁸¹, R. Cardarelli^{133a}, T. Carli³⁰, G. Carlino^{102a}, L. Carminati^{89a,89b}, B. Caron⁸⁵, S. Caron¹⁰⁴, E. Carquin^{32b}, G.D. Carrillo-Montoya¹⁷³, A.A. Carter⁷⁵, J.R. Carter²⁸, J. Carvalho^{124a,h}, D. Casadei¹⁰⁸, M.P. Casado¹², M. Cascella^{122a,122b}, C. Caso^{50a,50b,*}, A.M. Castaneda Hernandez^{173,i}, E. Castaneda-Miranda¹⁷³, V. Castillo Gimenez¹⁶⁷, N.F. Castro^{124a}, G. Cataldi^{72a}, P. Catastini⁵⁷, A. Catinaccio³⁰, J.R. Catmore³⁰, A. Cattai³⁰, G. Cattani^{133a,133b}, S. Caughron⁸⁸, V. Cavaliere¹⁶⁵, P. Cavalleri⁷⁸, D. Cavalli^{89a}, M. Cavalli-Sforza¹², V. Cavasinni^{122a,122b}, F. Ceradini^{134a,134b}, A.S. Cerqueira^{24b}, A. Cerri³⁰, L. Cerrito⁷⁵, F. Cerutti⁴⁷, S.A. Cetin^{19b}, A. Chafaq^{135a}, D. Chakraborty¹⁰⁶, I. Chalupkova¹²⁶, K. Chan³, P. Chang¹⁶⁵, B. Chapleau⁸⁵, J.D. Chapman²⁸, J.W. Chapman⁸⁷, E. Chareyre⁷⁸, D.G. Charlton¹⁸, V. Chavda⁸², C.A. Chavez Barajas³⁰, S. Cheatham⁸⁵, S. Chekanov⁶, S.V. Chekulaev^{159a}, G.A. Chelkov⁶⁴, M.A. Chelstowska¹⁰⁴, C. Chen⁶³, H. Chen²⁵, S. Chen^{33c}, X. Chen¹⁷³, Y. Chen³⁵, Y. Cheng³¹, A. Cheplakov⁶⁴, R. Cherkaoui El Moursli^{135e}, V. Chernyatin²⁵, E. Cheu⁷, S.L. Cheung¹⁵⁸, L. Chevalier¹³⁶, G. Chiefari^{102a,102b}, L. Chikovani^{51a,*}, J.T. Childers³⁰, A. Chilingarov⁷¹, G. Chiodini^{72a}, A.S. Chisholm¹⁸, R.T. Chislett⁷⁷, A. Chitan^{26a}, M.V. Chizhov⁶⁴, G. Choudalakis³¹, S. Chouridou¹³⁷, I.A. Christidi⁷⁷, A. Christov⁴⁸, D. Chromek-Burckhart³⁰, M.L. Chu¹⁵¹, J. Chudoba¹²⁵, G. Ciapetti^{132a,132b}, A.K. Ciftci^{4a}, R. Ciftci^{4a}, D. Cinca³⁴, V. Cindro⁷⁴, C. Ciocca^{20a,20b}, A. Ciocio¹⁵, M. Cirilli⁸⁷, P. Cirkovic^{13b}, Z.H. Citron¹⁷², M. Citterio^{89a}, M. Ciubancan^{26a}, A. Clark⁴⁹, P.J. Clark⁴⁶, R.N. Clarke¹⁵, W. Cleland¹²³, J.C. Clemens⁸³, B. Clement⁵⁵, C. Clement^{146a,146b}, Y. Coadou⁸³, M. Cobal^{164a,164c}, A. Coccaro¹³⁸, J. Cochran⁶³, L. Coffey²³, J.G. Cogan¹⁴³, J. Coggeshall¹⁶⁵, E. Cogneras¹⁷⁸, J. Colas⁵, S. Cole¹⁰⁶, A.P. Colijn¹⁰⁵, N.J. Collins¹⁸, C. Collins-Tooth⁵³, J. Collot⁵⁵, T. Colombo^{119a,119b}, G. Colon⁸⁴, G. Compostella⁹⁹, P. Conde Muiño^{124a}, E. Coniavitis¹⁶⁶, M.C. Conidi¹², S.M. Consonni^{89a,89b}, V. Consorti⁴⁸, S. Constantinescu^{26a}, C. Conta^{119a,119b}, G. Conti⁵⁷, F. Conventi^{102a,j}, M. Cooke¹⁵, B.D. Cooper⁷⁷, A.M. Cooper-Sarkar¹¹⁸, K. Copic¹⁵, T. Cornelissen¹⁷⁵, M. Corradi^{20a}, F. Corriveau^{85,k}, A. Cortes-Gonzalez¹⁶⁵, G. Cortiana⁹⁹, G. Costa^{89a}, M.J. Costa¹⁶⁷, D. Costanzo¹³⁹, D. Côté³⁰, L. Courneyea¹⁶⁹, G. Cowan⁷⁶, C. Cowden²⁸, B.E. Cox⁸², K. Cranmer¹⁰⁸, F. Crescioli^{122a,122b}, M. Cristinziani²¹, G. Crosetti^{37a,37b}, S. Crépe-Renaudin⁵⁵, C.-M. Cuciuic^{26a}, C. Cuenca Almenar¹⁷⁶, T. Cuhadar Donszelmann¹³⁹, M. Curatolo⁴⁷, C.J. Curtis¹⁸, C. Cuthbert¹⁵⁰, P. Cwetanski⁶⁰, H. Czirr¹⁴¹, P. Czodrowski⁴⁴, Z. Czyczula¹⁷⁶, S. D'Auria⁵³, M. D'Onofrio⁷³, A. D'Orazio^{132a,132b}, M.J. Da Cunha Sargedas De Sousa^{124a}, C. Da Via⁸², W. Dabrowski³⁸, A. Dafinca¹¹⁸, T. Dai⁸⁷, G. Dallapiccola⁸⁴, M. Dam³⁶, M. Dameri^{50a,50b}, D.S. Damiani¹³⁷, H.O. Danielsson³⁰, V. Dao⁴⁹, G. Darbo^{50a}, G.L. Darlea^{26b}, J.A. Dassoulas⁴², W. Davey²¹, T. Davidek¹²⁶, N. Davidson⁸⁶, R. Davidson⁷¹, E. Davies^{118,c}, M. Davies⁹³, O. Davignon⁷⁸, A.R. Davison⁷⁷, Y. Davygora^{58a}, E. Dawe¹⁴², I. Dawson¹³⁹, R.K. Daya-Ishmukhametova²³, K. De⁸, R. de Asmundis^{102a}, S. De Castro^{20a,20b}, S. De Cecco⁷⁸, J. de Graat⁹⁸, N. De Groot¹⁰⁴, P. de Jong¹⁰⁵, C. De La Taille¹¹⁵, H. De la Torre⁸⁰, F. De Lorenzi⁶³, L. de Mora⁷¹, L. De Nooij¹⁰⁵, D. De Pedis^{132a}, A. De Salvo^{132a}, U. De Sanctis^{164a,164c}, A. De Santo¹⁴⁹, J.B. De Vivie De Regie¹¹⁵, G. De Zorzi^{132a,132b}, W.J. Dearnaley⁷¹, R. Debebe²⁵, C. Debenedetti⁴⁶, B. Dechenaux⁵⁵, D.V. Dedovich⁶⁴, J. Degenhardt¹²⁰, C. Del Papa^{164a,164c}, J. Del Peso⁸⁰, T. Del Prete^{122a,122b}, T. Delemontex⁵⁵, M. Deliyergiyev⁷⁴, A. Dell'Acqua³⁰, L. Dell'Asta²², M. Della Pietra^{102a,j}, D. della Volpe^{102a,102b}, M. Delmastro⁵, P.A. Delsart⁵⁵, C. Deluca¹⁰⁵, S. Demers¹⁷⁶, M. Demichev⁶⁴, B. Demirkoz^{12,l}, J. Deng¹⁶³, S.P. Denisov¹²⁸, D. Derendarz³⁹, J.E. Derkaoui^{135d}, F. Derue⁷⁸, P. Dervan⁷³, K. Desch²¹, E. Devetak¹⁴⁸, P.O. Deviveiros¹⁰⁵, A. Dewhurst¹²⁹, B. DeWilde¹⁴⁸, S. Dhaliwal¹⁵⁸, R. Dhullipudi^{25,m}, A. Di Ciaccio^{133a,133b}, L. Di Ciaccio⁵, C. Di Donato^{102a,102b}, A. Di Girolamo³⁰, B. Di Girolamo³⁰, S. Di Luise^{134a,134b}, A. Di Mattia¹⁷³, B. Di Micco³⁰, R. Di Nardo⁴⁷, A. Di Simone^{133a,133b}, R. Di Sipio^{20a,20b}, M.A. Diaz^{32a}, E.B. Diehl⁸⁷, J. Dietrich⁴², T.A. Dietzsch^{58a}, S. Diglio⁸⁶, K. Dindar Yagci⁴⁰, J. Dingfelder²¹, F. Dinut^{26a}, C. Dionisi^{132a,132b}, P. Dita^{26a}, S. Dita^{26a}, F. Dittus³⁰, F. Djama⁸³, T. Djobava^{51b}, M.A.B. do Vale^{24c}, A. Do Valle Wemans^{124a,n}, T.K.O. Doan⁵, M. Dobbs⁸⁵, D. Dobos³⁰, E. Dobson^{30,o}, J. Dodd³⁵, C. Doglioni⁴⁹, T. Doherty⁵³, Y. Doi^{65,*}, J. Dolejsi¹²⁶, I. Dolenc⁷⁴, Z. Dolezal¹²⁶, B.A. Dolgoshein^{96,*}, T. Dohmae¹⁵⁵, M. Donadelli^{24d}, J. Donini³⁴, J. Dopke³⁰, A. Doria^{102a}, A. Dos Anjos¹⁷³, A. Dotti^{122a,122b}, M.T. Dova⁷⁰, A.D. Doxiadis¹⁰⁵, A.T. Doyle⁵³, N. Dressnandt¹²⁰, M. Dris¹⁰, J. Dubbert⁹⁹, S. Dube¹⁵, E. Duchovni¹⁷², G. Duckeck⁹⁸, D. Duda¹⁷⁵, A. Dudarev³⁰, F. Dudziak⁶³, M. Dührssen³⁰, I.P. Duerdoth⁸², L. Duflot¹¹⁵, M.-A. Dufour⁸⁵, L. Duguid⁷⁶, M. Dunford^{58a}, H. Duran Yildiz^{4a}, R. Duxfield¹³⁹, M. Dwuznik³⁸, F. Dydak³⁰, M. Düren⁵², W.L. Ebenstein⁴⁵, J. Ebke⁹⁸, S. Eckweiler⁸¹, K. Edmonds⁸¹, W. Edson², C.A. Edwards⁷⁶, N.C. Edwards⁵³, W. Ehrenfeld⁴², T. Eifert¹⁴³, G. Eigen¹⁴, K. Einsweiler¹⁵, E. Eisenhandler⁷⁵, T. Ekelof¹⁶⁶, M. El Kacimi^{135c}, M. Ellert¹⁶⁶, S. Elles⁵, F. Ellinghaus⁸¹, K. Ellis⁷⁵, N. Ellis³⁰, J. Elmsheuser⁹⁸, M. Elsing³⁰, D. Emeljanov¹²⁹, R. Engelmann¹⁴⁸, A. Engl⁹⁸, B. Epp⁶¹, J. Erdmann⁵⁴, A. Ereditato¹⁷, D. Eriksson^{146a}, J. Ernst², M. Ernst²⁵, J. Ernwein¹³⁶, D. Errede¹⁶⁵, S. Errede¹⁶⁵, E. Ertel⁸¹, M. Escalier¹¹⁵, H. Esch⁴³, C. Escobar¹²³, X. Espinal Curull¹², B. Esposito⁴⁷, F. Etienne⁸³, A.I. Etievre¹³⁶, E. Etzion¹⁵³, D. Evangelakou⁵⁴, H. Evans⁶⁰, L. Fabbri^{20a,20b}, C. Fabre³⁰, R.M. Fakhruddinov¹²⁸, S. Falciano^{132a}, Y. Fang¹⁷³, M. Fanti^{89a,89b}, A. Farbin⁸, A. Farilla^{134a}, J. Farley¹⁴⁸, T. Farooque¹⁵⁸, S. Farrell¹⁶³, S.M. Farrington¹⁷⁰, P. Farthouat³⁰, F. Fassi¹⁶⁷, P. Fassnacht³⁰, D. Fassouliotis⁹, B. Fatholahzadeh¹⁵⁸, A. Favareto^{89a,89b}, L. Fayard¹¹⁵, S. Fazio^{37a,37b}, R. Febbraro³⁴, P. Federic^{144a}, O.L. Fedin¹²¹, W. Fedorko⁸⁸, M. Fehling-Kaschek⁴⁸, L. Felgioni⁸³, D. Fellmann⁶,

C. Feng^{33d}, E.J. Feng⁶, A.B. Fenyuk¹²⁸, J. Ferencei^{144b}, W. Fernando⁶, S. Ferrag⁵³, J. Ferrando⁵³, V. Ferrara⁴², A. Ferrari¹⁶⁶, P. Ferrari¹⁰⁵, R. Ferrari^{119a}, D.E. Ferreira de Lima⁵³, A. Ferrer¹⁶⁷, D. Ferrere⁴⁹, C. Ferretti⁸⁷, A. Ferretto Parodi^{50a,50b}, M. Fiascaris³¹, F. Fiedler⁸¹, A. Filipčić⁷⁴, F. Filthaut¹⁰⁴, M. Fincke-Keeler¹⁶⁹, M.C.N. Fiolhais^{124a,h}, L. Fiorini¹⁶⁷, A. Firan⁴⁰, G. Fischer⁴², M.J. Fisher¹⁰⁹, M. Flechl⁴⁸, I. Fleck¹⁴¹, J. Fleckner⁸¹, P. Fleischmann¹⁷⁴, S. Fleischmann¹⁷⁵, T. Flick¹⁷⁵, A. Floderus⁷⁹, L.R. Flores Castillo¹⁷³, M.J. Flowerdew⁹⁹, T. Fonseca Martin¹⁷, A. Formica¹³⁶, A. Forti⁸², D. Fortin^{159a}, D. Fournier¹¹⁵, A.J. Fowler⁴⁵, H. Fox⁷¹, P. Francavilla¹², M. Franchini^{20a,20b}, S. Franchino^{119a,119b}, D. Francis³⁰, T. Frank¹⁷², M. Franklin⁵⁷, S. Franz³⁰, M. Fraternali^{119a,119b}, S. Fratina¹²⁰, S.T. French²⁸, C. Friedrich⁴², F. Friedrich⁴⁴, R. Froeschl³⁰, D. Froidevaux³⁰, J.A. Frost²⁸, C. Fukunaga¹⁵⁶, E. Fullana Torregrosa³⁰, B.G. Fulson¹⁴³, J. Fuster¹⁶⁷, C. Gabaldon³⁰, O. Gabizon¹⁷², T. Gadfort²⁵, S. Gadomski⁴⁹, G. Gagliardi^{50a,50b}, P. Gagnon⁶⁰, C. Galea⁹⁸, B. Galhardo^{124a}, E.J. Gallas¹¹⁸, V. Gallo¹⁷, B.J. Gallop¹²⁹, P. Gallus¹²⁵, K.K. Gan¹⁰⁹, Y.S. Gao^{143,e}, A. Gaponenko¹⁵, F. Garbersson¹⁷⁶, M. Garcia-Sciveres¹⁵, C. García¹⁶⁷, J.E. García Navarro¹⁶⁷, R.W. Gardner³¹, N. Garelli³⁰, H. Garitaonandia¹⁰⁵, V. Garonne³⁰, C. Gatti⁴⁷, G. Gaudio^{119a}, B. Gaur¹⁴¹, L. Gauthier¹³⁶, P. Gauzzi^{132a,132b}, I.L. Gavrilenko⁹⁴, C. Gay¹⁶⁸, G. Gaycken²¹, E.N. Gazis¹⁰, P. Ge^{33d}, Z. Gecse¹⁶⁸, C.N.P. Gee¹²⁹, D.A.A. Geerts¹⁰⁵, Ch. Geich-Gimbel²¹, K. Gellerstedt^{146a,146b}, C. Gemme^{50a}, A. Gemmell⁵³, M.H. Genest⁵⁵, S. Gentile^{132a,132b}, M. George⁵⁴, S. George⁷⁶, P. Gerlach¹⁷⁵, A. Gershon¹⁵³, C. Geweniger^{58a}, H. Ghazlane^{135b}, N. Ghodbane³⁴, B. Giacobbe^{20a}, S. Giagu^{132a,132b}, V. Giakoumopoulou⁹, V. Giangiobbe¹², F. Gianotti³⁰, B. Gibbard²⁵, A. Gibson¹⁵⁸, S.M. Gibson³⁰, M. Gilchriese¹⁵, D. Gillberg²⁹, A.R. Gillman¹²⁹, D.M. Gingrich^{3,d}, J. Ginzburg¹⁵³, N. Giokaris⁹, M.P. Giordani^{164c}, R. Giordano^{102a,102b}, F.M. Giorgi¹⁶, P. Giovannini⁹⁹, P.F. Giraud¹³⁶, D. Giugni^{89a}, M. Giunta⁹³, P. Giusti^{20a}, B.K. Gjelsten¹¹⁷, L.K. Gladilin⁹⁷, C. Glasman⁸⁰, J. Glatzer²¹, A. Glazov⁴², K.W. Glitza¹⁷⁵, G.L. Glonti⁶⁴, J.R. Goddard⁷⁵, J. Godfrey¹⁴², J. Godlewski³⁰, M. Goebel⁴², T. Göpfert⁴⁴, C. Goeringer⁸¹, C. Gössling⁴³, S. Goldfarb⁸⁷, T. Golling¹⁷⁶, A. Gomes^{124a,b}, L.S. Gomez Fajardo⁴², R. Gonçalves⁷⁶, J. Goncalves Pinto Firmino Da Costa⁴², L. Gonella²¹, S. González de la Hoz¹⁶⁷, G. Gonzalez Parra¹², M.L. Gonzalez Silva²⁷, S. Gonzalez-Sevilla⁴⁹, J.J. Goodson¹⁴⁸, L. Goossens³⁰, P.A. Gorbounov⁹⁵, H.A. Gordon²⁵, I. Gorelov¹⁰³, G. Gorfine¹⁷⁵, B. Gorini³⁰, E. Gorini^{72a,72b}, A. Gorišek⁷⁴, E. Gornicki³⁹, B. Gosdzik⁴², A.T. Goshaw⁶, M. Gosselink¹⁰⁵, M.I. Gostkin⁶⁴, I. Gough Eschrich¹⁶³, M. Gouighri^{135a}, D. Goujdami^{135c}, M.P. Goulette⁴⁹, A.G. Goussiou¹³⁸, C. Goy⁵, S. Gozpinar²³, I. Grabowska-Bold³⁸, P. Grafström^{20a,20b}, K.-J. Grahn⁴², E. Gramstad¹¹⁷, F. Grancagnolo^{72a}, S. Grancagnolo¹⁶, V. Grassi¹⁴⁸, V. Gratchev¹²¹, N. Grau³⁵, H.M. Gray³⁰, J.A. Gray¹⁴⁸, E. Graziani^{134a}, O.G. Grebenyuk¹²¹, T. Greenshaw⁷³, Z.D. Greenwood^{25,m}, K. Gregersen³⁶, I.M. Gregor⁴², P. Grenier¹⁴³, J. Griffiths⁸, N. Grigalashvili⁶⁴, A.A. Grillo¹³⁷, S. Grinstein¹², Ph. Gris³⁴, Y.V. Grishkevich⁹⁷, J.-F. Grivaz¹¹⁵, E. Gross¹⁷², J. Grosse-Knetter⁵⁴, J. Groth-Jensen¹⁷², K. Grybel¹⁴¹, D. Guest¹⁷⁶, C. Guichenev³⁴, S. Guindon⁵⁴, U. Gul⁵³, J. Gunther¹²⁵, B. Guo¹⁵⁸, J. Guo³⁵, P. Gutierrez¹¹¹, N. Guttman¹⁵³, O. Gutzwiller¹⁷³, C. Guyot¹³⁶, C. Gwenlan¹¹⁸, C.B. Gwilliam⁷³, A. Haas¹⁰⁸, S. Haas³⁰, C. Haber¹⁵, H.K. Hadavand⁸, D.R. Hadley¹⁸, P. Haefner²¹, F. Hahn³⁰, S. Haider³⁰, Z. Hajduk³⁹, H. Hakobyan¹⁷⁷, D. Hall¹¹⁸, K. Hamacher¹⁷⁵, P. Hamal¹¹³, K. Hamano⁸⁶, M. Hamer⁵⁴, A. Hamilton^{145b,p}, S. Hamilton¹⁶¹, L. Han^{33b}, K. Hanagaki¹¹⁶, K. Hanawa¹⁶⁰, M. Hance¹⁵, C. Handel⁸¹, P. Hanke^{58a}, J.R. Hansen³⁶, J.B. Hansen³⁶, J.D. Hansen³⁶, P.H. Hansen³⁶, P. Hansson¹⁴³, K. Hara¹⁶⁰, G.A. Hare¹³⁷, T. Harenberg¹⁷⁵, S. Harkusha⁹⁰, D. Harper⁸⁷, R.D. Harrington⁴⁶, O.M. Harris¹³⁸, J. Hartert⁴⁸, F. Hartjes¹⁰⁵, T. Haruyama⁶⁵, A. Harvey⁵⁶, S. Hasegawa¹⁰¹, Y. Hasegawa¹⁴⁰, S. Hassani¹³⁶, S. Haug¹⁷, M. Hauschild³⁰, R. Hauser⁸⁸, M. Havranek²¹, C.M. Hawkes¹⁸, R.J. Hawkins³⁰, A.D. Hawkins⁷⁹, T. Hayakawa⁶⁶, T. Hayashi¹⁶⁰, D. Hayden⁷⁶, C.P. Hays¹¹⁸, H.S. Hayward⁷³, S.J. Haywood¹²⁹, S.J. Head¹⁸, V. Hedberg⁷⁹, L. Heelan⁸, S. Heim⁸⁸, B. Heinemann¹⁵, S. Heisterkamp³⁶, L. Helary²², C. Heller⁹⁸, M. Heller³⁰, S. Hellman^{146a,146b}, D. Hellmich²¹, C. Helsen¹², R.C.W. Henderson⁷¹, M. Henke^{58a}, A. Henrichs¹⁷⁶, A.M. Henriques Correia³⁰, S. Henrot-Versille¹¹⁵, C. Hensel⁵⁴, T. Henß¹⁷⁵, C.M. Hernandez⁸, Y. Hernández Jiménez¹⁶⁷, R. Herrberg¹⁶, G. Herten⁴⁸, R. Hertenberger⁹⁸, L. Hervas³⁰, G.G. Hesketh⁷⁷, N.P. Hessey¹⁰⁵, E. Higón-Rodríguez¹⁶⁷, J.C. Hill²⁸, K.H. Hiller⁴², S. Hillert²¹, S.J. Hillier¹⁸, I. Hinchliffe¹⁵, E. Hines¹²⁰, M. Hirose¹¹⁶, F. Hirsch⁴³, D. Hirschbuehl¹⁷⁵, J. Hobbs¹⁴⁸, N. Hod¹⁵³, M.C. Hodgkinson¹³⁹, P. Hodgson¹³⁹, A. Hoecker³⁰, M.R. Hoferkamp¹⁰³, J. Hoffman⁴⁰, D. Hoffmann⁸³, M. Hohlfield⁸¹, M. Holder¹⁴¹, S.O. Holmgren^{146a}, T. Holy¹²⁷, J.L. Holzbauer⁸⁸, T.M. Hong¹²⁰, L. Hooft van Huysduynen¹⁰⁸, S. Horner⁴⁸, J.-Y. Hostachy⁵⁵, S. Hou¹⁵¹, A. Hoummada^{135a}, J. Howard¹¹⁸, J. Howarth⁸², I. Hristova¹⁶, J. Hrivnac¹¹⁵, T. Hryn'ova⁵, P.J. Hsu⁸¹, S.-C. Hsu¹⁵, D. Hu³⁵, Z. Hubacek¹²⁷, F. Hubaut⁸³, F. Huegging²¹, A. Huettmann⁴², T.B. Huffman¹¹⁸, E.W. Hughes³⁵, G. Hughes⁷¹, M. Huhtinen³⁰, M. Hurwitz¹⁵, N. Huseynov^{64,q}, J. Huston⁸⁸, J. Huth⁵⁷, G. Iacobucci⁴⁹, G. Iakovidis¹⁰, M. Ibbotson⁸², I. Ibragimov¹⁴¹, L. Iconomidou-Fayard¹¹⁵, J. Idarraga¹¹⁵, P. Iengo^{102a}, O. Igonkina¹⁰⁵, Y. Ikegami⁶⁵, M. Ikeno⁶⁵, D. Iliadis¹⁵⁴, N. Ilic¹⁵⁸, T. Ince⁹⁹, J. Inigo-Golfin³⁰, P. Ioannou⁹, M. Iodice^{134a}, K. Iordanidou⁹, V. Ippolito^{132a,132b}, A. Irls Quiles¹⁶⁷, C. Isaksson¹⁶⁶, M. Ishino⁶⁷, M. Ishitsuka¹⁵⁷, R. Ishmukhametov¹⁰⁹, C. Issever¹¹⁸, S. Istin^{19a}, A.V. Ivashin¹²⁸, W. Iwanski³⁹, H. Iwasaki⁶⁵, J.M. Izen⁴¹, V. Izzo^{102a}, B. Jackson¹²⁰, J.N. Jackson⁷³, P. Jackson¹, M.R. Jaekel³⁰, V. Jain⁶⁰, K. Jakobs⁴⁸, S. Jakobsen³⁶, T. Jakoubek¹²⁵, J. Jakubek¹²⁷, D.O. Jamin¹⁵¹, D.K. Jana¹¹¹, E. Jansen⁷⁷, H. Jansen³⁰, A. Jantsch⁹⁹, M. Janus⁴⁸, G. Jarlskog⁷⁹, L. Jeanty⁵⁷, I. Jen-La Plante³¹, D. Jennens⁸⁶, P. Jenni³⁰, A.E. Loevschall-Jensen³⁶, P. Jež³⁶, S. Jézéquel⁵, M.K. Jha^{20a}, H. Ji¹⁷³, W. Ji⁸¹, J. Jia¹⁴⁸, Y. Jiang^{33b},

M. Jimenez Belenguer⁴², S. Jin^{33a}, O. Jinnouchi¹⁵⁷, M.D. Joergensen³⁶, D. Joffe⁴⁰, M. Johansen^{146a,146b},
 K.E. Johansson^{146a}, P. Johansson¹³⁹, S. Johnert⁴², K.A. Johns⁷, K. Jon-And^{146a,146b}, G. Jones¹⁷⁰, R.W.L. Jones⁷¹,
 T.J. Jones⁷³, C. Joram³⁰, P.M. Jorge^{124a}, K.D. Joshi⁸², J. Jovicevic¹⁴⁷, T. Jovin^{13b}, X. Ju¹⁷³, C.A. Jung⁴³,
 R.M. Jungst³⁰, V. Juranek¹²⁵, P. Jussel⁶¹, A. Juste Rozas¹², S. Kabana¹⁷, M. Kaci¹⁶⁷, A. Kaczmarska³⁹,
 P. Kadlecik³⁶, M. Kado¹¹⁵, H. Kagan¹⁰⁹, M. Kagan⁵⁷, E. Kajomovitz¹⁵², S. Kalinin¹⁷⁵, L.V. Kalinovskaya⁶⁴,
 S. Kama⁴⁰, N. Kanaya¹⁵⁵, M. Kaneda³⁰, S. Kaneti²⁸, T. Kanno¹⁵⁷, V.A. Kantserov⁹⁶, J. Kanzaki⁶⁵, B. Kaplan¹⁰⁸,
 A. Kapliy³¹, J. Kaplon³⁰, D. Kar⁵³, M. Karagounis²¹, K. Karakostas¹⁰, M. Karnevskiy⁴², V. Kartvelishvili⁷¹,
 A.N. Karyukhin¹²⁸, L. Kashif¹⁷³, G. Kasieczka^{58b}, R.D. Kass¹⁰⁹, A. Kastanas¹⁴, M. Kataoka⁵, Y. Kataoka¹⁵⁵,
 E. Katsoufis¹⁰, J. Katzy⁴², V. Kaushik⁷, K. Kawagoe⁶⁹, T. Kawamoto¹⁵⁵, G. Kawamura⁸¹, M.S. Kayl¹⁰⁵,
 S. Kazama¹⁵⁵, V.A. Kazanin¹⁰⁷, M.Y. Kazarinov⁶⁴, R. Keeler¹⁶⁹, P.T. Keener¹²⁰, R. Kehoe⁴⁰, M. Keil⁵⁴,
 G.D. Kekelidze⁶⁴, J.S. Keller¹³⁸, M. Kenyon⁵³, O. Kepka¹²⁵, N. Kerschen³⁰, B.P. Kerševan⁷⁴, S. Kersten¹⁷⁵,
 K. Kessoku¹⁵⁵, J. Keung¹⁵⁸, F. Khalil-zada¹¹, H. Khandanyan^{146a,146b}, A. Khanov¹¹², D. Kharchenko⁶⁴,
 A. Khodinov⁹⁶, A. Khomich^{58a}, T.J. Khoo²⁸, G. Khoriali²¹, A. Khoroshilov¹⁷⁵, V. Khovanskiy⁹⁵, E. Khramov⁶⁴,
 J. Khubua^{51b}, H. Kim^{146a,146b}, S.H. Kim¹⁶⁰, N. Kimura¹⁷¹, O. Kind¹⁶, B.T. King⁷³, M. King⁶⁶, R.S.B. King¹¹⁸,
 J. Kirk¹²⁹, A.E. Kiryunin⁹⁹, T. Kishimoto⁶⁶, D. Kisielewska³⁸, T. Kitamura⁶⁶, T. Kittelmann¹²³, K. Kiuchi¹⁶⁰,
 E. Kladiva^{144b}, M. Klein⁷³, U. Klein⁷³, K. Kleinknecht⁸¹, M. Klemetti⁸⁵, A. Klier¹⁷², P. Klimek^{146a,146b},
 A. Klimentov²⁵, R. Klingenberg⁴³, J.A. Klinger⁸², E.B. Klinkby³⁶, T. Klioutchnikova³⁰, P.F. Klok¹⁰⁴, S. Klous¹⁰⁵,
 E.-E. Kluge^{58a}, T. Kluge⁷³, P. Kluit¹⁰⁵, S. Kluth⁹⁹, E. Kneringer⁶¹, E.B.F.G. Knoop⁸³, A. Knue⁵⁴, B.R. Ko⁴⁵,
 T. Kobayashi¹⁵⁵, M. Kobel⁴⁴, M. Kocian¹⁴³, P. Kodys¹²⁶, K. Köneke³⁰, A.C. König¹⁰⁴, S. Koenig⁸¹, L. Köpke⁸¹,
 F. Koetsveld¹⁰⁴, P. Koevesarki²¹, T. Koffas²⁹, E. Koffeman¹⁰⁵, L.A. Kogan¹¹⁸, S. Kohlmann¹⁷⁵, F. Kohn⁵⁴,
 Z. Kohout¹²⁷, T. Kohriki⁶⁵, T. Koj¹⁴³, G.M. Kolachev^{107,*}, H. Kolanoski¹⁶, V. Kolesnikov⁶⁴, I. Koletsou^{89a},
 J. Koll⁸⁸, A.A. Komar⁹⁴, Y. Komori¹⁵⁵, T. Kondo⁶⁵, T. Kono^{42,r}, A.I. Kononov⁴⁸, R. Konoplich^{108,s},
 N. Konstantinidis⁷⁷, R. Kopeliainsky¹⁵², S. Koperny³⁸, K. Korcyl³⁹, K. Kordas¹⁵⁴, A. Korn¹¹⁸, A. Korol¹⁰⁷,
 I. Korolkov¹², E.V. Korolkova¹³⁹, V.A. Korotkov¹²⁸, O. Kortner⁹⁹, S. Kortner⁹⁹, V.V. Kostyukhin²¹, S. Kotov⁹⁹,
 V.M. Kotov⁶⁴, A. Kotwal⁴⁵, C. Kourkoumelis⁹, V. Kouskoura¹⁵⁴, A. Koutsman^{159a}, R. Kowalewski¹⁶⁹,
 T.Z. Kowalski³⁸, W. Kozanecki¹³⁶, A.S. Kozhin¹²⁸, V. Kral¹²⁷, V.A. Kramarenko⁹⁷, G. Kramberger⁷⁴,
 M.W. Krasny⁷⁸, A. Krasznahorkay¹⁰⁸, J.K. Kraus²¹, S. Kreiss¹⁰⁸, F. Krejci¹²⁷, J. Kretschmar⁷³, N. Krieger⁵⁴,
 P. Krieger¹⁷, N. Krumnack⁶³, Z.V. Krumshteyn⁶⁴, T. Kubota⁸⁶, S. Kuday^{4a}, S. Kuehn⁴⁸, A. Kugel^{58c}, T. Kuhl⁴²,
 D. Kuhn⁶¹, V. Kukhtin⁶⁴, Y. Kulchitsky⁹⁰, S. Kuleshov^{32b}, C. Kummer⁹⁸, M. Kuna⁷⁸, J. Kunkle¹²⁰, A. Kupco¹²⁵,
 H. Kurashige⁶⁶, M. Kurata¹⁶⁰, Y.A. Kurochkin⁹⁰, V. Kus¹²⁵, E.S. Kuwertz¹⁴⁷, M. Kuze¹⁵⁷, J. Kvita¹⁴², R. Kwee¹⁶,
 A. La Rosa⁴⁹, L. La Rotonda^{37a,37b}, L. Labarga⁸⁰, J. Labbe⁵, S. Lablak^{135a}, C. Lacasta¹⁶⁷, F. Lacava^{132a,132b},
 J. Lacey²⁹, H. Lacker¹⁶, D. Lacour⁷⁸, V.R. Lacuesta¹⁶⁷, E. Ladygin⁶⁴, R. Lafaye⁵, B. Laforge⁷⁸, T. Lagouri¹⁷⁶,
 S. Lai⁴⁸, E. Laisne⁵⁵, M. Lamanna³⁰, L. Lambourne⁷⁷, C.L. Lampen⁷, W. Lampl⁷, E. Lancon¹³⁶, U. Landgraf⁴⁸,
 M.P.J. Landon⁷⁵, V.S. Lang^{58a}, C. Lange⁴², A.J. Lankford¹⁶³, F. Lanni²⁵, K. Lantzsch¹⁷⁵, S. Laplace⁷⁸,
 C. Lapoire²¹, J.F. Laporte¹³⁶, T. Lari^{89a}, A. Larner¹¹⁸, M. Lassnig³⁰, P. Laurelli⁴⁷, V. Lavorini^{37a,37b},
 W. Lavrijsen¹⁵, P. Laycock⁷³, O. Le Dortz⁷⁸, E. Le Guirriec⁸³, E. Le Menedeu¹², T. LeCompte⁶,
 F. Ledroit-Guillon⁵⁵, H. Lee¹⁰⁵, J.S.H. Lee¹¹⁶, S.C. Lee¹⁵¹, L. Lee¹⁷⁶, M. Lefebvre¹⁶⁹, M. Legendre¹³⁶, F. Legger⁹⁸,
 C. Leggett¹⁵, M. Lehmacher²¹, G. Lehmann Miotto³⁰, X. Lei⁷, M.A.L. Leite^{24d}, R. Leitner¹²⁶, D. Lellouch¹⁷²,
 B. Lemmer⁵⁴, V. Lendermann^{58a}, K.J.C. Leney^{145b}, T. Lenz¹⁰⁵, G. Lenzen¹⁷⁵, B. Lenzi³⁰, K. Leonhardt⁴⁴,
 S. Leontsinis¹⁰, F. Lepold^{58a}, C. Leroy⁹³, J-R. Lessard¹⁶⁹, C.G. Lester²⁸, C.M. Lester¹²⁰, J. Levêque⁵, D. Levin⁸⁷,
 L.J. Levinson¹⁷², A. Lewis¹¹⁸, G.H. Lewis¹⁰⁸, A.M. Leyko²¹, M. Leyton¹⁶, B. Li⁸³, H. Li¹⁴⁸, H.L. Li³¹, S. Li^{33b,t},
 X. Li⁸⁷, Z. Liang^{118,u}, H. Liao³⁴, B. Liberti^{133a}, P. Lichard³⁰, M. Lichtnecker⁹⁸, K. Lie¹⁶⁵, W. Liebig¹⁴,
 C. Limbach²¹, A. Limosani⁸⁶, M. Limper⁶², S.C. Lin^{151,v}, F. Linde¹⁰⁵, J.T. Linnemann⁸⁸, E. Lipeles¹²⁰,
 A. Lipniacka¹⁴, T.M. Liss¹⁶⁵, D. Lissauer²⁵, A. Lister⁴⁹, A.M. Litke¹³⁷, C. Liu²⁹, D. Liu¹⁵¹, H. Liu⁸⁷, J.B. Liu⁸⁷,
 L. Liu⁸⁷, M. Liu^{33b}, Y. Liu^{33b}, M. Livan^{119a,119b}, S.S.A. Livermore¹¹⁸, A. Lleres⁵⁵, J. Llorente Merino⁸⁰,
 S.L. Lloyd⁷⁵, E. Lobodzinska⁴², P. Loch⁷, W.S. Lockman¹³⁷, T. Loddenkoetter²¹, F.K. Loebinger⁸², A. Loginov¹⁷⁶,
 C.W. Loh¹⁶⁸, T. Lohse¹⁶, K. Lohwasser⁴⁸, M. Lokajicek¹²⁵, V.P. Lombardo⁵, R.E. Long⁷¹, L. Lopes^{124a},
 D. Lopez Mateos⁵⁷, J. Lorenz⁹⁸, N. Lorenzo Martinez¹¹⁵, M. Losada¹⁶², P. Loscutoff¹⁵, F. Lo Sterzo^{132a,132b},
 M.J. Losty^{159a,*}, X. Lou⁴¹, A. Lounis¹¹⁵, K.F. Loureiro¹⁶², J. Love⁶, P.A. Love⁷¹, A.J. Lowe^{143,e}, F. Lu^{33a},
 H.J. Lubatti¹³⁸, C. Luci^{132a,132b}, A. Lucotte⁵⁵, A. Ludwig⁴⁴, D. Ludwig⁴², I. Ludwig⁴⁸, J. Ludwig⁴⁸, F. Luehring⁶⁰,
 G. Luijckx¹⁰⁵, W. Lukas⁶¹, L. Luminari^{132a}, E. Lund¹¹⁷, B. Lund-Jensen¹⁴⁷, B. Lundberg⁷⁹, J. Lundberg^{146a,146b},
 O. Lundberg^{146a,146b}, J. Lundquist³⁶, M. Lungwitz⁸¹, D. Lynn²⁵, E. Lytken⁷⁹, H. Ma²⁵, L.L. Ma¹⁷³,
 G. Maccarrone⁴⁷, A. Macchiolo⁹⁹, B. Maček⁷⁴, J. Machado Miguens^{124a}, R. Mackeprang³⁶, R.J. Madaras¹⁵,
 H.J. Maddocks⁷¹, W.F. Mader⁴⁴, R. Maenner^{58c}, T. Maeno²⁵, P. Mättig¹⁷⁵, S. Mättig⁸¹, L. Magnoni¹⁶³,
 E. Magradze⁵⁴, K. Mahboubi⁴⁸, J. Mahlstedt¹⁰⁵, S. Mahmoud⁷³, G. Mahout¹⁸, C. Maiani¹³⁶, C. Maidantchik^{24a},
 A. Maio^{124a,b}, S. Majewski²⁵, Y. Makida⁶⁵, N. Makovec¹¹⁵, P. Mal¹³⁶, B. Malaescu³⁰, Pa. Malecki³⁹, P. Malecki³⁹,
 V.P. Maleev¹²¹, F. Malek⁵⁵, U. Mallik⁶², D. Malon⁶, C. Malone¹⁴³, S. Maltezos¹⁰, V. Malyshev¹⁰⁷, S. Malyukov³⁰,

R. Mameghani⁹⁸, J. Mamuzic^{13b}, A. Manabe⁶⁵, L. Mandelli^{89a}, I. Mandić⁷⁴, R. Mandrysch¹⁶, J. Maneira^{124a}, A. Manfredini⁹⁹, P.S. Mangedard⁸⁸, L. Manhaes de Andrade Filho^{24b}, J.A. Manjarres Ramos¹³⁶, A. Mann⁵⁴, P.M. Manning¹³⁷, A. Manousakis-Katsikakis⁹, B. Mansoulie¹³⁶, A. Mapelli³⁰, L. Mapelli³⁰, L. March¹⁶⁷, J.F. Marchand²⁹, F. Marchese^{133a,133b}, G. Marchiori⁷⁸, M. Marcisovsky¹²⁵, C.P. Marino¹⁶⁹, F. Marroquim^{24a}, Z. Marshall³⁰, F.K. Martens¹⁵⁸, L.F. Marti¹⁷, S. Marti-Garcia¹⁶⁷, B. Martin³⁰, B. Martin⁸⁸, J.P. Martin⁹³, T.A. Martin¹⁸, V.J. Martin⁴⁶, B. Martin dit Latour⁴⁹, S. Martin-Haugh¹⁴⁹, M. Martinez¹², V. Martinez Outschoorn⁵⁷, A.C. Martyniuk¹⁶⁹, M. Marx⁸², F. Marzano^{132a}, A. Marzin¹¹¹, L. Masetti⁸¹, T. Mashimo¹⁵⁵, R. Mashinistov⁹⁴, J. Masik⁸², A.L. Maslennikov¹⁰⁷, I. Massa^{20a,20b}, G. Massaro¹⁰⁵, N. Massol⁵, P. Mastrandrea¹⁴⁸, A. Mastroberardino^{37a,37b}, T. Masubuchi¹⁵⁵, P. Matricon¹¹⁵, H. Matsunaga¹⁵⁵, T. Matsushita⁶⁶, C. Mattravers^{118,c}, J. Maurer⁸³, S.J. Maxfield⁷³, A. Mayne¹³⁹, R. Mazini¹⁵¹, M. Mazur²¹, L. Mazzaferro^{133a,133b}, M. Mazzanti^{89a}, J. Mc Donald⁸⁵, S.P. Mc Kee⁸⁷, A. McCarn¹⁶⁵, R.L. McCarthy¹⁴⁸, T.G. McCarthy²⁹, N.A. McCubbin¹²⁹, K.W. McFarlane^{56,*}, J.A. Mcfayden¹³⁹, G. Mchedlidze^{51b}, T. McLaughlan¹⁸, S.J. McMahon¹²⁹, R.A. McPherson^{169,k}, A. Meade⁸⁴, J. Mechnich¹⁰⁵, M. Mechtel¹⁷⁵, M. Medinnis⁴², R. Meera-Lebbai¹¹¹, T. Meguro¹¹⁶, S. Mehlhase³⁶, A. Mehta⁷³, K. Meier^{58a}, B. Meirose⁷⁹, C. Melachrinou³¹, B.R. Mellado Garcia¹⁷³, F. Meloni^{89a,89b}, L. Mendoza Navas¹⁶², Z. Meng^{151,w}, A. Mengarelli^{20a,20b}, S. Menke⁹⁹, E. Meoni¹⁶¹, K.M. Mercurio⁵⁷, P. Mermod⁴⁹, L. Merola^{102a,102b}, C. Meroni^{89a}, F.S. Merritt³¹, H. Merritt¹⁰⁹, A. Messina^{30,x}, J. Metcalfe²⁵, A.S. Mete¹⁶³, C. Meyer⁸¹, C. Meyer³¹, J.-P. Meyer¹³⁶, J. Meyer¹⁷⁴, J. Meyer⁵⁴, T.C. Meyer³⁰, S. Michal³⁰, L. Micu^{26a}, R.P. Middleton¹²⁹, S. Migas⁷³, L. Mijović¹³⁶, G. Mikenberg¹⁷², M. Mikestikova¹²⁵, M. Mikuž⁷⁴, D.W. Miller³¹, R.J. Miller⁸⁸, W.J. Mills¹⁶⁸, C. Mills⁵⁷, A. Milov¹⁷², D.A. Milstead^{146a,146b}, D. Milstein¹⁷², A.A. Minaenko¹²⁸, M. Miñano Moya¹⁶⁷, I.A. Minashvili⁶⁴, A.I. Mincer¹⁰⁸, B. Mindur³⁸, M. Mineev⁶⁴, Y. Ming¹⁷³, L.M. Mir¹², G. Mirabelli^{132a}, J. Mitrevski¹³⁷, V.A. Mitsou¹⁶⁷, S. Mitsui⁶⁵, P.S. Miyagawa¹³⁹, J.U. Mjörnmark⁷⁹, T. Moa^{146a,146b}, V. Moeller²⁸, K. Mönig⁴², N. Möser²¹, S. Mohapatra¹⁴⁸, W. Mohr⁴⁸, R. Moles-Valls¹⁶⁷, A. Molfetas³⁰, J. Monk⁷⁷, E. Monnier⁸³, J. Montejo Berlingen¹², F. Monticelli⁷⁰, S. Monzani^{20a,20b}, R.W. Moore³, G.F. Moorhead⁸⁶, C. Mora Herrera⁴⁹, A. Moraes⁵³, N. Morange¹³⁶, J. Morel⁵⁴, G. Morello^{37a,37b}, D. Moreno⁸¹, M. Moreno Llácer¹⁶⁷, P. Morettini^{50a}, M. Morgenstern⁴⁴, M. Morii⁵⁷, A.K. Morley³⁰, G. Mornacchi³⁰, J.D. Morris⁷⁵, L. Morvaj¹⁰¹, H.G. Moser⁹⁹, M. Mosidze^{51b}, J. Moss¹⁰⁹, R. Mount¹⁴³, E. Mountricha^{10,y}, S.V. Mouraviev^{94,*}, E.J.W. Moyses⁸⁴, F. Mueller^{58a}, J. Mueller¹²³, K. Mueller²¹, T.A. Müller⁹⁸, T. Mueller⁸¹, D. Muenstermann³⁰, Y. Munwes¹⁵³, W.J. Murray¹²⁹, I. Mussche¹⁰⁵, E. Musto^{102a,102b}, A.G. Myagkov¹²⁸, M. Myska¹²⁵, O. Nackenhorst⁵⁴, J. Nadal¹², K. Nagai¹⁶⁰, R. Nagai¹⁵⁷, K. Nagano⁶⁵, A. Nagarkar¹⁰⁹, Y. Nagasaka⁵⁹, M. Nagel⁹⁹, A.M. Nairz³⁰, Y. Nakahama³⁰, K. Nakamura¹⁵⁵, T. Nakamura¹⁵⁵, I. Nakano¹¹⁰, G. Nanava²¹, A. Napier¹⁶¹, R. Narayan^{58b}, M. Nash^{77,c}, T. Nattermann²¹, T. Naumann⁴², G. Navarro¹⁶², H.A. Neal⁸⁷, P.Yu. Nechaeva⁹⁴, T.J. Neep⁸², A. Negri^{119a,119b}, G. Negri³⁰, M. Negrini^{20a}, S. Nektarijevic⁴⁹, A. Nelson¹⁶³, T.K. Nelson¹⁴³, S. Nemecek¹²⁵, P. Nemethy¹⁰⁸, A.A. Nepomuceno^{24a}, M. Nessi^{30,z}, M.S. Neubauer¹⁶⁵, M. Neumann¹⁷⁵, A. Neusiedl⁸¹, R.M. Neves¹⁰⁸, P. Nevski²⁵, F.M. Newcomer¹²⁰, P.R. Newman¹⁸, V. Nguyen Thi Hong¹³⁶, R.B. Nickerson¹¹⁸, R. Nicolaidou¹³⁶, B. Nicquevert³⁰, F. Niedercorn¹¹⁵, J. Nielsen¹³⁷, N. Nikiforou³⁵, A. Nikiforov¹⁶, V. Nikolaenko¹²⁸, I. Nikolic-Audit⁷⁸, K. Nikolics⁴⁹, K. Nikolopoulos¹⁸, H. Nilsen⁴⁸, P. Nilsson⁸, Y. Ninomiya¹⁵⁵, A. Nisati^{132a}, R. Nisius⁹⁹, T. Nobe¹⁵⁷, L. Nodulman⁶, M. Nomachi¹¹⁶, I. Nomidis¹⁵⁴, S. Norberg¹¹¹, M. Nordberg³⁰, P.R. Norton¹²⁹, J. Novakova¹²⁶, M. Nozaki⁶⁵, L. Nozka¹¹³, I.M. Nugent^{159a}, A.-E. Nuncio-Quiroz²¹, G. Nunes Hanninger⁸⁶, T. Nunnemann⁹⁸, E. Nurse⁷⁷, B.J. O'Brien⁴⁶, D.C. O'Neil¹⁴², V. O'Shea⁵³, L.B. Oakes⁹⁸, F.G. Oakham^{29,d}, H. Oberlack⁹⁹, J. Ocariz⁷⁸, A. Ochi⁶⁶, S. Oda⁶⁹, S. Odaka⁶⁵, J. Odier⁸³, H. Ogren⁶⁰, A. Oh⁸², S.H. Oh⁴⁵, C.C. Ohm³⁰, T. Ohshima¹⁰¹, W. Okamura¹¹⁶, H. Okawa²⁵, Y. Okumura³¹, T. Okuyama¹⁵⁵, A. Olariu^{26a}, A.G. Olchevski⁶⁴, S.A. Olivares Pino^{32a}, M. Oliveira^{124a,h}, D. Oliveira Damazio²⁵, E. Oliver Garcia¹⁶⁷, D. Olivito¹²⁰, A. Olszewski³⁹, J. Olszowska³⁹, A. Onofre^{124a,aa}, P.U.E. Onyisi³¹, C.J. Oram^{159a}, M.J. Oreglia³¹, Y. Oren¹⁵³, D. Orestano^{134a,134b}, N. Orlando^{72a,72b}, I. Orlov¹⁰⁷, C. Oropeza Barrera⁵³, R.S. Orr¹⁵⁸, B. Osculati^{50a,50b}, R. Ospanov¹²⁰, C. Osuna¹², G. Otero y Garzon²⁷, J.P. Ottersbach¹⁰⁵, M. Ouchrif^{135d}, E.A. Ouellette¹⁶⁹, F. Ould-Saada¹¹⁷, A. Ouraou¹³⁶, Q. Ouyang^{33a}, A. Ovcharova¹⁵, M. Owen⁸², S. Owen¹³⁹, V.E. Ozcan^{19a}, N. Ozturk⁸, A. Pacheco Pages¹², C. Padilla Aranda¹², S. Pagan Griso¹⁵, E. Paganis¹³⁹, C. Pahl⁹⁹, F. Paige²⁵, P. Pais⁸⁴, K. Pajchel¹¹⁷, G. Palacino^{159b}, C.P. Paleari⁷, S. Palestini³⁰, D. Pallin³⁴, A. Palma^{124a}, J.D. Palmer¹⁸, Y.B. Pan¹⁷³, E. Panagiotopoulou¹⁰, J.G. Panduro Vazquez⁷⁶, P. Pani¹⁰⁵, N. Panikashvili⁸⁷, S. Panitkin²⁵, D. Pantea^{26a}, A. Papadelis^{146a}, Th.D. Papadopoulou¹⁰, A. Paramonov⁶, D. Paredes Hernandez³⁴, W. Park^{25,ab}, M.A. Parker²⁸, F. Parodi^{50a,50b}, J.A. Parsons³⁵, U. Parzefall⁴⁸, S. Pashapour⁵⁴, E. Pasqualucci^{132a}, S. Passaggio^{50a}, A. Passeri^{134a}, F. Pastore^{134a,134b,*}, Fr. Pastore⁷⁶, G. Pásztor^{49,ac}, S. Pataria¹⁷⁵, N. Patel¹⁵⁰, J.R. Pater⁸², S. Patricelli^{102a,102b}, T. Pauly³⁰, M. Pecsny^{144a}, S. Pedraza Lopez¹⁶⁷, M.I. Pedraza Morales¹⁷³, S.V. Peleganchuk¹⁰⁷, D. Pelikan¹⁶⁶, H. Peng^{33b}, B. Penning³¹, A. Penson³⁵, J. Penwell⁶⁰, M. Perantoni^{24a}, K. Perez^{35,ad}, T. Perez Cavalcanti⁴², E. Perez Codina^{159a}, M.T. Pérez Garcia-Estañ¹⁶⁷, V. Perez Reale³⁵, L. Perini^{89a,89b}, H. Pernegger³⁰, R. Perrino^{72a}, P. Perrodo⁵, V.D. Peshekhonov⁶⁴, K. Peters³⁰, B.A. Petersen³⁰, J. Petersen³⁰, T.C. Petersen³⁶, E. Petit⁵, A. Petridis¹⁵⁴, C. Petridou¹⁵⁴, E. Petrolo^{132a}, F. Petrucci^{134a,134b}, D. Petschull⁴², M. Petteni¹⁴², R. Pezoa^{32b},

A. Phan⁸⁶, P.W. Phillips¹²⁹, G. Piacquadio³⁰, A. Picazio⁴⁹, E. Piccaro⁷⁵, M. Piccinini^{20a,20b}, S.M. Piec⁴²,
 R. Piegai²⁷, D.T. Pignotti¹⁰⁹, J.E. Pilcher³¹, A.D. Pilkington⁸², J. Pina^{124a,b}, M. Pinamonti^{164a,164c}, A. Pinder¹¹⁸,
 J.L. Pinfold³, B. Pinto^{124a}, C. Pizio^{89a,89b}, M. Plamondon¹⁶⁹, M.-A. Pleier²⁵, E. Plotnikova⁶⁴, A. Poblaguev²⁵,
 S. Poddar^{58a}, F. Podlyski³⁴, L. Poggioli¹¹⁵, D. Pohl²¹, M. Pohl⁴⁹, G. Polesello^{119a}, A. Policicchio^{37a,37b}, A. Polini^{20a},
 J. Poll⁷⁵, V. Polychronakos²⁵, D. Pomeroy²³, K. Pommès³⁰, L. Pontecorvo^{132a}, B.G. Pope⁸⁸, G.A. Popenciu^{26a},
 D.S. Popovic^{13a}, A. Poppleton³⁰, X. Portell Bueso³⁰, G.E. Pospelov⁹⁹, S. Pospisil¹²⁷, I.N. Potrap⁹⁹, C.J. Potter¹⁴⁹,
 C.T. Potter¹¹⁴, G. Poulard³⁰, J. Poveda⁶⁰, V. Pozdnyakov⁶⁴, R. Prabhu⁷⁷, P. Pralavorio⁸³, A. Pranko¹⁵,
 S. Prasad³⁰, R. Pravahan²⁵, S. Prell⁶³, K. Pretzl¹⁷, D. Price⁶⁰, J. Price⁷³, L.E. Price⁶, D. Prieur¹²³,
 M. Primavera^{72a}, K. Prokofiev¹⁰⁸, F. Prokoshin^{32b}, S. Protopopescu²⁵, J. Proudfoot⁶, X. Prudent⁴⁴,
 M. Przybycien³⁸, H. Przysieszniak⁵, S. Psoroulas²¹, E. Ptacek¹¹⁴, E. Pueschel⁸⁴, J. Purdham⁸⁷, M. Purohit^{25,ab},
 P. Puzo¹¹⁵, Y. Pylypchenko⁶², J. Qian⁸⁷, A. Quadt⁵⁴, D.R. Quarrie¹⁵, W.B. Quayle¹⁷³, F. Quinonez^{32a}, M. Raas¹⁰⁴,
 V. Radeka²⁵, V. Radescu⁴², P. Radloff¹¹⁴, T. Rador^{19a}, F. Ragusa^{89a,89b}, G. Rahal¹⁷⁸, A.M. Rahimi¹⁰⁹, D. Rahm²⁵,
 S. Rajagopalan²⁵, M. Rammensee⁴⁸, M. Rammes¹⁴¹, A.S. Randle-Conde⁴⁰, K. Randrianarivony²⁹, F. Rauscher⁹⁸,
 T.C. Rave⁴⁸, M. Raymond³⁰, A.L. Read¹¹⁷, D.M. Rebuffi^{119a,119b}, A. Redelbach¹⁷⁴, G. Redlinger²⁵, R. Reece¹²⁰,
 K. Reeves⁴¹, E. Reinherz-Aronis¹⁵³, A. Reinsch¹¹⁴, I. Reisinger⁴³, C. Rembser³⁰, Z.L. Ren¹⁵¹, A. Renaud¹¹⁵,
 M. Rescigno^{132a}, S. Resconi^{89a}, B. Resende¹³⁶, P. Reznicek⁹⁸, R. Rezvani¹⁵⁸, R. Richter⁹⁹, E. Richter-Was^{5,ae},
 M. Ridel⁷⁸, M. Rijpstra¹⁰⁵, M. Rijssenbeek¹⁴⁸, A. Rimoldi^{119a,119b}, L. Rinaldi^{20a}, R.R. Rios⁴⁰, I. Riu¹²,
 G. Rivoltella^{89a,89b}, F. Rizatdinova¹¹², E. Rizvi⁷⁵, S.H. Robertson^{85,k}, A. Robichaud-Veronneau¹¹⁸, D. Robinson²⁸,
 J.E.M. Robinson⁸², A. Robson⁵³, J.G. Rocha de Lima¹⁰⁶, C. Roda^{122a,122b}, D. Roda Dos Santos³⁰, A. Roe⁵⁴,
 S. Roe³⁰, O. Röhne¹¹⁷, S. Rolli¹⁶¹, A. Romaniouk⁹⁶, M. Romano^{20a,20b}, G. Romeo²⁷, E. Romero Adam¹⁶⁷,
 N. Rompotis¹³⁸, L. Roos⁷⁸, E. Ros¹⁶⁷, S. Rosati^{132a}, K. Rosbach⁴⁹, A. Rose¹⁴⁹, M. Rose⁷⁶, G.A. Rosenbaum¹⁵⁸,
 E.I. Rosenberg⁶³, P.L. Rosendahl¹⁴, O. Rosenthal¹⁴¹, L. Rosselet⁴⁹, V. Rossetti¹², E. Rossi^{132a,132b}, L.P. Rossi^{50a},
 M. Rotaru^{26a}, I. Roth¹⁷², J. Rothberg¹³⁸, D. Rousseau¹¹⁵, C.R. Royon¹³⁶, A. Rozanov⁸³, Y. Rozen¹⁵²,
 X. Ruan^{33a,af}, F. Rubbo¹², I. Rubinskiy⁴², N. Ruckstuhl¹⁰⁵, V.I. Rud⁹⁷, C. Rudolph⁴⁴, G. Rudolph⁶¹, F. Rühr⁷,
 A. Ruiz-Martinez⁶³, L. Rumyantsev⁶⁴, Z. Rurikova⁴⁸, N.A. Rusakovich⁶⁴, A. Ruschke⁹⁸, J.P. Rutherford⁷,
 P. Ruzicka¹²⁵, Y.F. Ryabov¹²¹, M. Rybar¹²⁶, G. Rybkin¹¹⁵, N.C. Ryder¹¹⁸, A.F. Saavedra¹⁵⁰, I. Sadeh¹⁵³,
 H.F.-W. Sadrozinski¹³⁷, R. Sadykov⁶⁴, F. Safai Tehrani^{132a}, H. Sakamoto¹⁵⁵, G. Salamanna⁷⁵, A. Salamon^{133a},
 M. Saleem¹¹¹, D. Salek³⁰, D. Salihagic⁹⁹, A. Salmikow¹⁴³, J. Salt¹⁶⁷, B.M. Salvachua Ferrando⁶, D. Salvatore^{37a,37b},
 F. Salvatore¹⁴⁹, A. Salvucci¹⁰⁴, A. Salzburger³⁰, D. Sampsonidis¹⁵⁴, B.H. Samset¹¹⁷, A. Sanchez^{102a,102b},
 V. Sanchez Martinez¹⁶⁷, H. Sandaker¹⁴, H.G. Sander⁸¹, M.P. Sanders⁹⁸, M. Sandhoff¹⁷⁵, T. Sandoval²⁸,
 C. Sandoval¹⁶², R. Sandstroem⁹⁹, D.P.C. Sankey¹²⁹, A. Sansoni⁴⁷, C. Santamarina Rios⁸⁵, C. Santoni³⁴,
 R. Santonicio^{133a,133b}, H. Santos^{124a}, J.G. Saraiva^{124a}, T. Sarangi¹⁷³, E. Sarkisyan-Grinbaum⁸, F. Sarri^{122a,122b},
 G. Sartiso¹⁷⁵, O. Sasaki⁶⁵, Y. Sasaki¹⁵⁵, N. Sasao⁶⁷, I. Satsounkevitch⁹⁰, G. Sauvage^{5,*}, E. Sauvan⁵,
 J.B. Sauvan¹¹⁵, P. Savard^{158,d}, V. Savinov¹²³, D.O. Savu³⁰, L. Sawyer^{25,m}, D.H. Saxon⁵³, J. Saxon¹²⁰, C. Sbarra^{20a},
 A. Sbrizzi^{20a,20b}, D.A. Scannicchio¹⁶³, M. Scarcella¹⁵⁰, J. Schaarschmidt¹¹⁵, P. Schacht⁹⁹, D. Schaefer¹²⁰,
 U. Schäfer⁸¹, A. Schaelicke⁴⁶, S. Schaepe²¹, S. Schaezel^{58b}, A.C. Schaffer¹¹⁵, D. Schaile⁹⁸, R.D. Schamberger¹⁴⁸,
 A.G. Schamov¹⁰⁷, V. Scharf^{58a}, V.A. Schegelsky¹²¹, D. Scheirich⁸⁷, M. Schernau¹⁶³, M.I. Scherzer³⁵,
 C. Schiavi^{50a,50b}, J. Schieck⁹⁸, M. Schioppa^{37a,37b}, S. Schlenker³⁰, E. Schmidt⁴⁸, K. Schmieden²¹, C. Schmitt⁸¹,
 S. Schmitt^{58b}, M. Schmitz²¹, B. Schneider¹⁷, U. Schnoor⁴⁴, L. Schoeffel¹³⁶, A. Schoening^{58b}, A.L.S. Schorlemmer⁵⁴,
 M. Schott³⁰, D. Schouten^{159a}, J. Schovancova¹²⁵, M. Schram⁸⁵, C. Schroeder⁸¹, N. Schroer^{58c}, M.J. Schultens²¹,
 J. Schultes¹⁷⁵, H.-C. Schultz-Coulon^{58a}, H. Schulz¹⁶, M. Schumacher⁴⁸, B.A. Schumm¹³⁷, Ph. Schune¹³⁶,
 C. Schwanenberger⁸², A. Schwartzman¹⁴³, Ph. Schwegler⁹⁹, Ph. Schwemling⁷⁸, R. Schwienhorst⁸⁸, R. Schwierz⁴⁴,
 J. Schwindling¹³⁶, T. Schwindt²¹, M. Schwoerer⁵, G. Sciolla²³, W.G. Scott¹²⁹, J. Searcy¹¹⁴, G. Sedov⁴²,
 E. Sedykh¹²¹, S.C. Seidel¹⁰³, A. Seiden¹³⁷, F. Seifert⁴⁴, J.M. Seixas^{24a}, G. Sekhniadze^{102a}, S.J. Sekula⁴⁰,
 K.E. Selbach⁴⁶, D.M. Seliverstov¹²¹, B. Sellden^{146a}, G. Sellers⁷³, M. Seman^{144b}, N. Semprini-Cesari^{20a,20b},
 C. Serfon⁹⁸, L. Serin¹¹⁵, L. Serkin⁵⁴, R. Seuster^{159a}, H. Severini¹¹¹, A. Sfyrla³⁰, E. Shabalina⁵⁴, M. Shamim¹¹⁴,
 L.Y. Shan^{33a}, J.T. Shank²², Q.T. Shao⁸⁶, M. Shapiro¹⁵, P.B. Shatalov⁹⁵, K. Shaw^{164a,164c}, D. Sherman¹⁷⁶,
 P. Sherwood⁷⁷, S. Shimizu¹⁰¹, M. Shimojima¹⁰⁰, T. Shin⁵⁶, M. Shiyakova⁶⁴, A. Shmeleva⁹⁴, M.J. Shochet³¹,
 D. Short¹¹⁸, S. Shrestha⁶³, E. Shulga⁹⁶, M.A. Shupe⁷, P. Sicho¹²⁵, A. Sidoti^{132a}, F. Siegert⁴⁸, Dj. Sijacki^{13a},
 O. Silbert¹⁷², J. Silva^{124a}, Y. Silver¹⁵³, D. Silverstein¹⁴³, S.B. Silverstein^{146a}, V. Simak¹²⁷, O. Simard¹³⁶,
 Lj. Simic^{13a}, S. Simion¹¹⁵, E. Simioni⁸¹, B. Simmons⁷⁷, R. Simonello^{89a,89b}, M. Simonyan³⁶, P. Sinervo¹⁵⁸,
 N.B. Sinev¹¹⁴, V. Sipica¹⁴¹, G. Siragusa¹⁷⁴, A. Sircar²⁵, A.N. Sisakyan^{64,*}, S.Yu. Sivoklokov⁹⁷, J. Sjölin^{146a,146b},
 T.B. Sjursen¹⁴, L.A. Skinnari¹⁵, H.P. Skottowe⁵⁷, K. Skovpen¹⁰⁷, P. Skubic¹¹¹, M. Slater¹⁸, T. Slavicek¹²⁷,
 K. Sliwa¹⁶¹, V. Smakhtin¹⁷², B.H. Smart⁴⁶, L. Smestad¹¹⁷, S.Yu. Smirnov⁹⁶, Y. Smirnov⁹⁶, L.N. Smirnova⁹⁷,
 O. Smirnova⁷⁹, B.C. Smith⁵⁷, D. Smith¹⁴³, K.M. Smith⁵³, M. Smizanska⁷¹, K. Smolek¹²⁷, A.A. Snesarev⁹⁴,
 S.W. Snow⁸², J. Snow¹¹¹, S. Snyder²⁵, R. Sobie^{169,k}, J. Sodomka¹²⁷, A. Soffer¹⁵³, C.A. Solans¹⁶⁷, M. Solar¹²⁷,
 J. Solc¹²⁷, E.Yu. Soldatov⁹⁶, U. Soldevila¹⁶⁷, E. Solfaroli Camillocci^{132a,132b}, A.A. Solodkov¹²⁸, O.V. Solovyanov¹²⁸,
 V. Solovyev¹²¹, N. Soni¹, V. Sopko¹²⁷, B. Sopko¹²⁷, M. Sosebee⁸, R. Soualah^{164a,164c}, A. Soukharev¹⁰⁷,

S. Spagnolo^{72a,72b}, F. Spano⁷⁶, R. Spighi^{20a}, G. Spigo³⁰, R. Spiwoks³⁰, M. Spousta^{126,ag}, T. Spreitzer¹⁵⁸, B. Spurlock⁸, R.D. St. Denis⁵³, J. Stahlman¹²⁰, R. Stamen^{58a}, E. Stanecka³⁹, R.W. Stanek⁶, C. Stanescu^{134a}, M. Stanescu-Bellu⁴², M.M. Stanitzki⁴², S. Stapnes¹¹⁷, E.A. Starchenko¹²⁸, J. Stark⁵⁵, P. Staroba¹²⁵, P. Starovoitov⁴², R. Staszewski³⁹, A. Staude⁹⁸, P. Stavina^{144a,*}, G. Steele⁵³, P. Steinbach⁴⁴, P. Steinberg²⁵, I. Stekl¹²⁷, B. Stelzer¹⁴², H.J. Stelzer⁸⁸, O. Stelzer-Chilton^{159a}, H. Stenzel⁵², S. Stern⁹⁹, G.A. Stewart³⁰, J.A. Stillings²¹, M.C. Stockton⁸⁵, K. Stoerig⁴⁸, G. Stoicea^{26a}, S. Stonjek⁹⁹, P. Strachota¹²⁶, A.R. Stradling⁸, A. Straessner⁴⁴, J. Strandberg¹⁴⁷, S. Strandberg^{146a,146b}, A. Strandlie¹¹⁷, M. Strang¹⁰⁹, E. Strauss¹⁴³, M. Strauss¹¹¹, P. Strizenc^{144b}, R. Ströhmer¹⁷⁴, D.M. Strom¹¹⁴, J.A. Strong^{76,*}, R. Stroyanowski⁴⁰, B. Stugu¹⁴, I. Stumer^{25,*}, J. Stupak¹⁴⁸, P. Sturm¹⁷⁵, N.A. Styles⁴², D.A. Soh^{151,u}, D. Su¹⁴³, HS. Subramania³, R. Subramaniam²⁵, A. Succuro¹², Y. Sugaya¹¹⁶, C. Suhr¹⁰⁶, M. Suk¹²⁶, V.V. Sulin⁹⁴, S. Sultansoy^{4d}, T. Sumida⁶⁷, X. Sun⁵⁵, J.E. Sundermann⁴⁸, K. Suruliz¹³⁹, G. Susinno^{37a,37b}, M.R. Sutton¹⁴⁹, Y. Suzuki⁶⁵, Y. Suzuki⁶⁶, M. Svatos¹²⁵, S. Swedish¹⁶⁸, I. Sykora^{144a}, T. Sykora¹²⁶, J. Sánchez¹⁶⁷, D. Ta¹⁰⁵, K. Tackmann⁴², A. Taffard¹⁶³, R. Tafirout^{159a}, N. Taiblum¹⁵³, Y. Takahashi¹⁰¹, H. Takai²⁵, R. Takashima⁶⁸, H. Takeda⁶⁶, T. Takeshita¹⁴⁰, Y. Takubo⁶⁵, M. Talby⁸³, A. Talyshv^{107,f}, M.C. Tamsett²⁵, K.G. Tan⁸⁶, J. Tanaka¹⁵⁵, R. Tanaka¹¹⁵, S. Tanaka¹³¹, S. Tanaka⁶⁵, A.J. Tanasijczuk¹⁴², K. Tani⁶⁶, N. Tannoury⁸³, S. Tapprogge⁸¹, D. Tardif¹⁵⁸, S. Tarem¹⁵², F. Tarrade²⁹, G.F. Tartarelli^{89a}, P. Tas¹²⁶, M. Tasevsky¹²⁵, E. Tassi^{37a,37b}, M. Tatarkhanov¹⁵, Y. Tayalati^{135d}, C. Taylor⁷⁷, F.E. Taylor⁹², G.N. Taylor⁸⁶, W. Taylor^{159b}, M. Teinturier¹¹⁵, F.A. Teischinger³⁰, M. Teixeira Dias Castanheira⁷⁵, P. Teixeira-Dias⁷⁶, K.K. Temming⁴⁸, H. Ten Kate³⁰, P.K. Teng¹⁵¹, S. Terada⁶⁵, K. Terashi¹⁵⁵, J. Terron⁸⁰, M. Testa⁴⁷, R.J. Teuscher^{158,k}, J. Therhaag²¹, T. Theveneaux-Pelzer⁷⁸, S. Thoma⁴⁸, J.P. Thomas¹⁸, E.N. Thompson³⁵, P.D. Thompson¹⁸, P.D. Thompson¹⁵⁸, A.S. Thompson⁵³, L.A. Thomsen³⁶, E. Thomson¹²⁰, M. Thomson²⁸, W.M. Thong⁸⁶, R.P. Thun⁸⁷, F. Tian³⁵, M.J. Tibbetts¹⁵, T. Tic¹²⁵, V.O. Tikhomirov⁹⁴, Y.A. Tikhonov^{107,f}, S. Timoshenko⁹⁶, E. Tiouchichine⁸³, P. Tipton¹⁷⁶, S. Tisserant⁸³, T. Todorov⁵, S. Todorova-Nova¹⁶¹, B. Toggerson¹⁶³, J. Tojo⁶⁹, S. Tokár^{144a}, K. Tokushuku⁶⁵, K. Tollefsen⁸⁸, M. Tomoto¹⁰¹, L. Tompkins³¹, K. Toms¹⁰³, A. Tonoyan¹⁴, C. Topfel¹⁷, N.D. Topilin⁶⁴, I. Torchiani³⁰, E. Torrence¹¹⁴, H. Torres⁷⁸, E. Torró Pastor¹⁶⁷, J. Toth^{83,ac}, F. Touchard⁸³, D.R. Tovey¹³⁹, T. Trefzger¹⁷⁴, L. Tremblet³⁰, A. Tricoli³⁰, I.M. Trigger^{159a}, S. Trincaz-Duvold⁷⁸, M.F. Tripiana⁷⁰, N. Triplett²⁵, W. Trischuk¹⁵⁸, B. Trocme⁵⁵, C. Troncon^{89a}, M. Trottier-McDonald¹⁴², P. True⁸⁸, M. Trzebinski³⁹, A. Trzupek³⁹, C. Tsarouchas³⁰, J.C.-L. Tseng¹¹⁸, M. Tsiakiris¹⁰⁵, P.V. Tsiareshka⁹⁰, D. Tsiounou^{5,ah}, G. Tsiopolitis¹⁰, S. Tsiskaridze¹², V. Tsiskaridze⁴⁸, E.G. Tskhadadze^{51a}, I.I. Tsukerman⁹⁵, V. Tsulaia¹⁵, J.-W. Tsung²¹, S. Tsuno⁶⁵, D. Tsybychev¹⁴⁸, A. Tua¹³⁹, A. Tudorache^{26a}, V. Tudorache^{26a}, J.M. Tuggle³¹, M. Turala³⁹, D. Turecek¹²⁷, I. Turk Cakir^{4e}, E. Turlay¹⁰⁵, R. Turra^{89a,89b}, P.M. Tuts³⁵, A. Tykhonov⁷⁴, M. Tylmad^{146a,146b}, M. Tyndel¹²⁹, G. Tzanakos⁹, K. Uchida²¹, I. Ueda¹⁵⁵, R. Ueno²⁹, M. Uglund¹⁴, M. Uhlenbrock²¹, M. Uhrmacher⁵⁴, F. Ukegawa¹⁶⁰, G. Unal³⁰, A. Undrus²⁵, G. Unel¹⁶³, Y. Unno⁶⁵, D. Urbaniec³⁵, P. Urquijo²¹, G. Usai⁸, M. Uslenghi^{119a,119b}, L. Vacavant⁸³, V. Vacek¹²⁷, B. Vachon⁸⁵, S. Vahsen¹⁵, J. Valenta¹²⁵, S. Valentinetti^{20a,20b}, A. Valero¹⁶⁷, S. Valkar¹²⁶, E. Valladolid Gallego¹⁶⁷, S. Vallecorsa¹⁵², J.A. Valls Ferrer¹⁶⁷, R. Van Berg¹²⁰, P.C. Van Der Deijl¹⁰⁵, R. van der Geer¹⁰⁵, H. van der Graaf¹⁰⁵, R. Van Der Leeuw¹⁰⁵, E. van der Poel¹⁰⁵, D. van der Ster³⁰, N. van Eldik³⁰, P. van Gemmeren⁶, I. van Vulpen¹⁰⁵, M. Vanadia⁹⁹, W. Vandelli³⁰, A. Vaniachine⁶, P. Vankov⁴², F. Vannucci⁷⁸, R. Vari^{132a}, T. Varol⁸⁴, D. Varouchas¹⁵, A. Vartapetian⁸, K.E. Varvell¹⁵⁰, V.I. Vassilakopoulos⁵⁶, F. Vazeille³⁴, T. Vazquez Schroeder⁵⁴, G. Vegni^{89a,89b}, J.J. Veillet¹¹⁵, F. Veloso^{124a}, R. Veness³⁰, S. Veneziano^{132a}, A. Ventura^{72a,72b}, D. Ventura⁸⁴, M. Venturi⁴⁸, N. Venturi¹⁵⁸, V. Vercesi^{119a}, M. Verducci¹³⁸, W. Verkerke¹⁰⁵, J.C. Vermeulen¹⁰⁵, A. Vest⁴⁴, M.C. Vetterli^{142,d}, I. Vichou¹⁶⁵, T. Vickey^{145b,ai}, O.E. Vickey Boeriu^{145b}, G.H.A. Viehhauser¹¹⁸, S. Viel¹⁶⁸, M. Villa^{20a,20b}, M. Villaplana Perez¹⁶⁷, E. Vilucchi⁴⁷, M.G. Vincker²⁹, E. Vinek³⁰, V.B. Vinogradov⁶⁴, M. Virchaux^{136,*}, J. Virzi¹⁵, O. Vitells¹⁷², M. Viti⁴², I. Vivarelli⁴⁸, F. Vives Vaque³, S. Vlachos¹⁰, D. Vladouiu⁹⁸, M. Vlasak¹²⁷, A. Vogel²¹, P. Vokac¹²⁷, G. Volpi⁴⁷, M. Volpi⁸⁶, G. Volpini^{89a}, H. von der Schmitt⁹⁹, H. von Radziewski⁴⁸, E. von Toerne²¹, V. Vorobel¹²⁶, V. Vorwerk¹², M. Vos¹⁶⁷, R. Voss³⁰, T.T. Voss¹⁷⁵, J.H. Vossebeld⁷³, N. Vranjes¹³⁶, M. Vranjes Milosavljevic¹⁰⁵, V. Vrba¹²⁵, M. Vreeswijk¹⁰⁵, T. Vu Anh⁴⁸, R. Vuillermet³⁰, I. Vukotic³¹, W. Wagner¹⁷⁵, P. Wagner¹²⁰, H. Wahlen¹⁷⁵, S. Wahrenmund⁴⁴, J. Wakabayashi¹⁰¹, S. Walch⁸⁷, J. Walder⁷¹, R. Walker⁹⁸, W. Walkowiak¹⁴¹, R. Wall¹⁷⁶, P. Waller⁷³, B. Walsh¹⁷⁶, C. Wang⁴⁵, H. Wang¹⁷³, H. Wang^{33b,aj}, J. Wang¹⁵¹, J. Wang⁵⁵, R. Wang¹⁰³, S.M. Wang¹⁵¹, T. Wang²¹, A. Warburton⁸⁵, C.P. Ward²⁸, D.R. Wardrope⁷⁷, M. Warsinsky⁴⁸, A. Washbrook⁴⁶, C. Wasicki⁴², I. Watanabe⁶⁶, P.M. Watkins¹⁸, A.T. Watson¹⁸, I.J. Watson¹⁵⁰, M.F. Watson¹⁸, G. Watts¹³⁸, S. Watts⁸², A.T. Waugh¹⁵⁰, B.M. Waugh⁷⁷, M.S. Weber¹⁷, P. Weber⁵⁴, J.S. Webster³¹, A.R. Weidberg¹¹⁸, P. Weigell⁹⁹, J. Weingarten⁵⁴, C. Weiser⁴⁸, P.S. Wells³⁰, T. Wenaus²⁵, D. Wendland¹⁶, Z. Weng^{151,u}, T. Wengler³⁰, S. Wenig³⁰, N. Wermes²¹, M. Werner⁴⁸, P. Werner³⁰, M. Werth¹⁶³, M. Wessels^{58a}, J. Wetter¹⁶¹, C. Weydert⁵⁵, K. Whalen²⁹, A. White⁸, M.J. White⁸⁶, S. White^{122a,122b}, S.R. Whitehead¹¹⁸, D. Whiteson¹⁶³, D. Whittington⁶⁰, F. Wicek¹¹⁵, D. Wicke¹⁷⁵, F.J. Wickens¹²⁹, W. Wiedenmann¹⁷³, M. Wielers¹²⁹, P. Wienemann²¹, C. Wiglesworth⁷⁵, L.A.M. Wiik-Fuchs²¹, P.A. Wijeratne⁷⁷, A. Wildauer⁹⁹, M.A. Wildt^{42,r}, I. Wilhelm¹²⁶, H.G. Wilkens³⁰, J.Z. Will⁹⁸, E. Williams³⁵, H.H. Williams¹²⁰, W. Willis³⁵, S. Willocq⁸⁴, J.A. Wilson¹⁸, M.G. Wilson¹⁴³, A. Wilson⁸⁷, I. Wingerter-Seez⁵,

S. Winkelmann⁴⁸, F. Winklmeier³⁰, M. Wittgen¹⁴³, S.J. Wollstadt⁸¹, M.W. Wolter³⁹, H. Wolters^{124a,h}, W.C. Wong⁴¹, G. Wooden⁸⁷, B.K. Wosiek³⁹, J. Wotschack³⁰, M.J. Woudstra⁸², K.W. Wozniak³⁹, K. Wraight⁵³, M. Wright⁵³, B. Wrona⁷³, S.L. Wu¹⁷³, X. Wu⁴⁹, Y. Wu^{33b,ak}, E. Wulf³⁵, B.M. Wynne⁴⁶, S. Xella³⁶, M. Xiao¹³⁶, S. Xie⁴⁸, C. Xu^{33b,y}, D. Xu¹³⁹, B. Yabsley¹⁵⁰, S. Yacoob^{145a,al}, M. Yamada⁶⁵, H. Yamaguchi¹⁵⁵, A. Yamamoto⁶⁵, K. Yamamoto⁶³, S. Yamamoto¹⁵⁵, T. Yamamura¹⁵⁵, T. Yamanaka¹⁵⁵, T. Yamazaki¹⁵⁵, Y. Yamazaki⁶⁶, Z. Yan²², H. Yang⁸⁷, U.K. Yang⁸², Y. Yang¹⁰⁹, Z. Yang^{146a,146b}, S. Yanush⁹¹, L. Yao^{33a}, Y. Yao¹⁵, Y. Yasu⁶⁵, G.V. Ybeles Smit¹³⁰, J. Ye⁴⁰, S. Ye²⁵, M. Yilmaz^{4c}, R. Yoosofmiya¹²³, K. Yorita¹⁷¹, R. Yoshida⁶, K. Yoshihara¹⁵⁵, C. Young¹⁴³, C.J. Young¹¹⁸, S. Youssef²², D. Yu²⁵, J. Yu⁸, J. Yu¹¹², L. Yuan⁶⁶, A. Yurkewicz¹⁰⁶, B. Zabinski³⁹, R. Zaidan⁶², A.M. Zaitsev¹²⁸, Z. Zajacova³⁰, L. Zanello^{132a,132b}, D. Zanzi⁹⁹, A. Zaytsev²⁵, C. Zeitnitz¹⁷⁵, M. Zeman¹²⁵, A. Zemla³⁹, C. Zender²¹, O. Zenin¹²⁸, T. Ženiš^{144a}, Z. Zinonos^{122a,122b}, S. Zenz¹⁵, D. Zerwas¹¹⁵, G. Zevi della Porta⁵⁷, D. Zhang^{33b,aj}, H. Zhang⁸⁸, J. Zhang⁶, X. Zhang^{33d}, Z. Zhang¹¹⁵, L. Zhao¹⁰⁸, Z. Zhao^{33b}, A. Zhemchugov⁶⁴, J. Zhong¹¹⁸, B. Zhou⁸⁷, N. Zhou¹⁶³, Y. Zhou¹⁵¹, C.G. Zhu^{33d}, H. Zhu⁴², J. Zhu⁸⁷, Y. Zhu^{33b}, X. Zhuang⁹⁸, V. Zhuravlov⁹⁹, A. Zibell⁹⁸, D. Zieminska⁶⁰, N.I. Zimin⁶⁴, R. Zimmermann²¹, S. Zimmermann²¹, S. Zimmermann⁴⁸, M. Ziolkowski¹⁴¹, R. Zitoun⁵, L. Živković³⁵, V.V. Zmouchko^{128,*}, G. Zobernig¹⁷³, A. Zoccoli^{20a,20b}, M. zur Nedden¹⁶, V. Zutshi¹⁰⁶, L. Zwalinski³⁰.

¹ School of Chemistry and Physics, University of Adelaide, Adelaide, Australia

² Physics Department, SUNY Albany, Albany NY, United States of America

³ Department of Physics, University of Alberta, Edmonton AB, Canada

⁴ (a) Department of Physics, Ankara University, Ankara; (b) Department of Physics, Dumlupinar University, Kutahya; (c) Department of Physics, Gazi University, Ankara; (d) Division of Physics, TOBB University of Economics and Technology, Ankara; (e) Turkish Atomic Energy Authority, Ankara, Turkey

⁵ LAPP, CNRS/IN2P3 and Université de Savoie, Annecy-le-Vieux, France

⁶ High Energy Physics Division, Argonne National Laboratory, Argonne IL, United States of America

⁷ Department of Physics, University of Arizona, Tucson AZ, United States of America

⁸ Department of Physics, The University of Texas at Arlington, Arlington TX, United States of America

⁹ Physics Department, University of Athens, Athens, Greece

¹⁰ Physics Department, National Technical University of Athens, Zografou, Greece

¹¹ Institute of Physics, Azerbaijan Academy of Sciences, Baku, Azerbaijan

¹² Institut de Física d'Altes Energies and Departament de Física de la Universitat Autònoma de Barcelona and ICREA, Barcelona, Spain

¹³ (a) Institute of Physics, University of Belgrade, Belgrade; (b) Vinca Institute of Nuclear Sciences, University of Belgrade, Belgrade, Serbia

¹⁴ Department for Physics and Technology, University of Bergen, Bergen, Norway

¹⁵ Physics Division, Lawrence Berkeley National Laboratory and University of California, Berkeley CA, United States of America

¹⁶ Department of Physics, Humboldt University, Berlin, Germany

¹⁷ Albert Einstein Center for Fundamental Physics and Laboratory for High Energy Physics, University of Bern, Bern, Switzerland

¹⁸ School of Physics and Astronomy, University of Birmingham, Birmingham, United Kingdom

¹⁹ (a) Department of Physics, Bogazici University, Istanbul; (b) Division of Physics, Dogus University, Istanbul; (c) Department of Physics Engineering, Gaziantep University, Gaziantep; (d) Department of Physics, Istanbul Technical University, Istanbul, Turkey

²⁰ (a) INFN Sezione di Bologna; (b) Dipartimento di Fisica, Università di Bologna, Bologna, Italy

²¹ Physikalisches Institut, University of Bonn, Bonn, Germany

²² Department of Physics, Boston University, Boston MA, United States of America

²³ Department of Physics, Brandeis University, Waltham MA, United States of America

²⁴ (a) Universidade Federal do Rio De Janeiro COPPE/EE/IF, Rio de Janeiro; (b) Federal University of Juiz de Fora (UFJF), Juiz de Fora; (c) Federal University of Sao Joao del Rei (UFSJ), Sao Joao del Rei; (d) Instituto de Fisica, Universidade de Sao Paulo, Sao Paulo, Brazil

²⁵ Physics Department, Brookhaven National Laboratory, Upton NY, United States of America

²⁶ (a) National Institute of Physics and Nuclear Engineering, Bucharest; (b) University Politehnica Bucharest, Bucharest; (c) West University in Timisoara, Timisoara, Romania

²⁷ Departamento de Física, Universidad de Buenos Aires, Buenos Aires, Argentina

²⁸ Cavendish Laboratory, University of Cambridge, Cambridge, United Kingdom

²⁹ Department of Physics, Carleton University, Ottawa ON, Canada

³⁰ CERN, Geneva, Switzerland

³¹ Enrico Fermi Institute, University of Chicago, Chicago IL, United States of America

- 32 ^(a) Departamento de Física, Pontificia Universidad Católica de Chile, Santiago; ^(b) Departamento de Física, Universidad Técnica Federico Santa María, Valparaíso, Chile
- 33 ^(a) Institute of High Energy Physics, Chinese Academy of Sciences, Beijing; ^(b) Department of Modern Physics, University of Science and Technology of China, Anhui; ^(c) Department of Physics, Nanjing University, Jiangsu; ^(d) School of Physics, Shandong University, Shandong, China
- 34 Laboratoire de Physique Corpusculaire, Clermont Université and Université Blaise Pascal and CNRS/IN2P3, Clermont-Ferrand, France
- 35 Nevis Laboratory, Columbia University, Irvington NY, United States of America
- 36 Niels Bohr Institute, University of Copenhagen, Kobenhavn, Denmark
- 37 ^(a) INFN Gruppo Collegato di Cosenza; ^(b) Dipartimento di Fisica, Università della Calabria, Arcavata di Rende, Italy
- 38 AGH University of Science and Technology, Faculty of Physics and Applied Computer Science, Krakow, Poland
- 39 The Henryk Niewodniczanski Institute of Nuclear Physics, Polish Academy of Sciences, Krakow, Poland
- 40 Physics Department, Southern Methodist University, Dallas TX, United States of America
- 41 Physics Department, University of Texas at Dallas, Richardson TX, United States of America
- 42 DESY, Hamburg and Zeuthen, Germany
- 43 Institut für Experimentelle Physik IV, Technische Universität Dortmund, Dortmund, Germany
- 44 Institut für Kern- und Teilchenphysik, Technical University Dresden, Dresden, Germany
- 45 Department of Physics, Duke University, Durham NC, United States of America
- 46 SUPA - School of Physics and Astronomy, University of Edinburgh, Edinburgh, United Kingdom
- 47 INFN Laboratori Nazionali di Frascati, Frascati, Italy
- 48 Fakultät für Mathematik und Physik, Albert-Ludwigs-Universität, Freiburg, Germany
- 49 Section de Physique, Université de Genève, Geneva, Switzerland
- 50 ^(a) INFN Sezione di Genova; ^(b) Dipartimento di Fisica, Università di Genova, Genova, Italy
- 51 ^(a) E. Andronikashvili Institute of Physics, Iv. Javakishvili Tbilisi State University, Tbilisi; ^(b) High Energy Physics Institute, Tbilisi State University, Tbilisi, Georgia
- 52 II Physikalisches Institut, Justus-Liebig-Universität Giessen, Giessen, Germany
- 53 SUPA - School of Physics and Astronomy, University of Glasgow, Glasgow, United Kingdom
- 54 II Physikalisches Institut, Georg-August-Universität, Göttingen, Germany
- 55 Laboratoire de Physique Subatomique et de Cosmologie, Université Joseph Fourier and CNRS/IN2P3 and Institut National Polytechnique de Grenoble, Grenoble, France
- 56 Department of Physics, Hampton University, Hampton VA, United States of America
- 57 Laboratory for Particle Physics and Cosmology, Harvard University, Cambridge MA, United States of America
- 58 ^(a) Kirchhoff-Institut für Physik, Ruprecht-Karls-Universität Heidelberg, Heidelberg; ^(b) Physikalisches Institut, Ruprecht-Karls-Universität Heidelberg, Heidelberg; ^(c) ZITI Institut für technische Informatik, Ruprecht-Karls-Universität Heidelberg, Mannheim, Germany
- 59 Faculty of Applied Information Science, Hiroshima Institute of Technology, Hiroshima, Japan
- 60 Department of Physics, Indiana University, Bloomington IN, United States of America
- 61 Institut für Astro- und Teilchenphysik, Leopold-Franzens-Universität, Innsbruck, Austria
- 62 University of Iowa, Iowa City IA, United States of America
- 63 Department of Physics and Astronomy, Iowa State University, Ames IA, United States of America
- 64 Joint Institute for Nuclear Research, JINR Dubna, Dubna, Russia
- 65 KEK, High Energy Accelerator Research Organization, Tsukuba, Japan
- 66 Graduate School of Science, Kobe University, Kobe, Japan
- 67 Faculty of Science, Kyoto University, Kyoto, Japan
- 68 Kyoto University of Education, Kyoto, Japan
- 69 Department of Physics, Kyushu University, Fukuoka, Japan
- 70 Instituto de Física La Plata, Universidad Nacional de La Plata and CONICET, La Plata, Argentina
- 71 Physics Department, Lancaster University, Lancaster, United Kingdom
- 72 ^(a) INFN Sezione di Lecce; ^(b) Dipartimento di Matematica e Fisica, Università del Salento, Lecce, Italy
- 73 Oliver Lodge Laboratory, University of Liverpool, Liverpool, United Kingdom
- 74 Department of Physics, Jožef Stefan Institute and University of Ljubljana, Ljubljana, Slovenia
- 75 School of Physics and Astronomy, Queen Mary University of London, London, United Kingdom
- 76 Department of Physics, Royal Holloway University of London, Surrey, United Kingdom
- 77 Department of Physics and Astronomy, University College London, London, United Kingdom
- 78 Laboratoire de Physique Nucléaire et de Hautes Energies, UPMC and Université Paris-Diderot and CNRS/IN2P3, Paris, France
- 79 Fysiska institutionen, Lunds universitet, Lund, Sweden

- 80 Departamento de Fisica Teorica C-15, Universidad Autonoma de Madrid, Madrid, Spain
- 81 Institut für Physik, Universität Mainz, Mainz, Germany
- 82 School of Physics and Astronomy, University of Manchester, Manchester, United Kingdom
- 83 CPPM, Aix-Marseille Université and CNRS/IN2P3, Marseille, France
- 84 Department of Physics, University of Massachusetts, Amherst MA, United States of America
- 85 Department of Physics, McGill University, Montreal QC, Canada
- 86 School of Physics, University of Melbourne, Victoria, Australia
- 87 Department of Physics, The University of Michigan, Ann Arbor MI, United States of America
- 88 Department of Physics and Astronomy, Michigan State University, East Lansing MI, United States of America
- 89 ^(a) INFN Sezione di Milano; ^(b) Dipartimento di Fisica, Università di Milano, Milano, Italy
- 90 B.I. Stepanov Institute of Physics, National Academy of Sciences of Belarus, Minsk, Republic of Belarus
- 91 National Scientific and Educational Centre for Particle and High Energy Physics, Minsk, Republic of Belarus
- 92 Department of Physics, Massachusetts Institute of Technology, Cambridge MA, United States of America
- 93 Group of Particle Physics, University of Montreal, Montreal QC, Canada
- 94 P.N. Lebedev Institute of Physics, Academy of Sciences, Moscow, Russia
- 95 Institute for Theoretical and Experimental Physics (ITEP), Moscow, Russia
- 96 Moscow Engineering and Physics Institute (MEPhI), Moscow, Russia
- 97 Skobeltsyn Institute of Nuclear Physics, Lomonosov Moscow State University, Moscow, Russia
- 98 Fakultät für Physik, Ludwig-Maximilians-Universität München, München, Germany
- 99 Max-Planck-Institut für Physik (Werner-Heisenberg-Institut), München, Germany
- 100 Nagasaki Institute of Applied Science, Nagasaki, Japan
- 101 Graduate School of Science and Kobayashi-Maskawa Institute, Nagoya University, Nagoya, Japan
- 102 ^(a) INFN Sezione di Napoli; ^(b) Dipartimento di Scienze Fisiche, Università di Napoli, Napoli, Italy
- 103 Department of Physics and Astronomy, University of New Mexico, Albuquerque NM, United States of America
- 104 Institute for Mathematics, Astrophysics and Particle Physics, Radboud University Nijmegen/Nikhef, Nijmegen, Netherlands
- 105 Nikhef National Institute for Subatomic Physics and University of Amsterdam, Amsterdam, Netherlands
- 106 Department of Physics, Northern Illinois University, DeKalb IL, United States of America
- 107 Budker Institute of Nuclear Physics, SB RAS, Novosibirsk, Russia
- 108 Department of Physics, New York University, New York NY, United States of America
- 109 Ohio State University, Columbus OH, United States of America
- 110 Faculty of Science, Okayama University, Okayama, Japan
- 111 Homer L. Dodge Department of Physics and Astronomy, University of Oklahoma, Norman OK, United States of America
- 112 Department of Physics, Oklahoma State University, Stillwater OK, United States of America
- 113 Palacký University, RCPTM, Olomouc, Czech Republic
- 114 Center for High Energy Physics, University of Oregon, Eugene OR, United States of America
- 115 LAL, Université Paris-Sud and CNRS/IN2P3, Orsay, France
- 116 Graduate School of Science, Osaka University, Osaka, Japan
- 117 Department of Physics, University of Oslo, Oslo, Norway
- 118 Department of Physics, Oxford University, Oxford, United Kingdom
- 119 ^(a) INFN Sezione di Pavia; ^(b) Dipartimento di Fisica, Università di Pavia, Pavia, Italy
- 120 Department of Physics, University of Pennsylvania, Philadelphia PA, United States of America
- 121 Petersburg Nuclear Physics Institute, Gatchina, Russia
- 122 ^(a) INFN Sezione di Pisa; ^(b) Dipartimento di Fisica E. Fermi, Università di Pisa, Pisa, Italy
- 123 Department of Physics and Astronomy, University of Pittsburgh, Pittsburgh PA, United States of America
- 124 ^(a) Laboratorio de Instrumentacao e Fisica Experimental de Particulas - LIP, Lisboa, Portugal; ^(b) Departamento de Fisica Teorica y del Cosmos and CAFPE, Universidad de Granada, Granada, Spain
- 125 Institute of Physics, Academy of Sciences of the Czech Republic, Praha, Czech Republic
- 126 Faculty of Mathematics and Physics, Charles University in Prague, Praha, Czech Republic
- 127 Czech Technical University in Prague, Praha, Czech Republic
- 128 State Research Center Institute for High Energy Physics, Protvino, Russia
- 129 Particle Physics Department, Rutherford Appleton Laboratory, Didcot, United Kingdom
- 130 Physics Department, University of Regina, Regina SK, Canada
- 131 Ritsumeikan University, Kusatsu, Shiga, Japan
- 132 ^(a) INFN Sezione di Roma I; ^(b) Dipartimento di Fisica, Università La Sapienza, Roma, Italy
- 133 ^(a) INFN Sezione di Roma Tor Vergata; ^(b) Dipartimento di Fisica, Università di Roma Tor Vergata, Roma, Italy
- 134 ^(a) INFN Sezione di Roma Tre; ^(b) Dipartimento di Fisica, Università Roma Tre, Roma, Italy

- 135 ^(a) Faculté des Sciences Ain Chock, Réseau Universitaire de Physique des Hautes Energies - Université Hassan II, Casablanca; ^(b) Centre National de l'Energie des Sciences Techniques Nucleaires, Rabat; ^(c) Faculté des Sciences Semlalia, Université Cadi Ayyad, LPHEA-Marrakech; ^(d) Faculté des Sciences, Université Mohamed Premier and LPTPM, Oujda; ^(e) Faculté des sciences, Université Mohammed V-Agdal, Rabat, Morocco
- 136 DSM/IRFU (Institut de Recherches sur les Lois Fondamentales de l'Univers), CEA Saclay (Commissariat a l'Energie Atomique), Gif-sur-Yvette, France
- 137 Santa Cruz Institute for Particle Physics, University of California Santa Cruz, Santa Cruz CA, United States of America
- 138 Department of Physics, University of Washington, Seattle WA, United States of America
- 139 Department of Physics and Astronomy, University of Sheffield, Sheffield, United Kingdom
- 140 Department of Physics, Shinshu University, Nagano, Japan
- 141 Fachbereich Physik, Universität Siegen, Siegen, Germany
- 142 Department of Physics, Simon Fraser University, Burnaby BC, Canada
- 143 SLAC National Accelerator Laboratory, Stanford CA, United States of America
- 144 ^(a) Faculty of Mathematics, Physics & Informatics, Comenius University, Bratislava; ^(b) Department of Subnuclear Physics, Institute of Experimental Physics of the Slovak Academy of Sciences, Kosice, Slovak Republic
- 145 ^(a) Department of Physics, University of Johannesburg, Johannesburg; ^(b) School of Physics, University of the Witwatersrand, Johannesburg, South Africa
- 146 ^(a) Department of Physics, Stockholm University; ^(b) The Oskar Klein Centre, Stockholm, Sweden
- 147 Physics Department, Royal Institute of Technology, Stockholm, Sweden
- 148 Departments of Physics & Astronomy and Chemistry, Stony Brook University, Stony Brook NY, United States of America
- 149 Department of Physics and Astronomy, University of Sussex, Brighton, United Kingdom
- 150 School of Physics, University of Sydney, Sydney, Australia
- 151 Institute of Physics, Academia Sinica, Taipei, Taiwan
- 152 Department of Physics, Technion: Israel Institute of Technology, Haifa, Israel
- 153 Raymond and Beverly Sackler School of Physics and Astronomy, Tel Aviv University, Tel Aviv, Israel
- 154 Department of Physics, Aristotle University of Thessaloniki, Thessaloniki, Greece
- 155 International Center for Elementary Particle Physics and Department of Physics, The University of Tokyo, Tokyo, Japan
- 156 Graduate School of Science and Technology, Tokyo Metropolitan University, Tokyo, Japan
- 157 Department of Physics, Tokyo Institute of Technology, Tokyo, Japan
- 158 Department of Physics, University of Toronto, Toronto ON, Canada
- 159 ^(a) TRIUMF, Vancouver BC; ^(b) Department of Physics and Astronomy, York University, Toronto ON, Canada
- 160 Faculty of Pure and Applied Sciences, University of Tsukuba, Tsukuba, Japan
- 161 Department of Physics and Astronomy, Tufts University, Medford MA, United States of America
- 162 Centro de Investigaciones, Universidad Antonio Narino, Bogota, Colombia
- 163 Department of Physics and Astronomy, University of California Irvine, Irvine CA, United States of America
- 164 ^(a) INFN Gruppo Collegato di Udine; ^(b) ICTP, Trieste; ^(c) Dipartimento di Chimica, Fisica e Ambiente, Università di Udine, Udine, Italy
- 165 Department of Physics, University of Illinois, Urbana IL, United States of America
- 166 Department of Physics and Astronomy, University of Uppsala, Uppsala, Sweden
- 167 Instituto de Física Corpuscular (IFIC) and Departamento de Física Atómica, Molecular y Nuclear and Departamento de Ingeniería Electrónica and Instituto de Microelectrónica de Barcelona (IMB-CNM), University of Valencia and CSIC, Valencia, Spain
- 168 Department of Physics, University of British Columbia, Vancouver BC, Canada
- 169 Department of Physics and Astronomy, University of Victoria, Victoria BC, Canada
- 170 Department of Physics, University of Warwick, Coventry, United Kingdom
- 171 Waseda University, Tokyo, Japan
- 172 Department of Particle Physics, The Weizmann Institute of Science, Rehovot, Israel
- 173 Department of Physics, University of Wisconsin, Madison WI, United States of America
- 174 Fakultät für Physik und Astronomie, Julius-Maximilians-Universität, Würzburg, Germany
- 175 Fachbereich C Physik, Bergische Universität Wuppertal, Wuppertal, Germany
- 176 Department of Physics, Yale University, New Haven CT, United States of America
- 177 Yerevan Physics Institute, Yerevan, Armenia
- 178 Centre de Calcul de l'Institut National de Physique Nucléaire et de Physique des Particules (IN2P3), Villeurbanne, France
- ^a Also at Laboratório de Instrumentação e Física Experimental de Partículas - LIP, Lisboa, Portugal

- ^b Also at Faculdade de Ciencias and CFNUL, Universidade de Lisboa, Lisboa, Portugal
- ^c Also at Particle Physics Department, Rutherford Appleton Laboratory, Didcot, United Kingdom
- ^d Also at TRIUMF, Vancouver BC, Canada
- ^e Also at Department of Physics, California State University, Fresno CA, United States of America
- ^f Also at Novosibirsk State University, Novosibirsk, Russia
- ^g Also at Fermilab, Batavia IL, United States of America
- ^h Also at Department of Physics, University of Coimbra, Coimbra, Portugal
- ⁱ Also at Department of Physics, UASLP, San Luis Potosi, Mexico
- ^j Also at Università di Napoli Parthenope, Napoli, Italy
- ^k Also at Institute of Particle Physics (IPP), Canada
- ^l Also at Department of Physics, Middle East Technical University, Ankara, Turkey
- ^m Also at Louisiana Tech University, Ruston LA, United States of America
- ⁿ Also at Dep Fisica and CEFITEC of Faculdade de Ciencias e Tecnologia, Universidade Nova de Lisboa, Caparica, Portugal
- ^o Also at Department of Physics and Astronomy, University College London, London, United Kingdom
- ^p Also at Department of Physics, University of Cape Town, Cape Town, South Africa
- ^q Also at Institute of Physics, Azerbaijan Academy of Sciences, Baku, Azerbaijan
- ^r Also at Institut für Experimentalphysik, Universität Hamburg, Hamburg, Germany
- ^s Also at Manhattan College, New York NY, United States of America
- ^t Also at CPPM, Aix-Marseille Université and CNRS/IN2P3, Marseille, France
- ^u Also at School of Physics and Engineering, Sun Yat-sen University, Guanzhou, China
- ^v Also at Academia Sinica Grid Computing, Institute of Physics, Academia Sinica, Taipei, Taiwan
- ^w Also at School of Physics, Shandong University, Shandong, China
- ^x Also at Dipartimento di Fisica, Università La Sapienza, Roma, Italy
- ^y Also at DSM/IRFU (Institut de Recherches sur les Lois Fondamentales de l'Univers), CEA Saclay (Commissariat à l'Energie Atomique), Gif-sur-Yvette, France
- ^z Also at Section de Physique, Université de Genève, Geneva, Switzerland
- ^{aa} Also at Departamento de Fisica, Universidade de Minho, Braga, Portugal
- ^{ab} Also at Department of Physics and Astronomy, University of South Carolina, Columbia SC, United States of America
- ^{ac} Also at Institute for Particle and Nuclear Physics, Wigner Research Centre for Physics, Budapest, Hungary
- ^{ad} Also at California Institute of Technology, Pasadena CA, United States of America
- ^{ae} Also at Institute of Physics, Jagiellonian University, Krakow, Poland
- ^{af} Also at LAL, Université Paris-Sud and CNRS/IN2P3, Orsay, France
- ^{ag} Also at Nevis Laboratory, Columbia University, Irvington NY, United States of America
- ^{ah} Also at Department of Physics and Astronomy, University of Sheffield, Sheffield, United Kingdom
- ^{ai} Also at Department of Physics, Oxford University, Oxford, United Kingdom
- ^{aj} Also at Institute of Physics, Academia Sinica, Taipei, Taiwan
- ^{ak} Also at Department of Physics, The University of Michigan, Ann Arbor MI, United States of America
- ^{al} Also at Discipline of Physics, University of KwaZulu-Natal, Durban, South Africa
- * Deceased